NAVAL POSTGRADUATE SCHOOL
MONTEREY, CALIFORNIA

THESIS

A 15-YEAR CLIMATOLOGY OF SYNOPTICAL DISTURBANCE OVER TROPICAL NORTHWESTERN PACIFIC DURING SUMMER

by

Cheng,Chu-Chai

March, 1995

Thesis Advisor: Chih-Pei Chang
Co-Advisor: Jeng-Ming Chen

Approved for public release; distribution is unlimited.

REPORT DOCUMENTATION PAGE

Form Approved OMB No. 0704-0188

1. AGENCY USE ONLY *(Leave blank)*	2. REPORT DATE March, 1995.	3. REPORT TYPE AND DATES COVERED Master's Thesis

4. TITLE AND SUBTITLE A 15-YEAR CLIMATOLOGY OF SYNOPTICAL DISTURBANCE OVER TROPICAL NORTHWESTERN PACIFIC DURING SUMMER

5. FUNDING NUMBERS

6. AUTHOR(S) Cheng, Chu-Chai

7. PERFORMING ORGANIZATION NAME(S) AND ADDRESS(ES)
Naval Postgraduate School
Monterey CA 93943-5000

8. PERFORMING ORGANIZATION REPORT NUMBER

9. SPONSORING/MONITORING AGENCY NAME(S) AND ADDRESS(ES)

10. SPONSORING/MONITORING AGENCY REPORT NUMBER

11. SUPPLEMENTARY NOTES The views expressed in this thesis are those of the author and do not reflect the official policy or position of the Department of Defense or the U.S. Government.

12a. DISTRIBUTION/AVAILABILITY STATEMENT
Approved for public release; distribution is unlimited.

12b. DISTRIBUTION CODE

13. ABSTRACT *(maximum 200 words)*

This work investigated the suumertime northwestward propagating waves over the tropical western North Pacific and their relationship with tropical cyclone activities. The 15-season (May-October 1974-1988) Navy tropical global band data were separated into three groups according to the degree of organization in the multiple-set canonical correlation (MCC) modes that were computed from the surface v wind. Groups A (6 seasons) and B (5 seasons) showed orderly large-scale propagating patterns at the surface and 700 hPa with an average period of 8 days and a wavelength of about 2500-3000 km. The structure is robust whether the MCC analysis was performed on each of the seasons individually or on groups of years. A strong in-phase relationship between the low-level disturbance cyclonic cells and tropical cyclone centers was found. Composite analysese of all cases in these two groups whose MCC mode 1 amplitude exceeded 1.5 m/s showed organized northwestward propagating divergence/convergence patterns at 200 hPa. Group C (4 seasons) shows the least organized structure, with a large difference between MCC modes obtained from the entire group and those from each individual season. The possibility that group C contains irregular tropical cyclone tracks was discussed.

14. SUBJECT TERMS MULTIPLE-SET CANONICAL CORRELATION, SINGLE POINT CORRELATION AND COMPOSITE ANALYSIS.			15. NUMBER OF PAGES 161
			16. PRICE CODE
17. SECURITY CLASSIFICATION OF REPORT Unclassified	18. SECURITY CLASSIFICATION OF THIS PAGE Unclassified	19. SECURITY CLASSIFICATION OF ABSTRACT Unclassified	20. LIMITATION OF ABSTRACT UL

NSN 7540-01-280-5500

Standard Form 298 (Rev. 2-89)
Prescribed by ANSI Std. 239-18 298-102

Approved for public release; distribution is unlimited.

A 15-YEAR CLIMATOLOGY OF SYNOPTICAL DISTURBANCE OVER TROPICAL NORTHWESTERN PACIFIC DURING SUMMER

Cheng, Chu-Chai
Lieutenant Commander, Taiwan(R.O.C)Navy
B.S., Chinese naval academy, 1982

Submitted in partial fulfillment
of the requirements for the degree of

MASTER OF SCIENCE IN METEOROLOGY

from the

NAVAL POSTGRADUATE SCHOOL
March 1995

Author: Cheng, Chu-Chai
Cheng,Chu-Chai

Approved by: C P Chang
C.P.Chang,Thesis Advisor

Jeng-My Chen
J.M. Chen, Co-Advisor

R.L. Haney
R.L. Haney, Chairman
Department of Meteorology

ABSTRACT

This work investigated the suumertime northwestward propagating waves over the tropical western North Pacific and their relationship with tropical cyclone activities. The 15-season (May-October 1974-1988) Navy tropical global band data were separated into three groups according to the degree of organization in the multiple-set canonical correlation (MCC) modes that were computed from the surface v wind. Groups A (6 seasons) and B (5 seasons) showed orderly large-scale propagating patterns at the surface and 700 hPa with an average period of 8 days and a wavelength of about 2500-3000 km. The structure is robust whether the MCC analysis was performed on each of the seasons individually or on groups of years. A strong in-phase relationship between the low-level disturbance cyclonic cells and tropical cyclone centers was found. Composite analysese of all cases in these two groups whose MCC mode 1 amplitude exceeded 1.5 m/s showed organized northwestward propagating divergence/convergence patterns at 200 hPa. Group C (4 seasons) shows the least organized structure, with a large difference between MCC modes obtained from the entire group and those from each individual season. The possibility that group C contains irregular tropical cyclone tracks was discussed.

TABLE OF CONTENTS

LIST OF FIGURES

ACKNOWLEDGMENTS

The author wishes to express his appreciation for the guidance by Prof. C.P. Chang and Dr. J.M. Chen, without which this researh could never have been completed.

Thanks are also due to Dr. Patrick Harr for helping with the plotting of the tropical cyclone center positions and reading the manuscript, and to Ms. Bao-Fong Jeng for providing invaluable computational support.

This work was supported in part by the National Science Foundation, under Grant ATM9106495. The global band analysis data were provided by the Fleet Numerical Meteorology and Oceanograkphy Center, Monterey, California.

I. INTRODUCTION

The tropical easterly wave disturbance was first recognized by Piersig(1936) and Regular(1936), using surface data, they found these disturbances traveling from western Africa toward the Atlantic. These waves disturbances have a relatively well defined period of around 4 or 5 days with a horizontal wavelength of 2000-4000 Km in the lower troposphere. Dunn(1940) used surface pressure data to trace the movement of an isallobaric center across the western Atlantic ocean and Caribbean sea. During and after World War II ,using upper air data from the Caribbean area, Riehl(1945) and associates developed the theory of easterly wave model. The term " easterly waves " is used to described these synoptic disturbances, and their propagation characteristic are believed to be near those of Rossby waves. These waves, which have maximum intensity in the layer from 700 hpa to 500 hpa, slope eastward with height.

Yanai et al. (1968) also found westward propagating waves, which have 4-5 days period with 6000-10000 Km wave length and eastward tilt vertical structure. Between the late 1960's and the early 1970's, most of the study of tropical tropospheric synoptic disturbances, using station radiosonde data and satellite cloud pictures, were made over the tropical western pacific. Over the western North Pacific, Wallace and Chang 1969, Chang et al. 1970 and Reed and Recker 1971 used spectrum and composite analyses to study the characteristics of the easterly wave disturbance. They found that these waves have a well-defined 4-5 day period and with a horizontal wavelength of 2000-4000 Km there is also a northeast-southwest horizontal tilt, which implies by a northward momentum flux. The waves contain a warm core vertical structure, which is equivalent barotropic

with very little tilt the over central part of the western Pacific, and have a slight westward tilt with height over the western part of the western Pacific. The influense of the vertical shear in the ambientflow, on the change in vertical tilt across the western Pacific bases was verified in a linear model by Holton (1971).

The easterly waves are Rossby like waves. Over the eastern part of the western Pacific, the disturbance sometimes have a longer-wavelength. The vertical structure contains an eastward tilt with height below 300 hpa and westward with height above it. These waves are sometimes identified with mixed-Rossby-gravity waves. Using the internal variation of sea surface temperature Chang and Miller (1977) and Dunkerton(1993) and Chang and Zambresky (1994) , used suced seasonal variation to explain the change in the wave disturbance.

The expanded observation platforms of the 1979 First GAPP Global Experiment (FGGE) facilitated further investigation into the behavior of tropical wave disturbance at locations where only few station data were available before. Nitta et al. (1985), Nitta and Takayaba (1985) and Tai and Ogura (1987) use these data to examine synoptic scale disturbance throughout the tropics. They identified various regions with active summer-time transient activities in the northern tropics by examining band-pass-filtered data of meridional wind(v) and outgoing longwave radiation (OLR). They concentrated on spectral characteristics and the vertical structure of the wave disturbance. Nitta and Takayabu (1985) and Tai and Ogura (1987), found west-northwestward propagating disturbances in the eastern tropical Pacific. They also observed cold anomalies below 700 hpa and stronger warm anomalies at about 300 hpa. Recently, because of the increase in quality of numerical

model analyses and satellite data over the tropics, we are no longer limited to only station data. Reed et al. (1988a,1988b) studied the synoptic evolution of Africa wave disturbances appearing in the European Center for medium Range Weather Forecast (ECMWF) for the summer of 1985. They found two preferred tracks for Africa wave disturbance and also confirm much of the previous studies of the wave disturbances. They found over data sparse area the African wave disturbance features depicted by the ECMWF analysis are substantiated by independent satellite data. Liebman and Henton (1990) used the initialized data from ECMWF and outgoing longwave radiation (OLR) data during fall(September - December), 1980-1987 to study the zonal variation of the 3- day equatorial synoptic scale waves. Lau and Lau (1990) also used the ECMWF data and OLR data for summer (June - August), 1980-1987 to study the tropical waves disturbance over the western Pacific. They used single point correlation and rotated " extended empirical orthogonal function " (EEOF) analysis to show a northwestward phase propagation, with a wavelength around 2800 Km and period of 6 days. This result is within Liebman and Henton's (1990) estimate. The summertime phase propagation pattern with the northeast-southwest elongated wave structure is more well defined than the fall pattern and it may be track back to 5°N,155-160°E. Their results show that the mixed Rossby Gravity waves(MRG) will dominate the equatorial eastern Pacific and Rossby wave-like, west-northwest propagating waves dominate the western Pacific. The strong northwestward tilt with height is found in the equatorial region, and convection (as indicated by OLR) is ahead of low level troughs. The vertical tilt and convection-trough phase difference both decrease downstream, and disappear toward the south coast of China.

Takayaba and Nitta (1993), used the summer ECMWF data (1980-1989) along with satellite cloud data from Japanese GMS, to study the northwestward propagating wave pattern in the western North Pacific. They found the same westward propagating mixed Rossby-gravity wave (3-5 days) patterns which may dominate because to the mean vertical shear and sea-surface temperature. Their results in agreed with Chang and Miller's (1977) finding,which was based on radiosoude data. They also suggest that these northwestward propagating wave disturbances may develop from the mixed Rossby Gravity waves in the equatorial central pacific. This downstream development appears plausible as both type of waves have the same 3-5 days period in their study. Nevertheless, Lau and Lau (1990) considered this link unlikely owing to the weakening of the central Pacific equatorial wave near the dateline.

Chang et al.(1994) Who used multiple canonical correlation analysis(MCCA) with analyzed data from the Navy Operational Global Atmosphere Analysis and Prediction Model (NOGAPS) studied these northwestward propagating waves during the summer of 1989-1991. To focus in the synoptic scale disturbance they used high-pass filtered deta to remove features with a period greater than 12 days. The wave disturbance have patterns that are similar to those found by Lau and Lau (1990) but have a longer period of 8 days. They concluded that most of these waves are related to tropical cyclone activities, and postulated that nonlinear barotropic effects, which cause anticyclogenesis southeast of the main cyclone center with a southeast propagating of wave energy, favors a continuous development of the wave disturbance. These are Rossby-like waves where the beta effect plays a major role in the propagation and development.

In addition to synoptic waves discussed above,

intraseasonal oscillations have been known to affect tropical weather significantly. Madden and Julian (1971,1972), using spectra and cross spectra with data from other stations, found two propagating waves , a westward propagating was found with a 5-6 days period and a global horizontal scale, (Maddan and Julian 1972b), the other is the 40-50 dsys oscillation which called Madden-Julian Oscillation(MJO). These 40-50 days waves propagate eastward with planetary scale Zonal wavenumber one. The dominant signal is in the zonal(U) wind component. There are many studies on the MJO and its' role in tropical convection, especially over the Indian monsoon region(Krishnamurti and Subrahmanyan, 1982; Lorenc, 1984; Krishnamurti, 1985; Lau and Chan, 1986).

Krishnamurti et al. ,(1985) clearly identifies a planetary-scale divergence wave that travel eastward around the globe throughout the FGGE year. The divergence or convergence centers usually show up over the western equatorial Indian ocean. These centers then propagate to the western Pacific. Hayashi and Sumi(1986) and Lau and Peng(1987), Used a numerical study to suggest that cumulus convection is an important factor in generating the 40-50 day low frequency mode. The northwestward propagation of the divergent mode might be attributed to the supply of available water vapor and cumulus convection over the entire Asian Monsoon region. The theoretical studies have suggested that the MJO is likely moist Kelvin waves(Chang, 1977; Lau and Peng, 1987;Chang and Lim,1988), and also may have a Rossby component that couple the convection with the planetary boundary layer(Wang, 1988).

There is another intraseasonal signal that appear in the tropical wave disturbances that occurs in the period range between the synoptic wave and the MJO. Wallace and

Chang(1969) found that the meridional(V) winds at the tropical western Pacific show a 10-20 day peak. This quasi-biweekly periodicity was also found in various studies of the Asian summer monsoon region (Krishnamurti, 1973; Murakami and Frydrych, 1974; Zangvil, 1975; and Chan and Chen, 1993). These 10-20 day oscillations generally propagate westward and have a near barotropic vertical structure. Many of the previous studies associated this oscillation with the activity of the Indian summer monsoon. the studies of Krishnamurti and Bhalme (1976) and LI and Zhou (1992) show that the biweekly oscillation dominates the fluctuation of wind and surface pressure over the Indian monsoon region and documented its interaction with MJO. Harr (1993) studing the effect of variation of large scale circulation on tropical cyclone characteristics over the tropical western North Pacific. He identified six recurrent 700 hpa circulation patterns that represent large-scale variabilities associated with the monsoon trough and subtropical ridge. There are many possible transitions among recurrent circulation patterns, but significant transitions occur over a very limited set of paths which are associated with interactions with tropical and midlatitude circulation systems. Furthermore their transitions can explain much of the observed intraseasonal variability in the occurrence and track types of tropical cyclones.

The quasi-biweekly oscillations and the MJO both have strong signals over the northern summer monsoon region. This suggests that the intraseasonal oscillation may be the manifestation of a large-scale monsoon oscillation over the entire Indian Ocean-western Pacific region. (Krishnamurti and Subrahmanyan, 1982; Lau and Chen, 1986; Chan et al. , 1988). The near 10 day period disturbance (Chang et al. , 1994), nearly overlaps with the short end of the period

range of the quasi-biweekly oscillation. Most previous studies have relied on a time frequency filter, typically band-pass filters, to separate the MJO and quasi-biweekly systems. This may pre-determine the period window to be studied and may leave out structures that are outside of the predetermined window. The MCCA (Chen and Chang, 1993; Chen et al. ,1994) effectively isolate the synoptic scale, west-northwestward propagating disturbance in the tropical western Pacific from the NOGAPS analysis during summer of 1989-1991, Although intraseasonal frequencies were removed by a high-pass filter that truncates the spectrum at a period of 12 days, narrow band pass filtering was not used. Because the technique of MCCA is mainly a spatial decomposition, is used to find the structure of the synoptic waves, which have a period close to 8 days during the three summers. This is longer than the previously assumed 3-6 day period.

The purpose of this work is to study the properties of the tropical northwestward propagating wave disturbances over the western Pacific during 15-years(May-October, 1974-1988), and to compare the results with tropical cyclone activities. The focus of this study will be on intraseasonal oscillations other than the MJO. So the MCCA will be applied to the meridional wind component. This will bring out the non-MJO signal, Since the MJO is base on the zonal wind component. As we expected, The MCCA method successfully separates out tropical synoptic wave disturbances which we are interested in this study.

In section 2 we describe the data and methodology used. Section 3 will show the leading MCC structure of v wind component. Section 4 will show one-point correlation and the relation between the synoptic wave disturbance and the tropical cyclone position. Section 5 discuss the results of

a composite study which show the contour and vector map of V vector from selected strong cases. Section 6 include a summary and the conclusion.

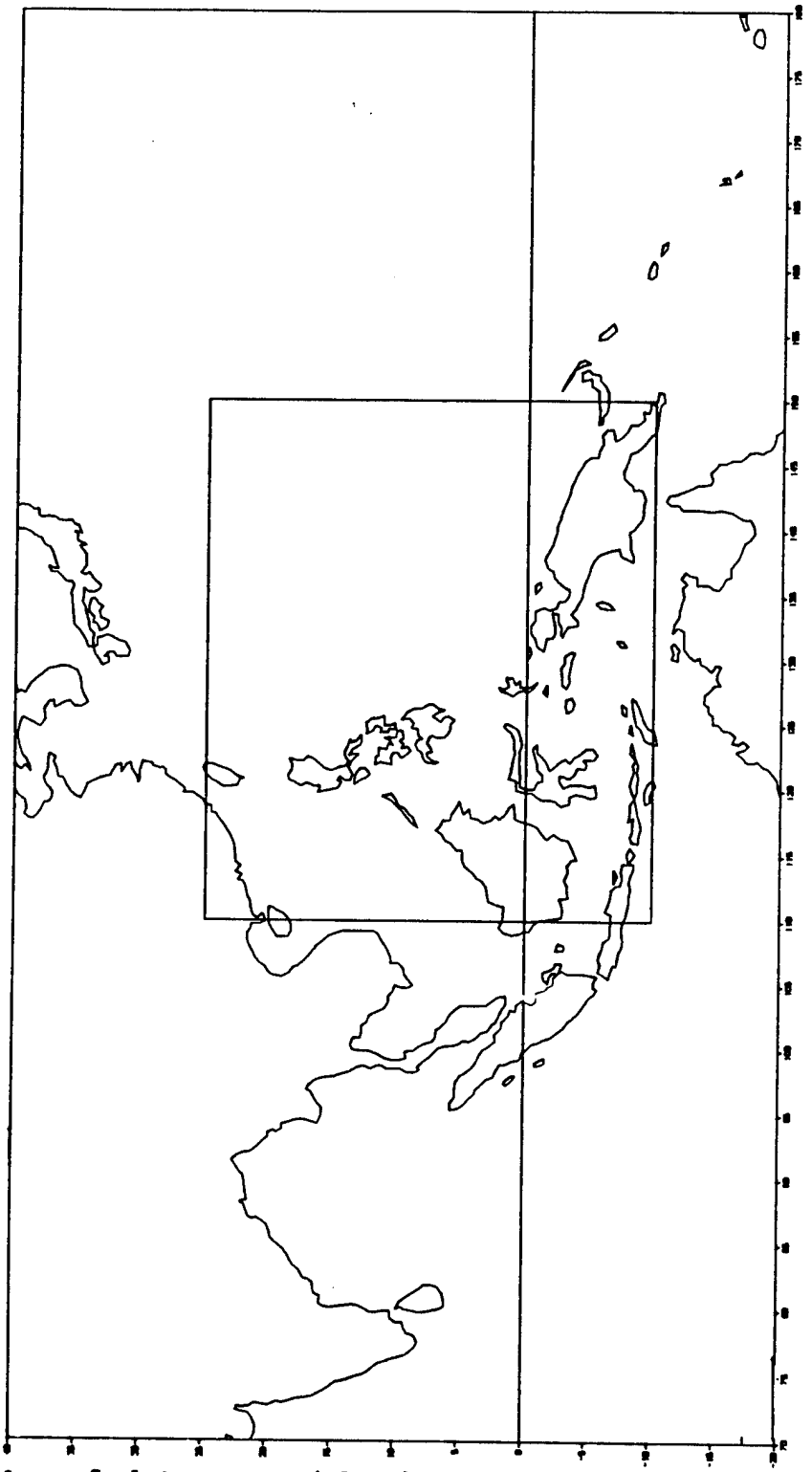

Figure 1:Map of data area (showing core domain for MCCA and large domain for single point correlation and composites)

II. DATA AND METHODOLOGY

A 15 year (May-October) wind data set is used, except for 1974, which only contain July-October. analyzed fields are from the operational Global Band Analysis (GBA) of the Fleet Numerical Meteorology and Oceanographys Center, Monterey, California, during 1974-1988. These data were produced four times daily by objective procedures on a mercator grid which extended from 60°N to 40°S. The objective analysis scheme was designed to take advantage of all the reports from the operational data base. Although, data were available every six hours for the surface, 700, 400, 250, and 200 hpa level, We only use twice daily data (00h and 12h) and surface, 700 hpa, 200 hpa (V) wind data. The domain of the study is shown in Fig 1. A core region of 110°-150°E, 10°S-25°N is embedded in the large domain of 70°-180°E, 20°S-40°N. Because of major progress in computer technology and the availability of large amounts of data, researchers have used different kind of statistical methods in the meteorological data fields. One of these is the Principal Component Analysis (PCA) which was used by Pearson(1901) in a biological context when he recast linear regression analysis into a new form so as to avoid the weak asymmetrical relationship between "dependent" and "independent" variables. Lorenz (1956) used the technique in the field of statistical-dynamical approaches to weather prediction. The term PCA, sometime called "empirical orthogonal function analysis" (EOFA) concentrates the internal variation within one data field to a set of leading components. These are used to transform the original set of variables to a new set of uncorrelated variables called principle component(PC). These are used to find a linear combination of the original data variable such that

the principal component, which is a function of time over a set of grid point(17x15 in our study) and is also referred to as an "amplitude", has the maximum variance under the condition that the weighting function is orthogonal to those of all preceding PC's. Subsequent PC's can be found under the same maximum variance,unitary weighting function, and orthogonality requirements. If a data pattern is proportional to its own weighting function, all other PC's will vanish due to the spatial orthogonality. These weighting functions are often called EOF's in meteorological study, also we can reduce the dimensionality of the data in order to simplify later analysis. Chen et al., (1993) have shown that direct application of PCA to data from a well-chosen network is particularly efficient.

PCA gives us the internal variation within one data field to the leading component, but does not tell us the information of relationship between different fields. The relationships between two data fields in term of correlation coefficient can be determined by the canonical correlation analysis (CCA). The CCA is basically a search for optimal correlation between two variable fields by linearly combining the elements of each fields. These combinations are called canonical component(CC). The CCA method pairs data patterns(one for each field) so as to identify those parts of the patterns that are significantly correlated and their respective variance contributions. Conventional CCA can be used for investigating the correlation between two fields, but it can only show maximum correlations without regard to the variance significance. So we always perform the PCA before the CCA does. It is hoped that with PCA, the leading component may represent different physical processes, or at least, component truncation can help to delete noise and errors which may be associated with small

variabilities.

The multiple-set canonical component analysis(MCCA) method is a generalization of the traditional two variable CCA to multiple variables(e.g. Steel, 1955; Horst, 1965; Kettenring, 1971; Gifi, 1990). This method tries to find the maximum correlation among more than two data fields. Through a diaganolization of the product or the square product of the correlation matrices, Chen et al.,(1994) not only simplify the MCCA procedures to be used in studies with large dimensioned data, but also can select the correlation between the two fields we need. The results are accepted when the largest residual (cross-component) correlation is negligible compare to the average correlation. The application of the MCCA method follows that of Chen and Chang(1993,1994), where the different data fields are constructed from an overlaping-sliding time window that contains consecutive fields of the same variable. In our study, we use MCCA on v_{sfc}, 700 and 200 hpa within the core region to find the basic disturbance structure mode, the basic structure mode is correlated with other variables to find the entire structure of the disturbance.

The data on 255 grid points within the core domain are first pre-processed with an EOF analysis, that will truncate the data to include the first 18 principal components, which retain 79% of the total variance in the core domain. A high pass filter, 20 days, is applied to each of the components by removing all waves whose period longer than 20 days, which may masks significant synoptic time scale events. This will leave the higher frequency, synoptic-scale events. The data set, which contains 12 consecutive twice-daily data, are formed as the window (00h(time t0) to 132h(time t11)slides forward at 12-hour intervals. The squared product of correlation matrices between fields of adjacent times are

optimized. The reliability of this application procedure of the MCCA method for the field data has been tested and found satisfactory by Chen and Chang(1994).

The MCCA results in 12 MCC modes that are ranked according to the average correlation through any 132 h(5.5 days) period. The first mode always contains the largest correlation coefficience, which will show the best defined pattern. The comparisons between the wave patterns in different time frames will tell the characteristics of transient phenomena occurring in the area covered in this study.

At any given time MCC mode contains both horizontal spatial and time structure, which includes the 12 consecutive 12-hour time frame from day 0 to day 5.5. Therefore, we also produce a time-integrated amplitude coefficient. This coefficient is the average amplitude of the 12 consecutive 12-hour structure and is plotted in the time domain according to the first time frame,(t0).

To study the U,V structure over large domain and at other level, we use one point correlation. The v_{sfc}, v_{700}, v_{200} wind component are determined by the single point correlation between these field and the time-integrated amplitude coefficient of the MCC mode one. A sequence of correlation plots based on different time lags may be produced. The correlation plots will give us some idea of how well the MCC mode is done in the mean removed data. We also use the correlation plots to find the possible relationship between the propagating wave and tropical cyclone activities. This is done by identifing the time of the maximum point in the time series and then correlate it with the tropical cyclone center positions.

Another approach to reveal the three dimensional and time pattens of the leading MCC modes are to composite the

strongest cases chosen on the time-integrated amplitude coefficient time series. The composite was with respect to the time lag from the large amplitude time points. Because the cases selected are based on a particular MCC mode, it is likely that each case is indeed similar and that the composite does provide a useful representation.

III. LEADING MCC STRUCTURE

All MCC modes are determined from the May-October v_{sfc} fields. Several calculations are performed based on different periods of the data. First, the entire 15-year summer data are used to find a set of MCC modes, which are referred to as the 15Y MCC modes. The MCCA is then performed on each of the 15 individual years, resulting in 15 sets of MCCs, one for each year. The individual year's leading MCC mode are compared to the 15Y's, and are found to resemble the 15Y leading mode in various degrees. We then group the individual years into three groups, with Group A containing years whose MCC mode 1 resembles that of 15Y, Group B contains years whose MCC mode 1 resembles 15Y to a slightly lesser degree, and Group C containing years whose MCC mode 1 dose not resemble that of 15Y. Finally, the MCCA is performed on each of the three groups, resulting in yet another three sets of MCCs.

In most cases, MCC modes 1-2 form a pair of propagating modes with similar horizontal structure, fractional variance, averaged correlation, and approximately one quarter cycle phase difference. Higher order modes are normally associated with small variance and smaller scale, less coherent structure. Thus, our study focuses on mode 1 only.

A. MCC MODES DETERMINED FROM 15-YEAR DATA

The first two MCC modes for the 15Y are shown in Fig. 2. The 12-hour frames show a synoptic-scale, west-northwestward propagating pattern with a wavelength of about 2500-3000 km. The propagation track starts from the tropical western Pacific, across the Philippines and reaches southeastern coast of China. Any two time frames that are

96 h apart demonstrate a near 180° out-of-phase relationship in the main features. For example, time frame T2 shows a positive cell center over the northern Philippines and a negative cell center at 15°N, 135°E; while time frame T10 shows a negative center over the northern Philippines and a positive cell center at 12°N, 133°E. Thus, a period of approximately 8 days may be inferred. These horizontal structures and periodicity are very close to those estimated by Chang et al. (1995) based on NOGAPS data of 1989-1991 using the same MCCA technique. The structures also resemble those found by Lau and Lau (1990) using simple lag correlations on the 1981-89 ECMWF data, although they estimated a period range of 6-8 days.

The averaged correlation between each consecutive 12-hour frame is about 0.87 for both modes 1 and 2, which is slightly less than the 1989-1991 NOGAPS results of 0.94. The total fractional variance for the two modes is about 25%. Because of different filters used, a direct comparison of the present results and the three-year NOGAPS study can not be made, but it is possible to state that this variance is slightly less than that obtained by Chang et al. (1995). These slightly reduced correlations and variances are not significant, considering the fact that the GBA data set does not use model forecasts as a first guess. The present variance estimate is significantly larger than Lau and Lau's (1990) results of about 9% for the northwestward propagating wave. This is likely due to the bogus typhoon data used in the GBA which is not used in the ECMWF analysis. In addition, Chen and Chang (1993) and Chen et al. (1994) found that the multiple-time correlations over a synoptic period can isolate a significantly larger signal than simple lag correlations. The latter represents only a partial view of the time variability based on two time points. The signals

isolated depend on how much these two time points can represent the entire variability. On the other hand, the former method seeks for the variability based on a more complete sampling of several time points throughout the synoptic period, and may give rise to a more complete representation of the coherent motion system.

B. MCC MODES DETERMINED FROM INDIVIDUAL YEARS

A main purpose of the present study is to see how representative the 8-day northwestward propagating wave is for each individual year in the GBA data set We therefore conducted an MCCA for each of the 15 years. In all cases modes after the first two do not contain consistent-varying, large scale structures throughout the 5.5 day period of the MCCA, so again only the leading pair of MCC modes 1-2 are considered interesting. The individual MCC mode 1 structure, derived from individual year from 1974 to 1988, are included in Appendix A (Fig. A1). In general, the structures may be classified into three broad categories based on their resemblance or difference from the 15Y mode 1. These categories are termed groups A, B, and C, respectively. Group A contains the six years that best resemble the 15Y. Group B contains five years that partially resemble 15Y. Finally, group C includes four years that appear to be significantly different from 15Y. The years within each group are listed below:

Group A:1975, 1977, 1979, 1985, 1986, 1987

Group B:1974, 1980, 1981, 1982, 1983

Group C:1976, 1978, 1984, 1988.

In this categorization Group B years usually show the basic cell structure of the 15Y pattern, but are considered to have only partial resemblance because either the structure in a number of time frames shows smaller-scale or

other anomaly features, appreciably depart from the straight northwestward track, or the whole pattern appears stationary over part of the period.

The total fractional variance and the averaged correlation for MCC modes 1 and 2 for the individual years are listed in Table I. The fractional variance, in general, ranges between 24% and 40%, mostly above the total variance determined from the 15Y MCC modes 1-2. The single exception is 1978, a group C year, with a very low variance of 8%. We have examined other modes of this year, none of which show patterns that resemble the leading 15Y MCC modes. The variance of group A years, on the average, is slightly higher than the other groups, and that of group C years, even after removing 1978, is the lowest, although the differences are not large. The correlation for individual years ranges between 0.75 and 0.93, as compared to the 15Y value of 0.87. There is no systematic change among the three groups.

YEAR	GROUP	TOTAL VARIANCE	CORRELATION
15		25%	0.87
1974	B	37%	0.91
1975	A	27%	0.89
1976	C	31%	0.93
1977	A	31%	0.90
1978	C	8%	0.90
1979	A	40%	0.93
1980	B	33%	0.93
1981	B	32%	0.88
1982	B	28%	0.80
1983	B	29%	0.85
1984	C	26%	0.88
1985	A	39%	0.92
1986	A	38%	0.89
1987	A	34%	0.85
1988	C	24%	0.75

Table I:Variance and correlation for 15Y and individual years MCC mode#1 and #2

Since individual years in group have their leading MCC mode patterns appreciably different from the 15Y, it will be interesting to see how an MCCA for the entire group (combining all years within the group) will compare with the 15Y patterns. Therefore, we carried out the MCCA for each of the individual groups. The resultant MCC modes 1-2 patterns are shown in Figs. 3, 4, 5, respectively, for groups A, B, and C. The total fractional variance and the

average correlation for these group modes are shown in Table 2. As expected, the group A mode 1 pattern (Fig. 3a) shows the northwestward propagating wave pattern with similar spatial and time scales as that of 15Y. In this case mode 2 of group A (Fig. 3b) is nearly in phase with the 15Y mode 1 (Fig. 2a), and vice versa. The total modes 1-2 fractional variance is 32% (Table II), which is considerably higher than the 15Y value of 25%. The average correlation of 0.88 is very close to the 15Y's 0.87.

YEAR	GROUP	TOTAL VARIANCE	CORRELATION
A		32%	0.88
B		28%	0.86
C		13%	0.83
CC		23%	0.83

Table II:Same as Table I except for Group

The group B modes 1-2 patterns (Fig. 4) also resemble the 15Y patterns, almost as close as that of group A, with its mode 1 corresponding to the 15Y mode 2 and vice versa. The resemblance is an improvement over those of the individual B years. Therefore, the five years, when combined, give a more clearly defined large-scale wave signal than individual years. The total fractional variance is 28%, and the average correlation is 0.86, which is again very close to the 15Y's value. The group C modes 1-2 are shown in Fig. 5. Different from each of its four individual years, Fig. 5 reveals a pattern that contain some aspects of the northwestward propagating wave pattern shown in the 15Y modes. Fig. 5b shows that main features of group C's mode 2

have a small phase difference (somewhat less than 90°) with the 15Y mode 1 (Fig. 2a). In the meantime, the main features of group C's mode 1 (Fig. 5a), particularly in the vicinity of the Philippines, are roughly half a cycle out-of-phase with the 15Y mode 2 (Fig. 2b). Thus, group C modes 1-2 roughly describe a propagating wave that is about 180° out-of-phase with the 15Y modes 1-2. This partial resemblance of the 15Y modes by the group C result is a significant difference from each of the four individual years. It indicates that the common structure among these four "abnormal" (relative to the 15Y structure) years is closer to the 15Y modes than that is revealed by any individual year's MCC modes. The total mode 1-2 fractional variance of group C is 13%, considerably smaller than the 15Y, apparently because of the very low variance in 1978 (Table 1). The average correlation is 0.83, which is only marginally less than 15Y and groups A and B.

In order to see whether the low-variance 1978 has any special impact on the group C results, we conducted the MCCA on the three other years of group C. This shall be termed group CC, and the resultant MCC modes 1-2 are shown in Fig. 6. The patterns are much the same as those from group C. Table II also shows that the total mode 1-2 fractional variance for group CC is 23%, considerably higher than group C (when 1978 is included in the group), but smaller than group A's 32% and group B's 28%. This systematic decrease in the fractional variance from groups A to C suggests that the northwestward propagating wave pattern is the domainant organized motion system in this region during the northern summer. When this motion system is more active, the v_{sfc} field is more organized, which leads to larger fractional variances of MCC modes 1-2. The fact that groups B and C's modes reveal a structure closer to the 15Y modes than the

individual years within their respective groups is an additional indication that the northwestward propagating wave pattern is a common structure among most years.

C. TIME VARIATIONS OF THE MCC MODE AMPLITUDES

The time variations of the MCC mode amplitudes are shown both as a composite time series and a power spectrum. The reason of a composite time series is that, at any given time, a mode contains both horizontal and time structures, with the latter encompassing 12 consecutive twelve-hourly frames from day 0 to day 5.5. Thus, the time variation of each mode should be described by considering the fact that each mode is a space-time volume function that covers not just the horizontal spatial domain but also a time domain of 5.5 days. In order to take into account this time domain, the coefficient of each mode is constructed by a time-integrated amplitude coefficient. This coefficient is the average amplitude of the 12 consecutive twelve-hour structures, and is plotted in the time domain according to the time of the first (day 0) time frame.

We have conducted the MCCA on the 15-year data set as one group (15Y), in three different groups (A, B, C), and for each individual years, For each year three time-integrated amplitude series of mode 1 can be constructed. Fig. 7 shows the three time series for each of the six group A years, and Figs. 8-9 show those for the groups B and C years, respectively. For each year the top panel is the time series from the 15Y mode 1, the middle panel is from the respective group's mode 1, and the lower panel is from mode 1 based on the single-year data. The power spectra are shown to the right of the time series. In general, the six member of group A show a high correlation among the three time series, particularly between the 15Y

and the group A series, which are mostly in-phase throughout the season. The single-year series are also correlated to the respective 15Y and group A series, an occasional a phase shift of around one quarter cycle is simply due to identification of the T0 time frame in applying the MCCA procedure to different lengths of data. As long as the mode pattern also has a one-quarter cycle shift (approximately two days), the results coincide with each other. In some years (e.g., 1985), the single-year phase shift during the early part of the season (May-July) is larger than during the late part of the season (August-October). As will be shown in the next section, the northwestward propagating wave patterns can often be associated with tropical cyclone activities. These activities are normally more active during the latter period. Therefore, the better correspondence during late summer between the single-year MCC mode 1 series and that of the group A and 15Y may be due to the increased presence of tropical cyclones.

The good correspondence among all three time series for each year is also obvious in the group B years (Fig. 8). Since the group C modes 1-2 describe a propagating wave pattern that is roughly 180° out-of-phase with 15Y, in Fig. 9 the sign of the group C series has been reversed in order to help the comparison. For group C years, the 15Y and group C time series are in good agreement, but their correspondence with the single-year series is less. This is consistent with the fact that the single-year MCC modes least resemble the 15Y modes.

Figs. 7-9 show that the power spectra for the different MCC modes and different years often have spectral peaks in the 6-12 day range. The most frequent peak occurs around 8 days. In order to identify the dominate spectral peaks, we composited the spectra shown in Figs. 7-9 for the entire 15

years, and for each of the three groups. The 15-year composite is based on the 15Y modes 1-2 spectra and is shown in Fig. 10a. Each group composite is based on the group's modes 1-2 (not the 15Y modes), and is shown in Figs. 10b-d for groups A, B and C, respectively. The 15Y composite shows a broad, but well-defined, power peak in the 6-12 day period band. The group A composite shows a sharply defined peak at around 8 days, the same period that was observed in the 15Y MCC modes 1-2 patterns (Figs. 2-3), and is the period that was reported by Chang et al (1995) using the northern summer 1989-1991 NOGAPS data. The group B composite is different from group A. It shows a double peak at 6 and 11 days, respectively, and the 8-day period appears as a local power minimum within a broad 6-12 day maximum. The group C composite contains large difference from group A. There is a broad spectral maximum that covers a range from 6-days to longer periods. The drop in power beyond 20-days in Fig. 10d is likely due to the use of a high-pass filter. Thus, group C, which has the least organized signal of the northwestward propagating waves in its MCC modes, also has the smallest percentage of its power in the 6-12 day range.

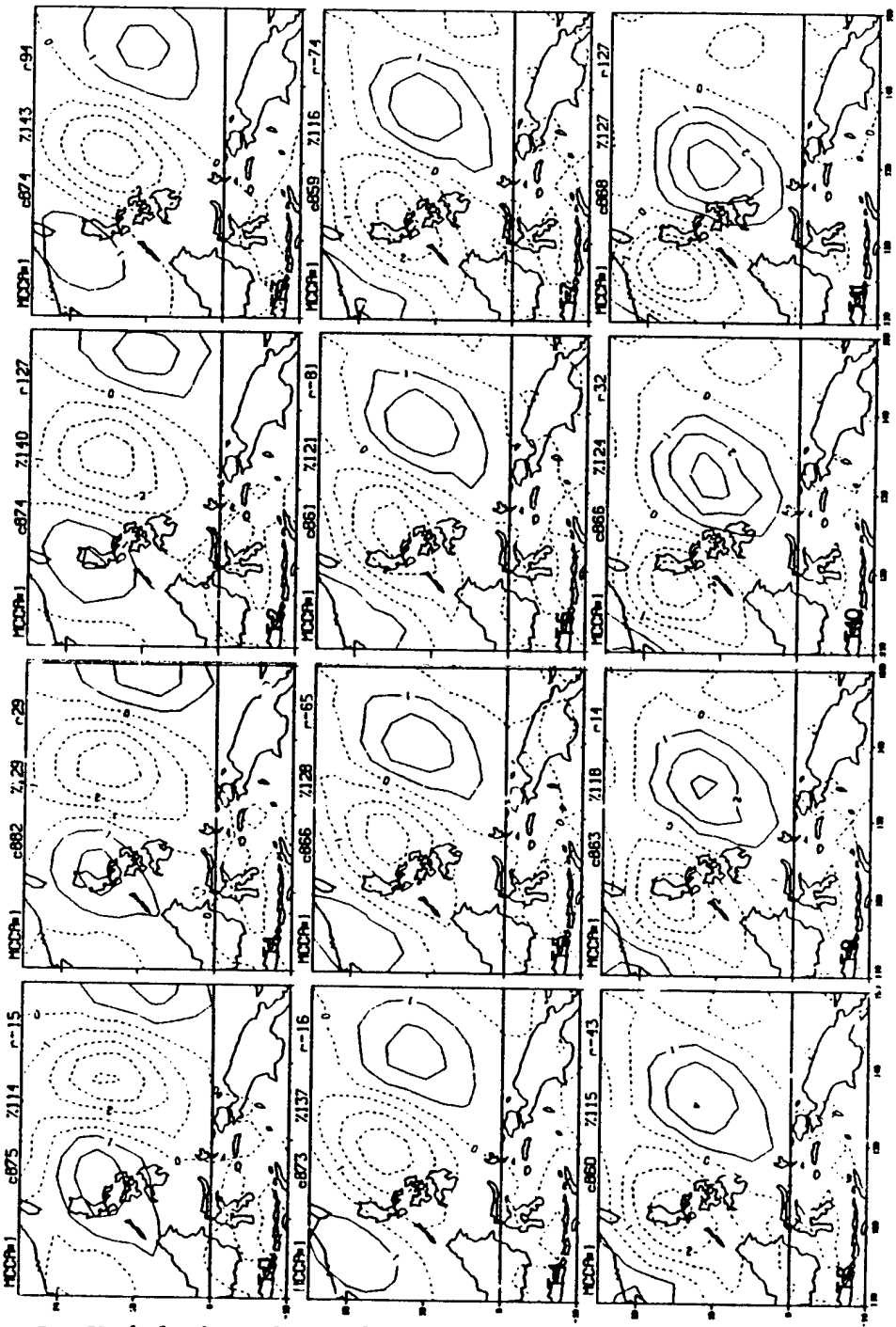

Figure 2a:Weighting function for 15Y MCC mode#1(equivalent to MCC mode#1 structure) of surface meridional wind(v) for 12 consecutive 12-hour frames from 00 h to 132 h(5.5 day). Contour interval is 0.06 and dashed lined correspond to northerly winds when MCC mode#1 amplidtude is positive

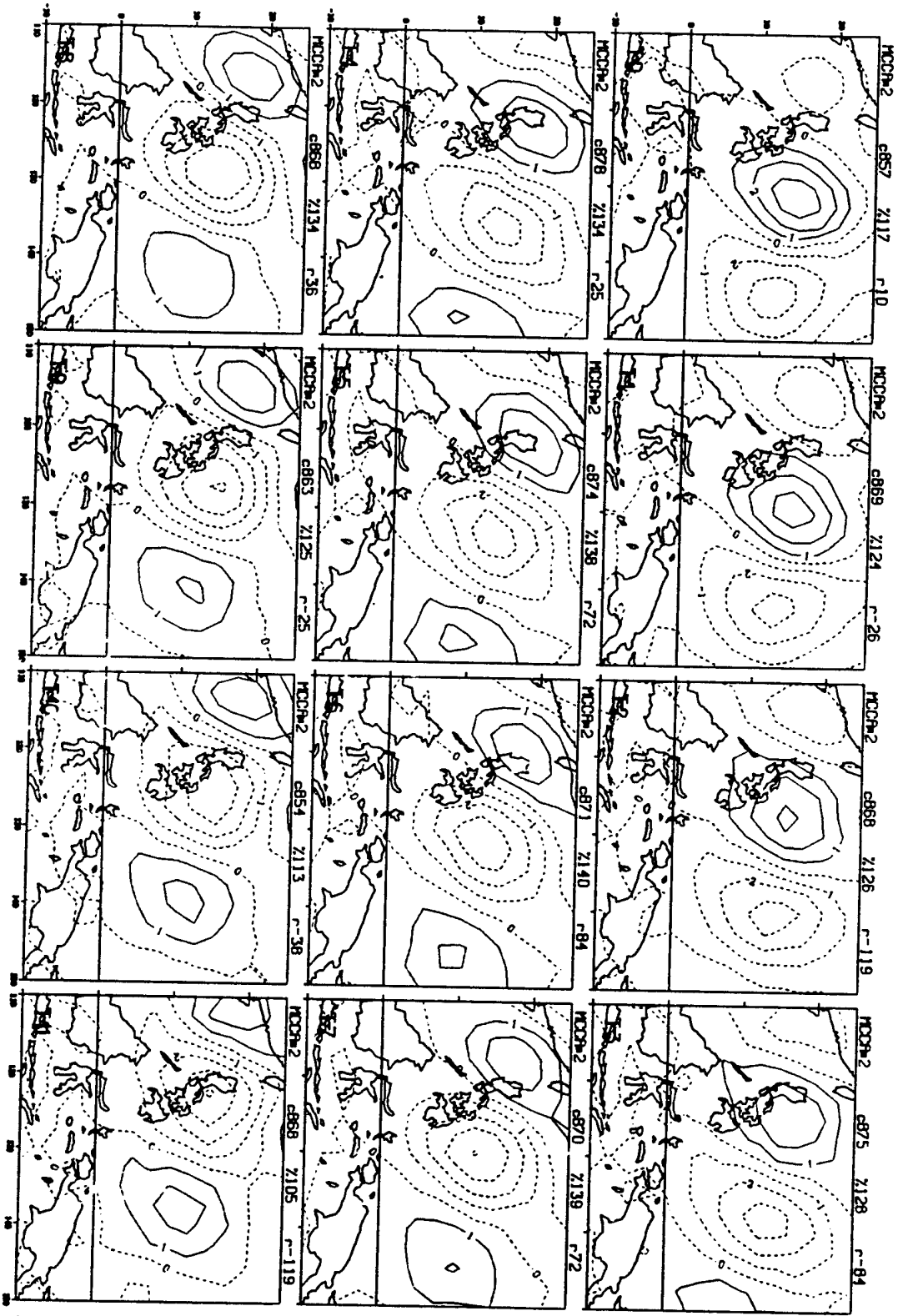

Figure 2b: Same as Figure 2a except for MCC mode#2

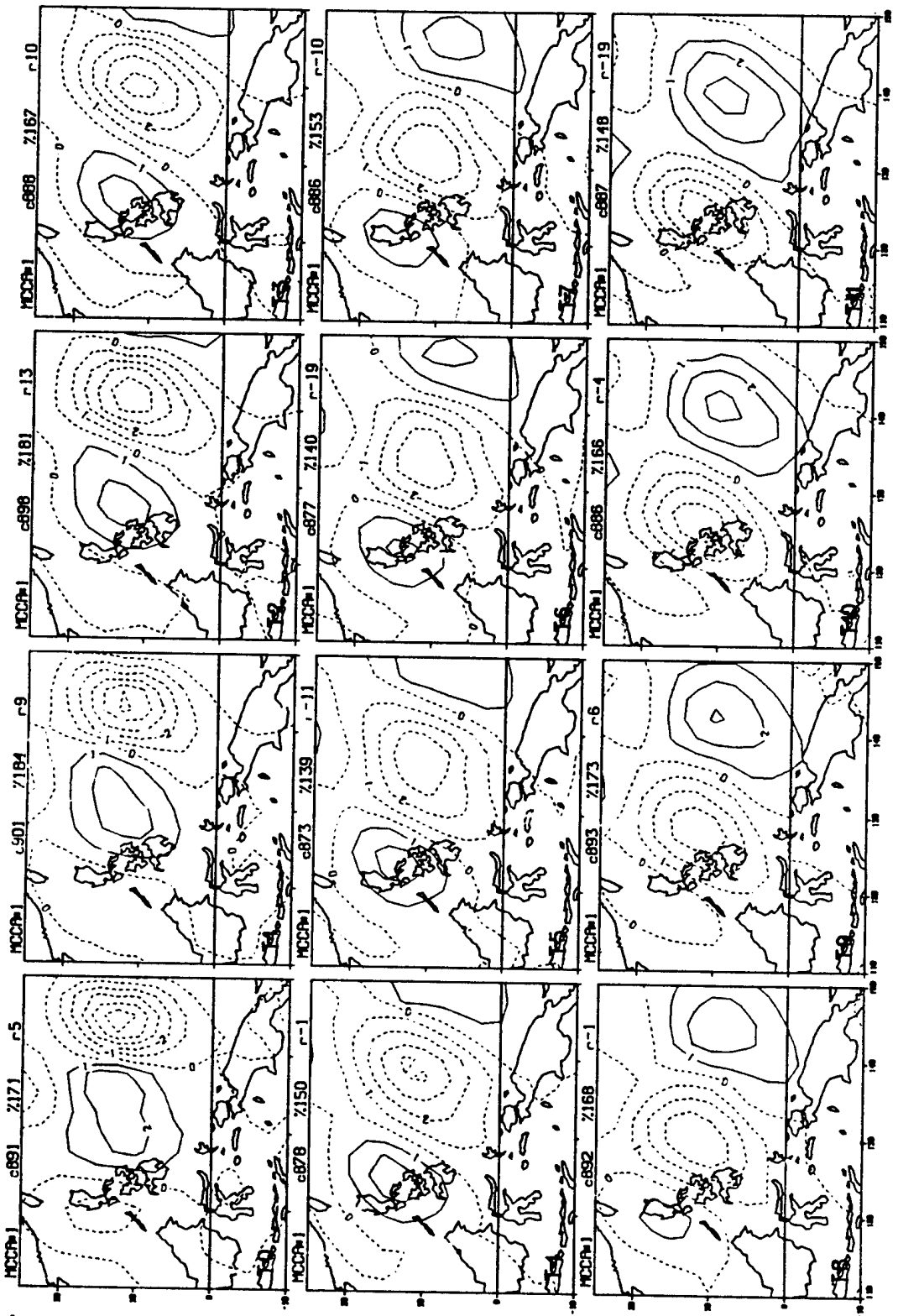

Figure 3a: Same as Figure 2 except for Group A MCC mode#1

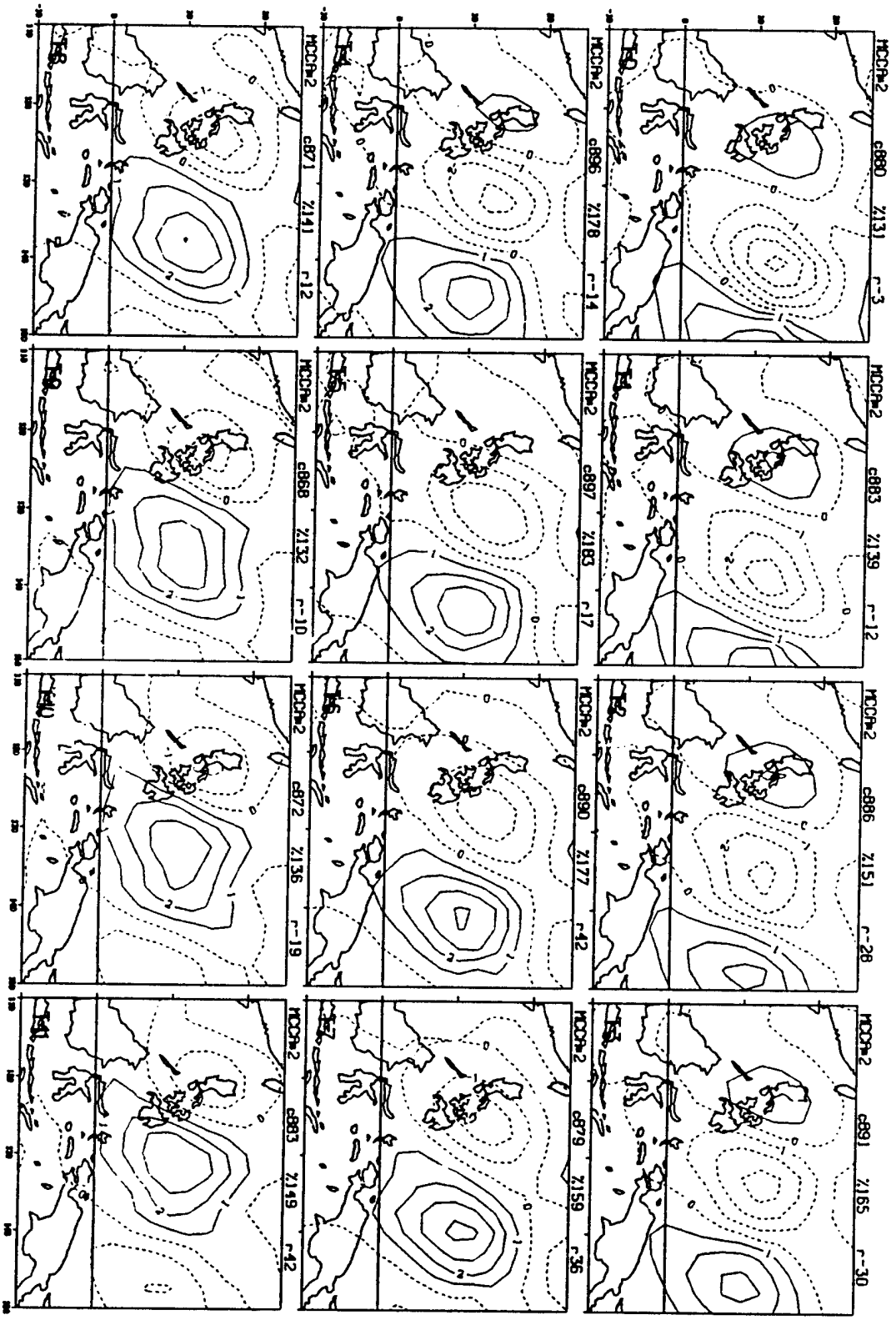

Figure 3b: Same as Figure 2 except for Group A MCC mode#2

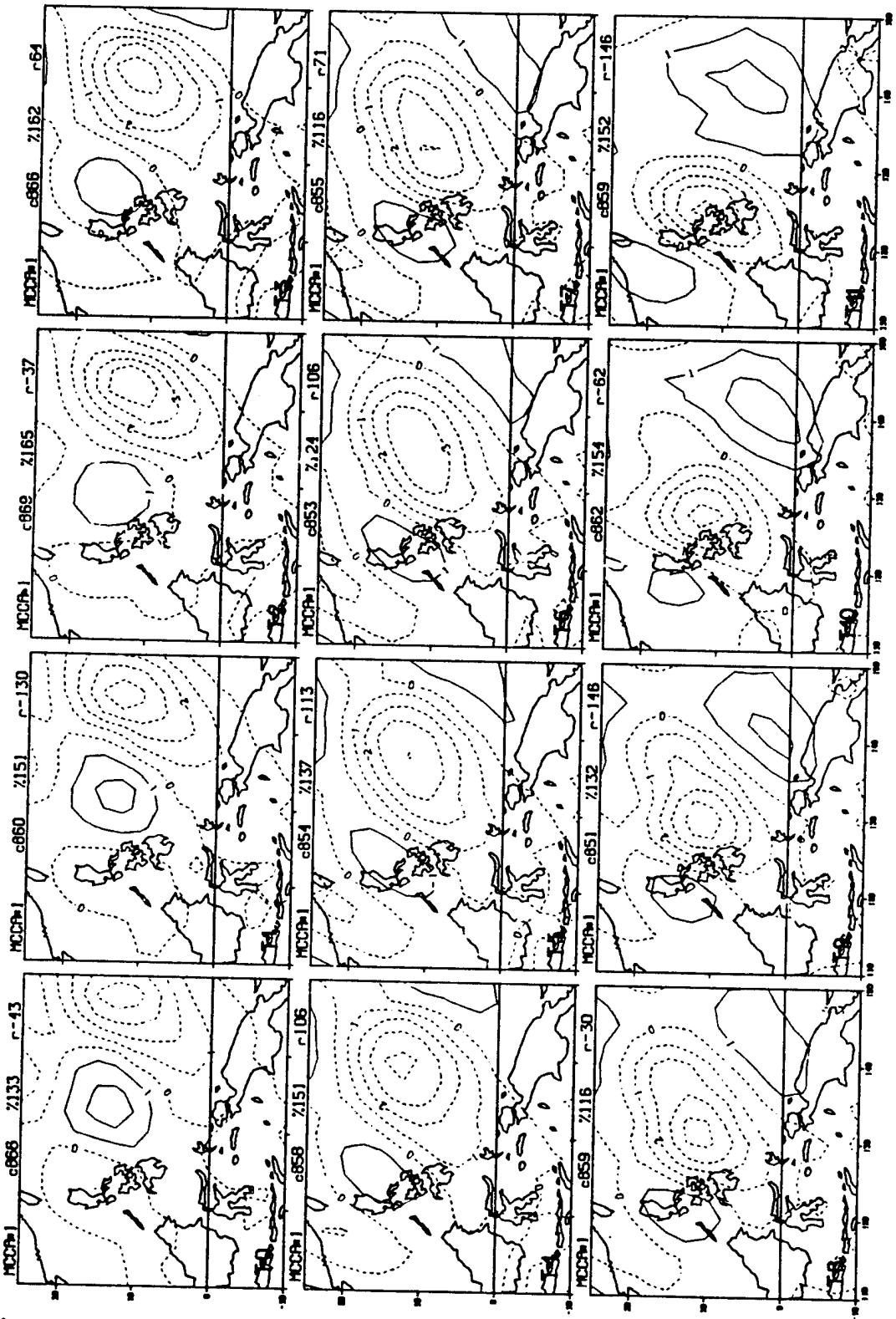

Figure 4a: Same as Figure 2 except for Group B MCC mode#1

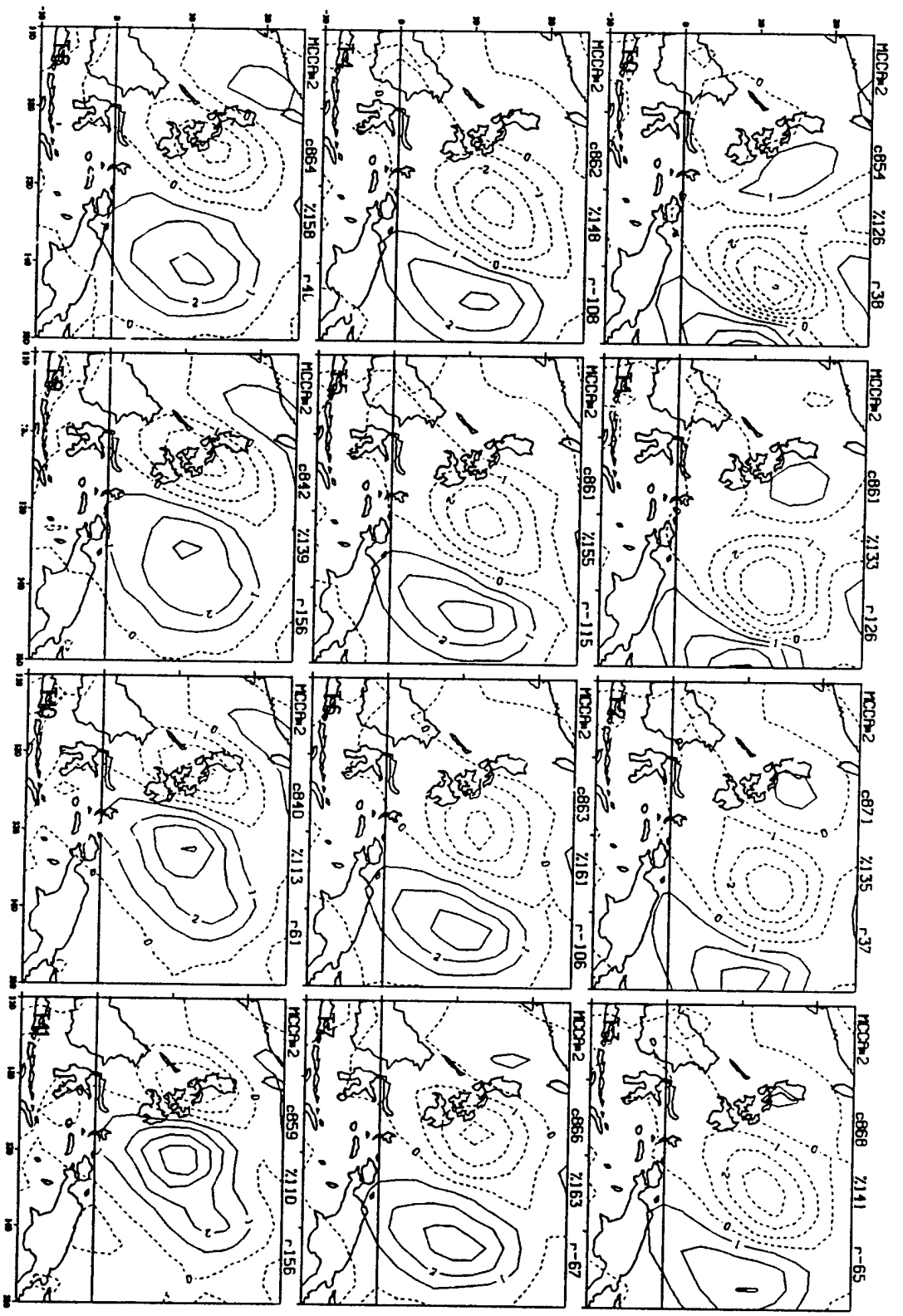

Figure 4b: same as Figure 2 except for Group B MCC mode#2

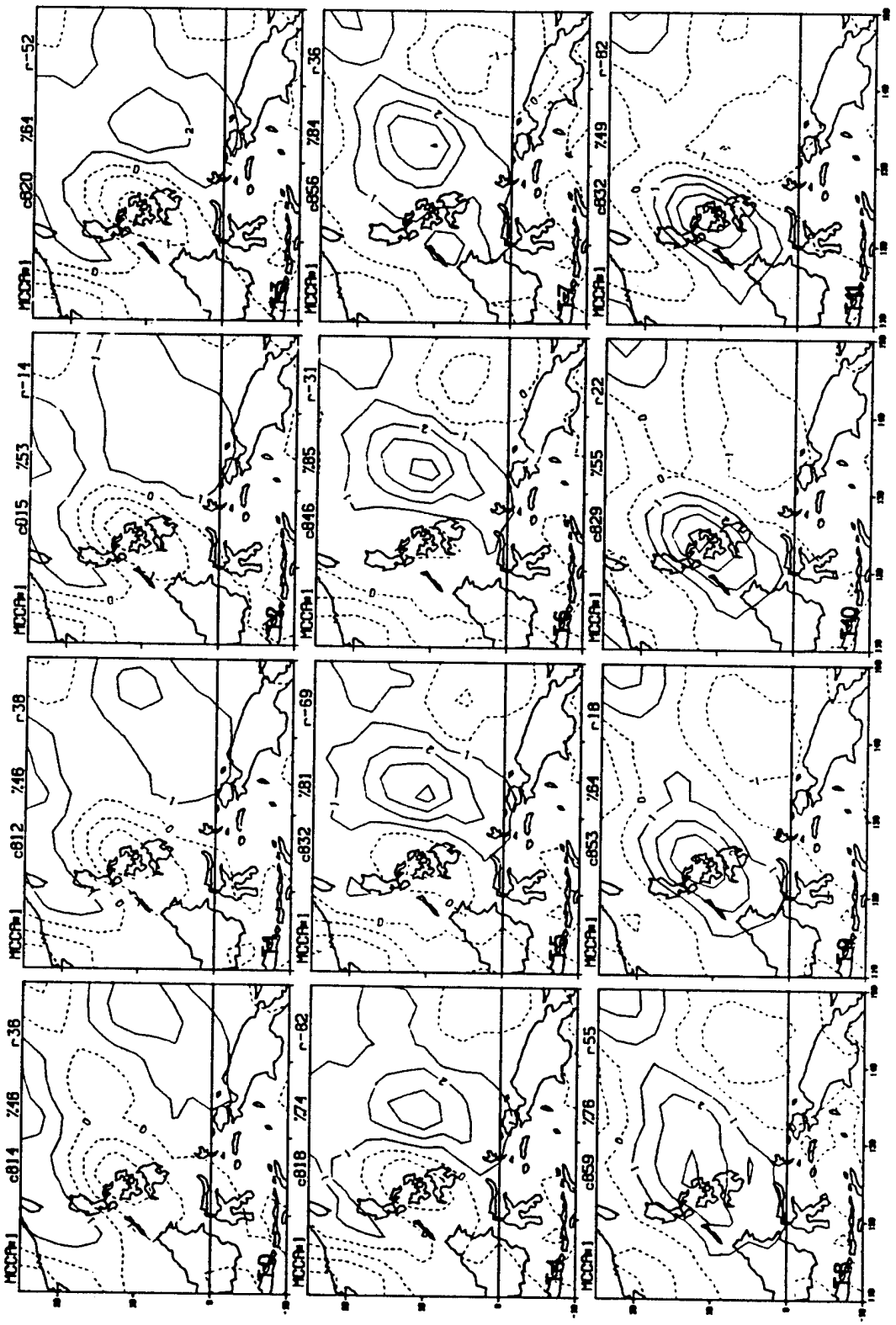

Figure 5a: Same as Figure 2 except for Group C MCC mode#1

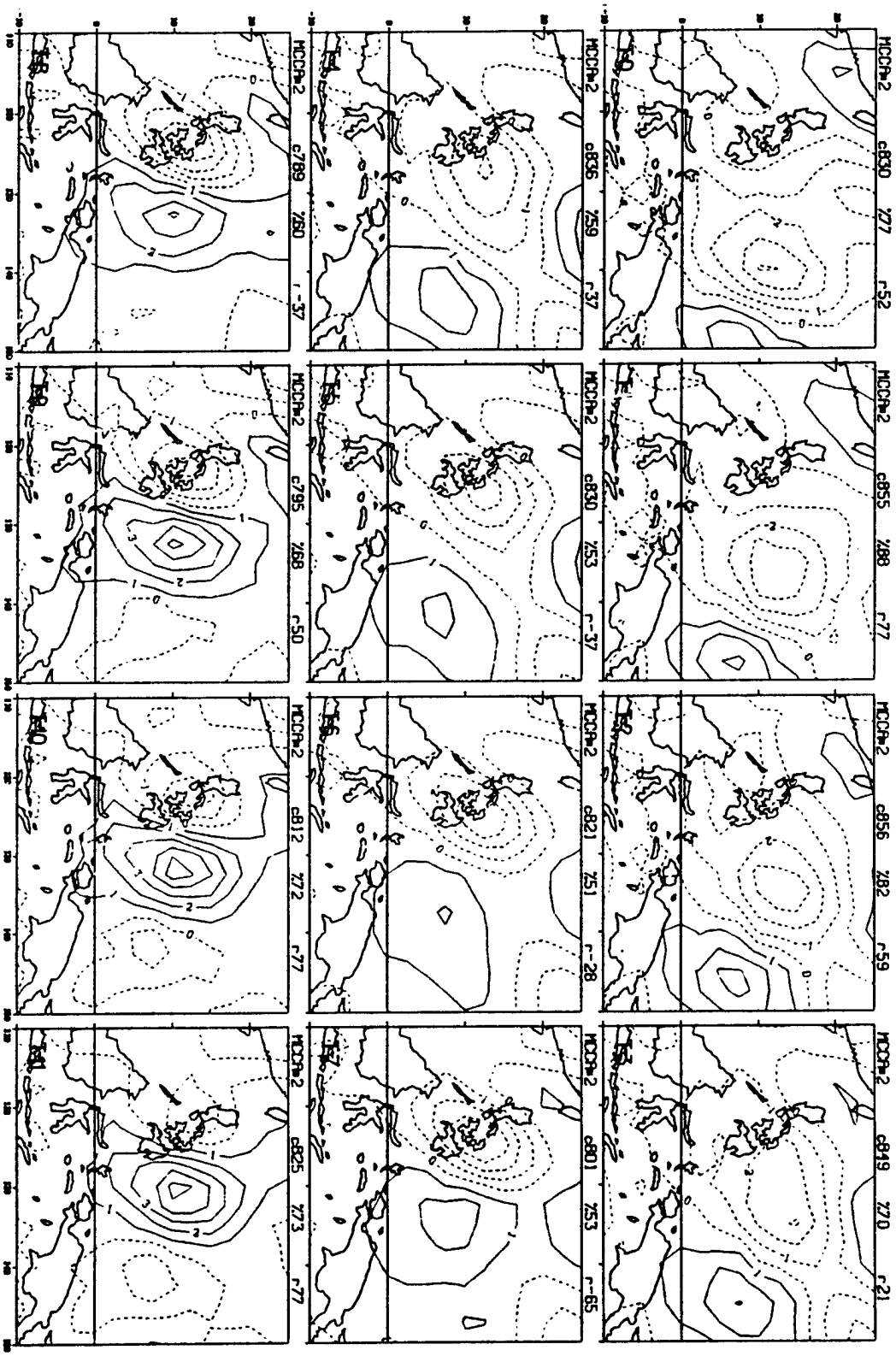

Figure 5b: Same as Figure 2 except for Group C MCC mode#2

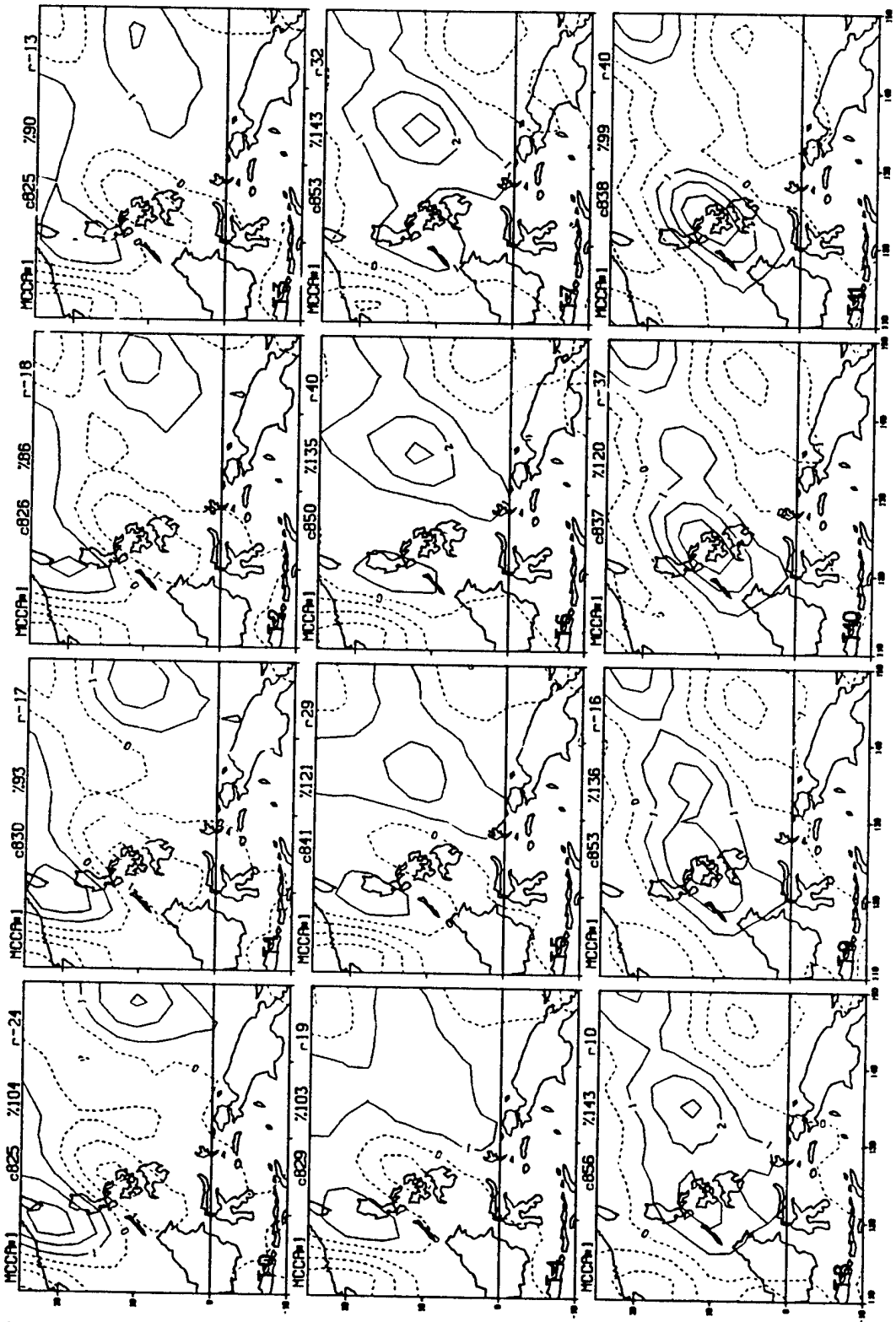

Figure 6a: Same as Figure 2 except for Group CC MCC mode#1

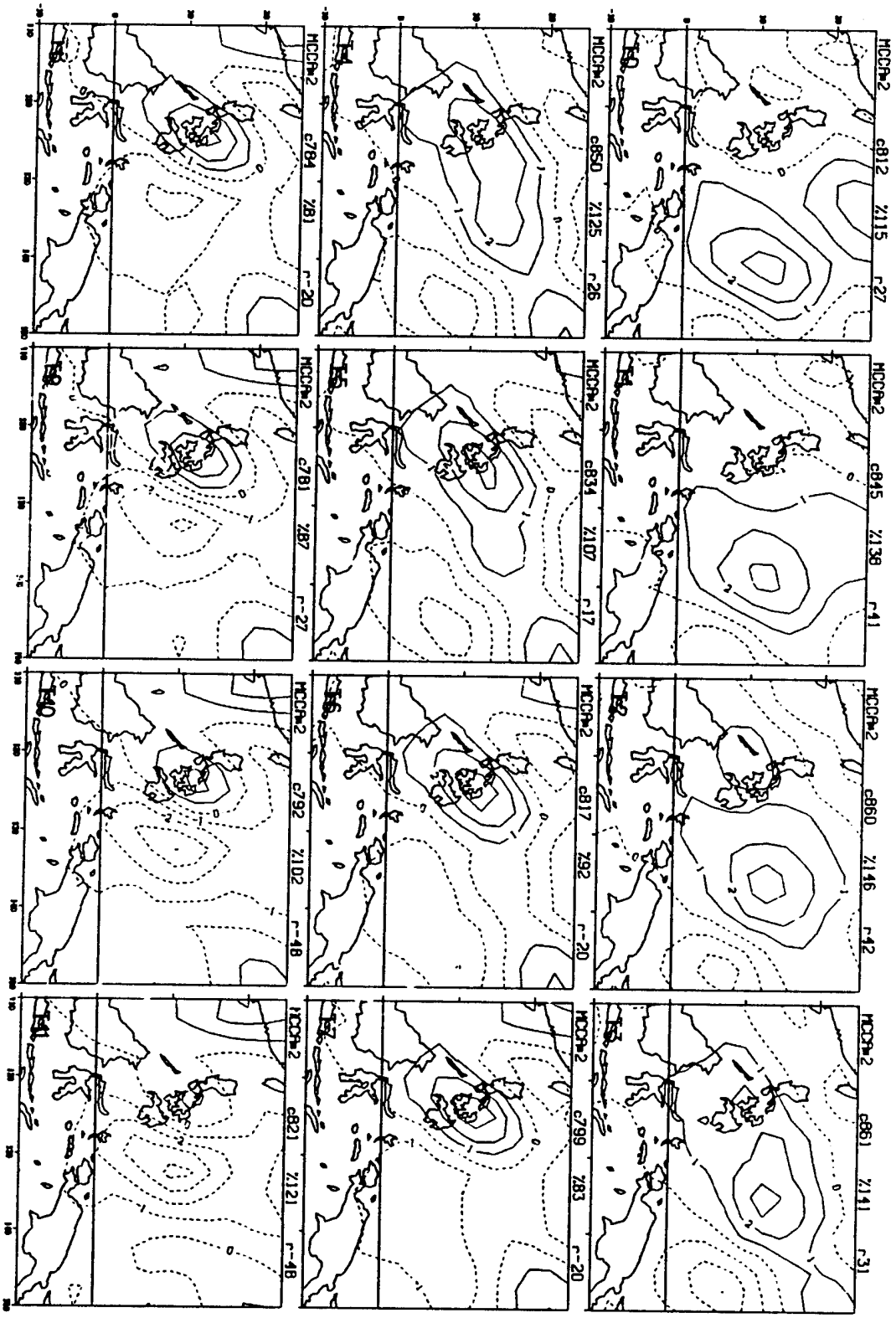

Figure 6b: Same as Figure 2 except for Group CC MCC mode#2

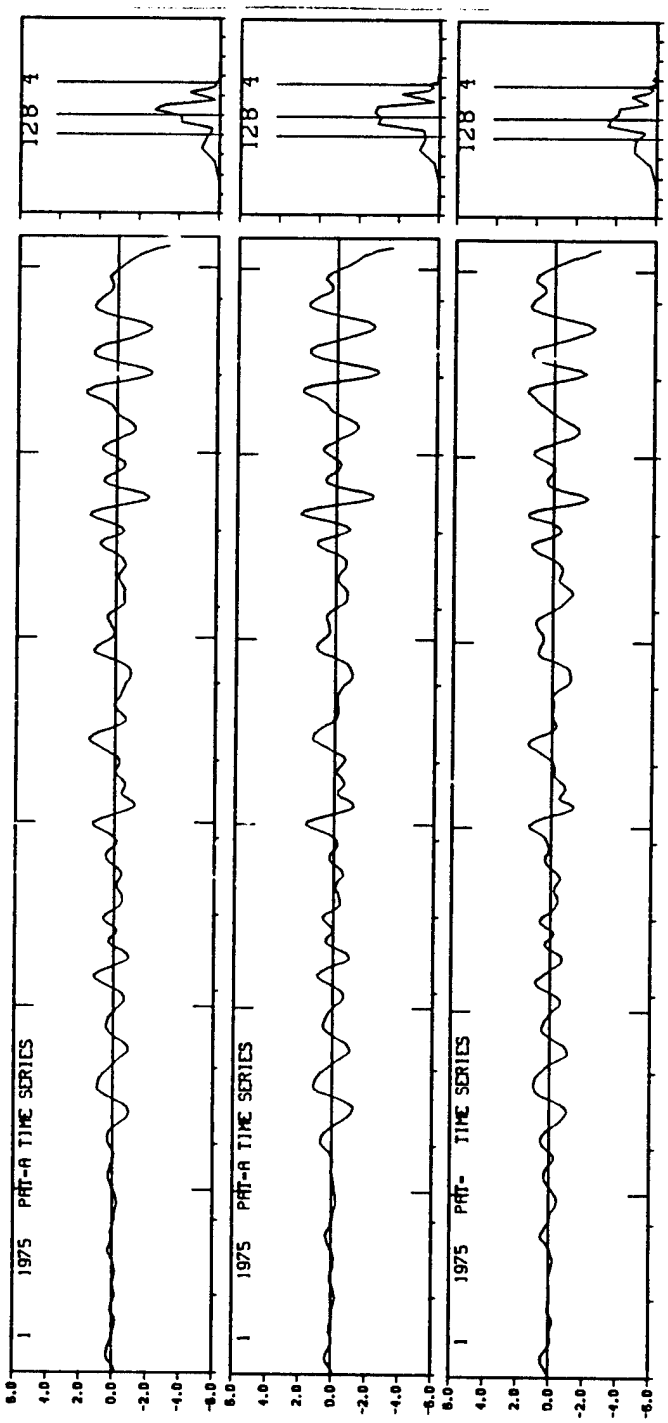

Figure 7a: Time series of time-integrated amplitude coefficients of MCC mode#1 for the 1975(May-October). Top panel shows 15Y, Group and individual years respectivity. Power spectrum of the time series is shown at right

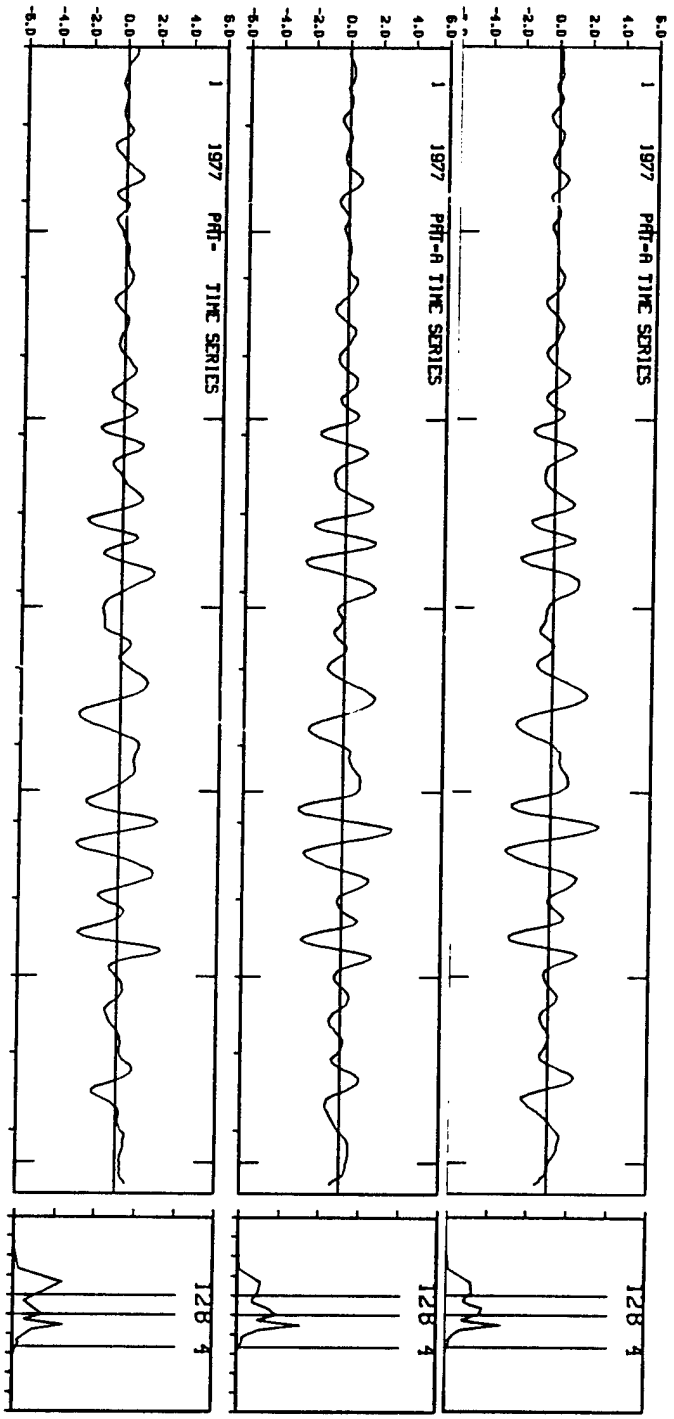

Figure 7b: Same as Figure 7a except for year 1977

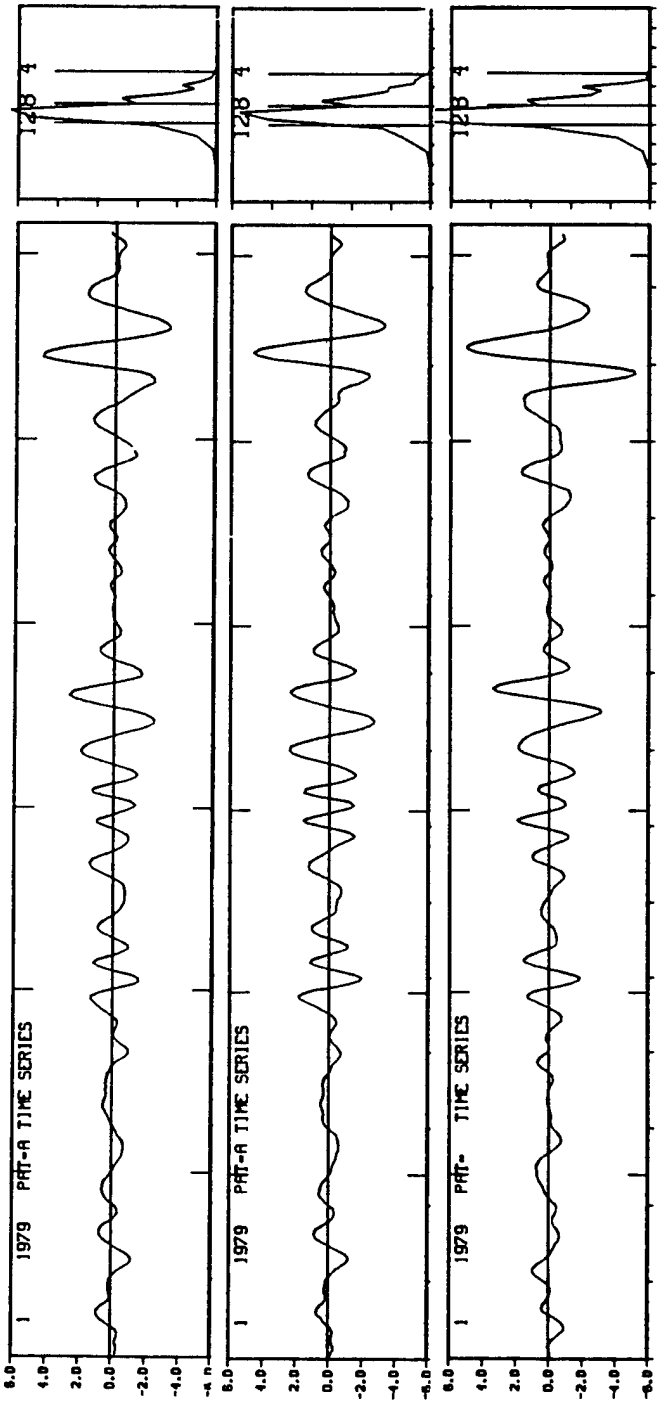

Figure 7c: Same as Figure 7a except for the year 1979

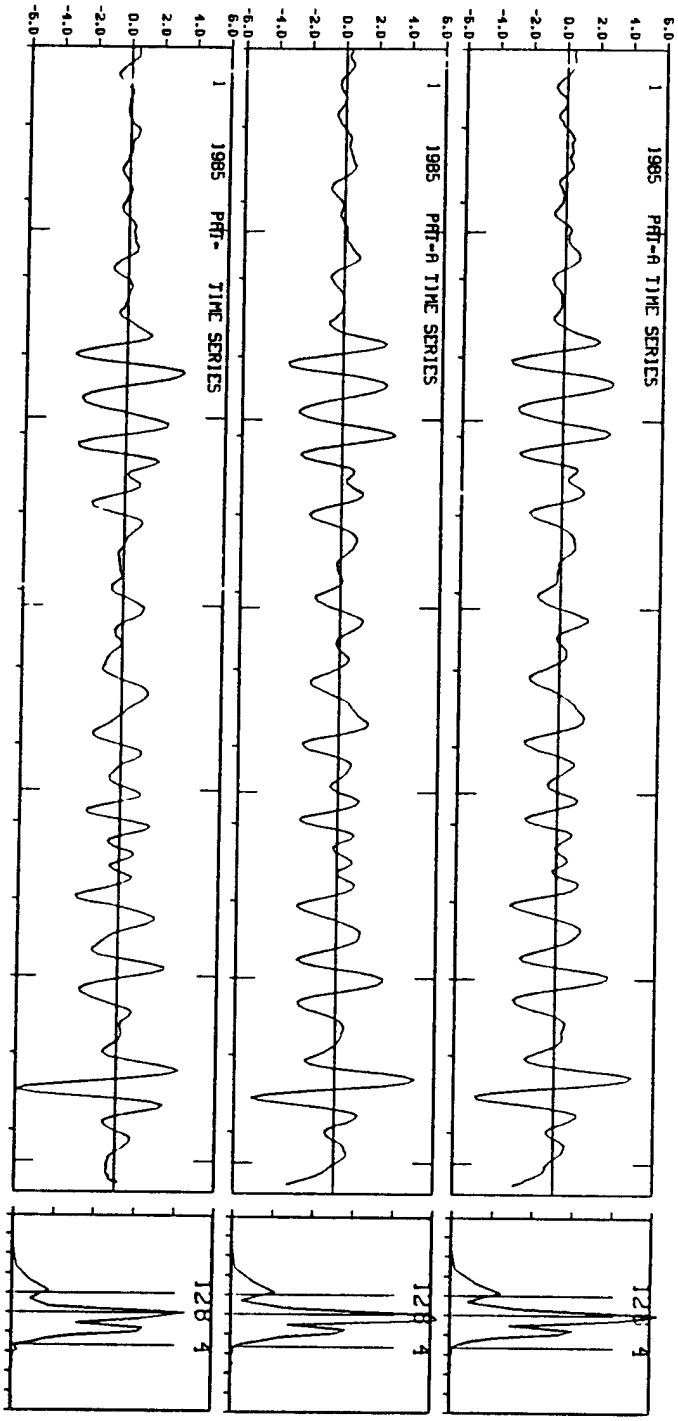

Figure 7d: Same as Figure 7a except for the year 1985

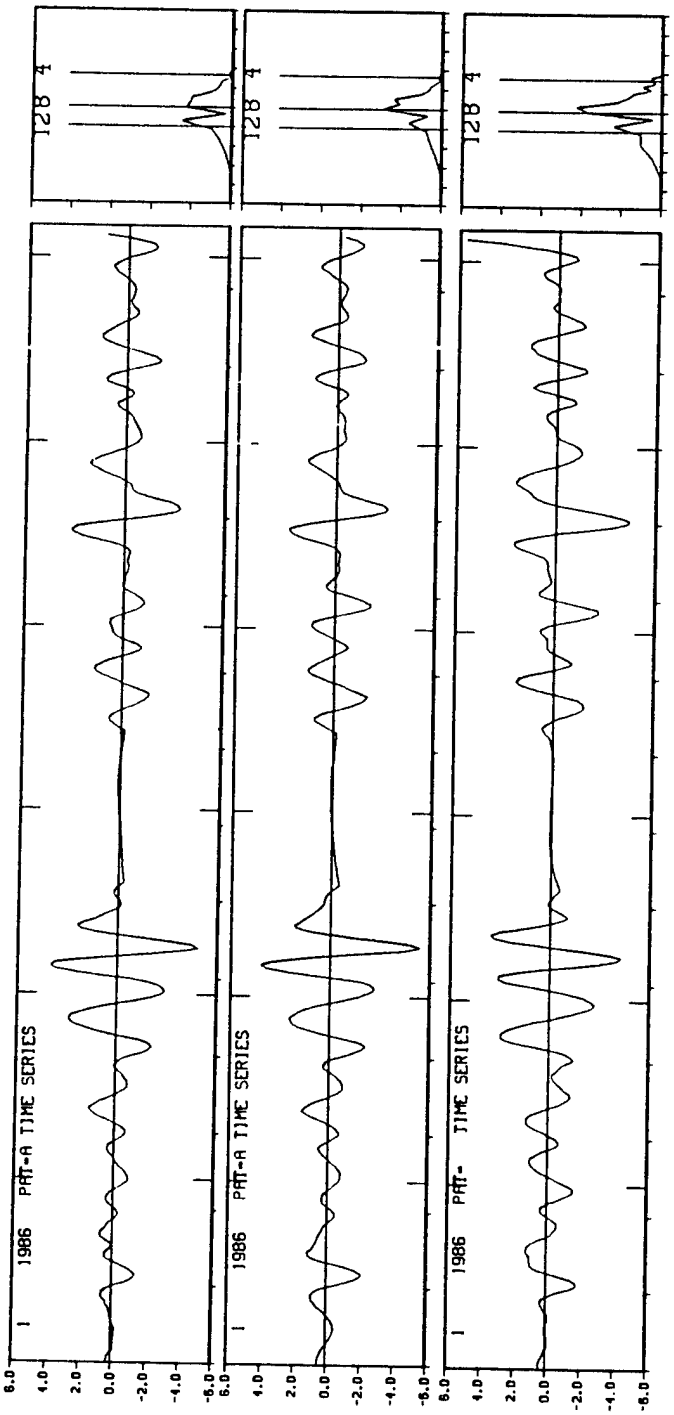

Figure 7e: Same as Figure 7a except for the year 1986

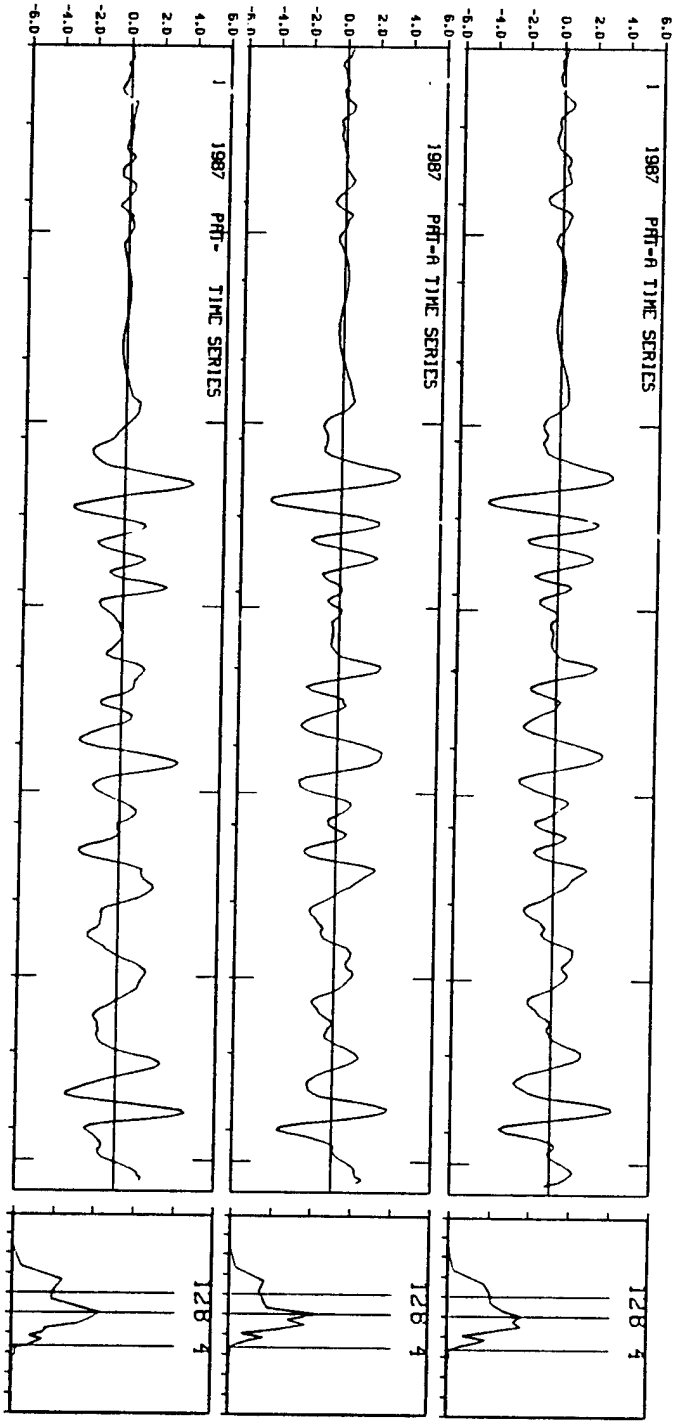

Figure 7f: Same as Figure 7a except for the year 1987

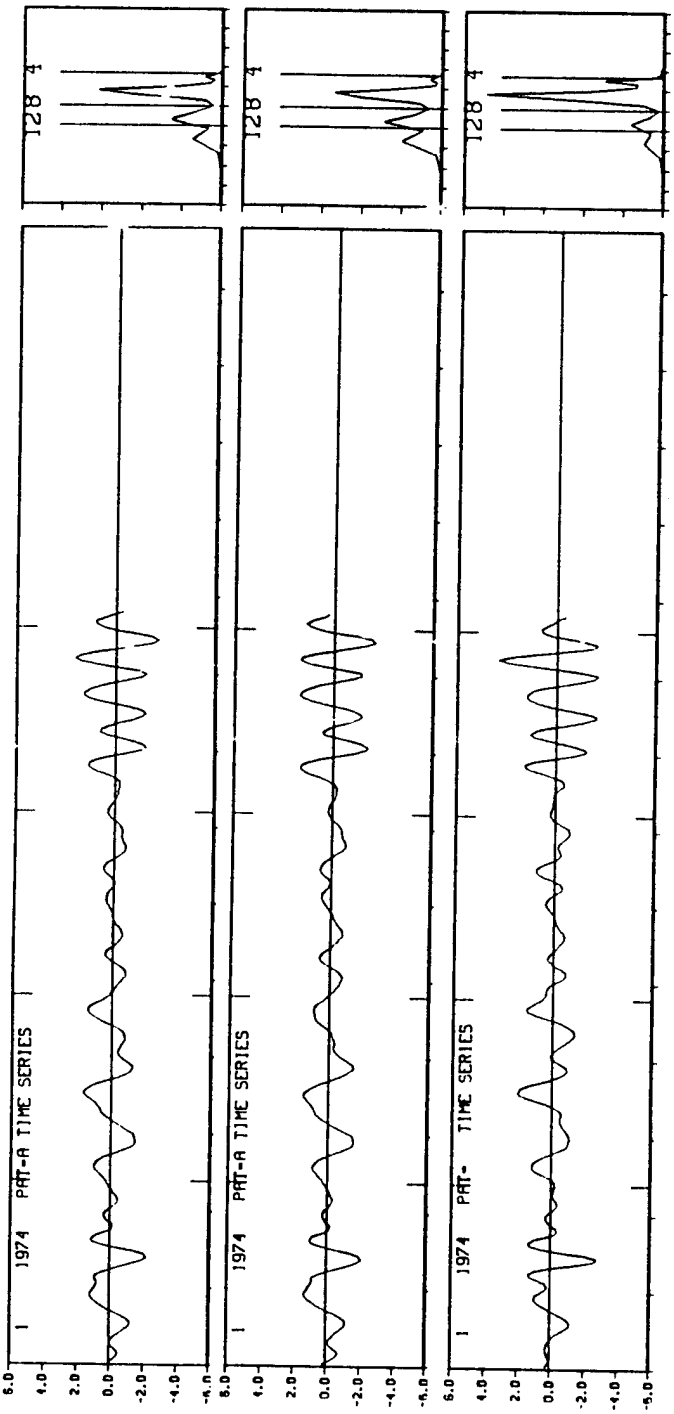

Figure 8a: Same as Figure 7a except for the year 1974

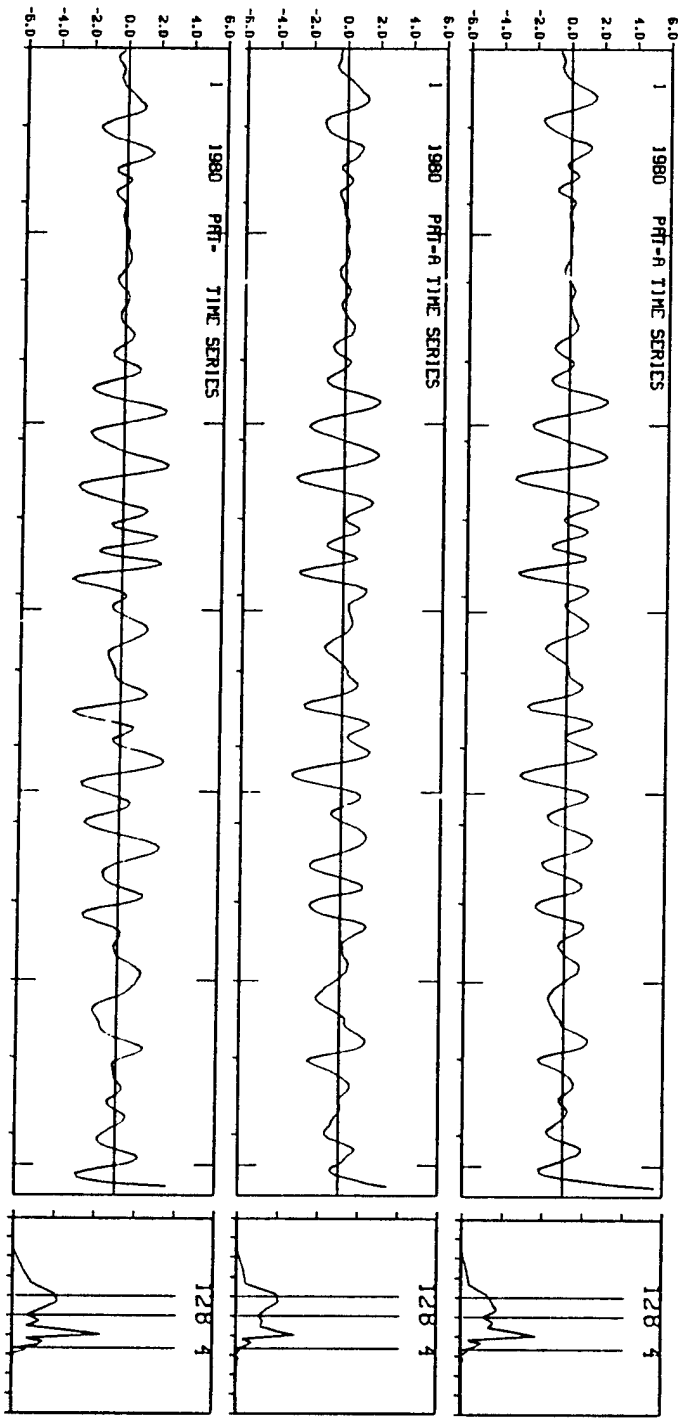

Figure 8b: Same as Figure 7 except for the year 1980

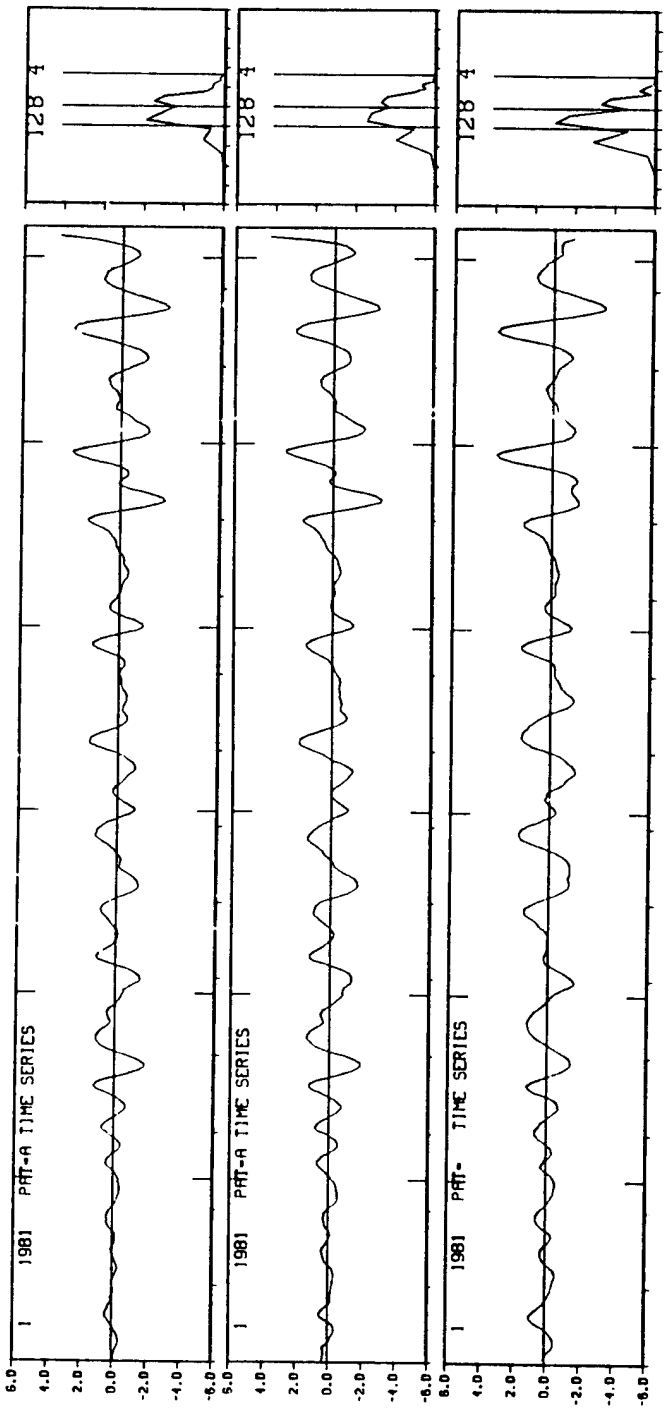

Figure 8c: Same as Figure 7 except for the year 1981

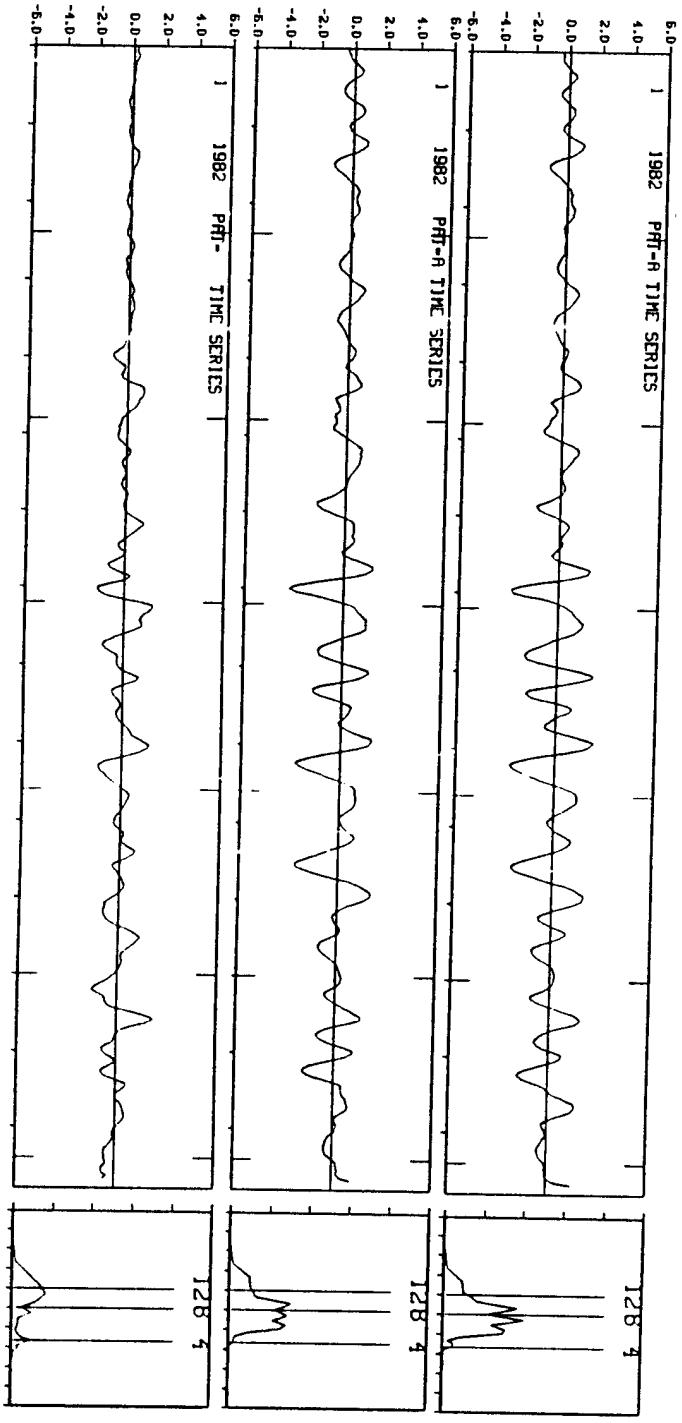

Figure 8d: Same as Figure 7 except for the year 1982

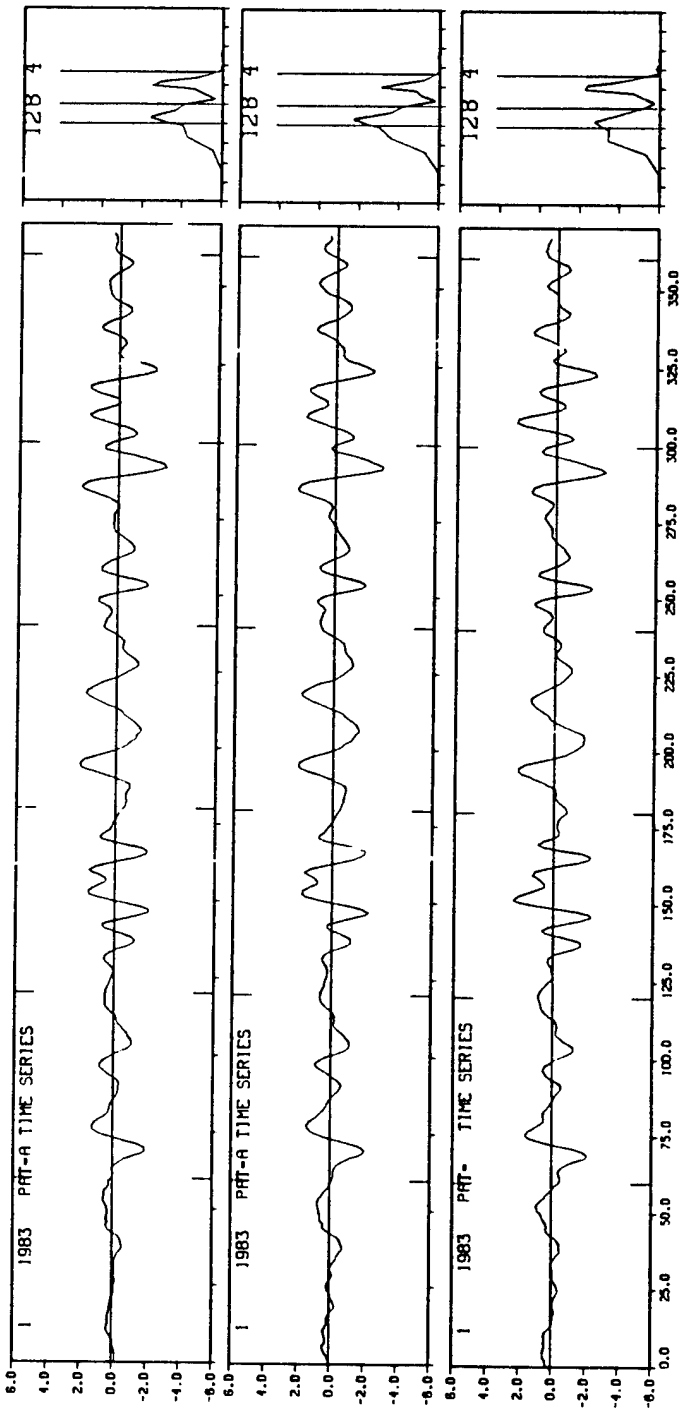

Figure 8e: Same as Figure 7 except for the year 1983

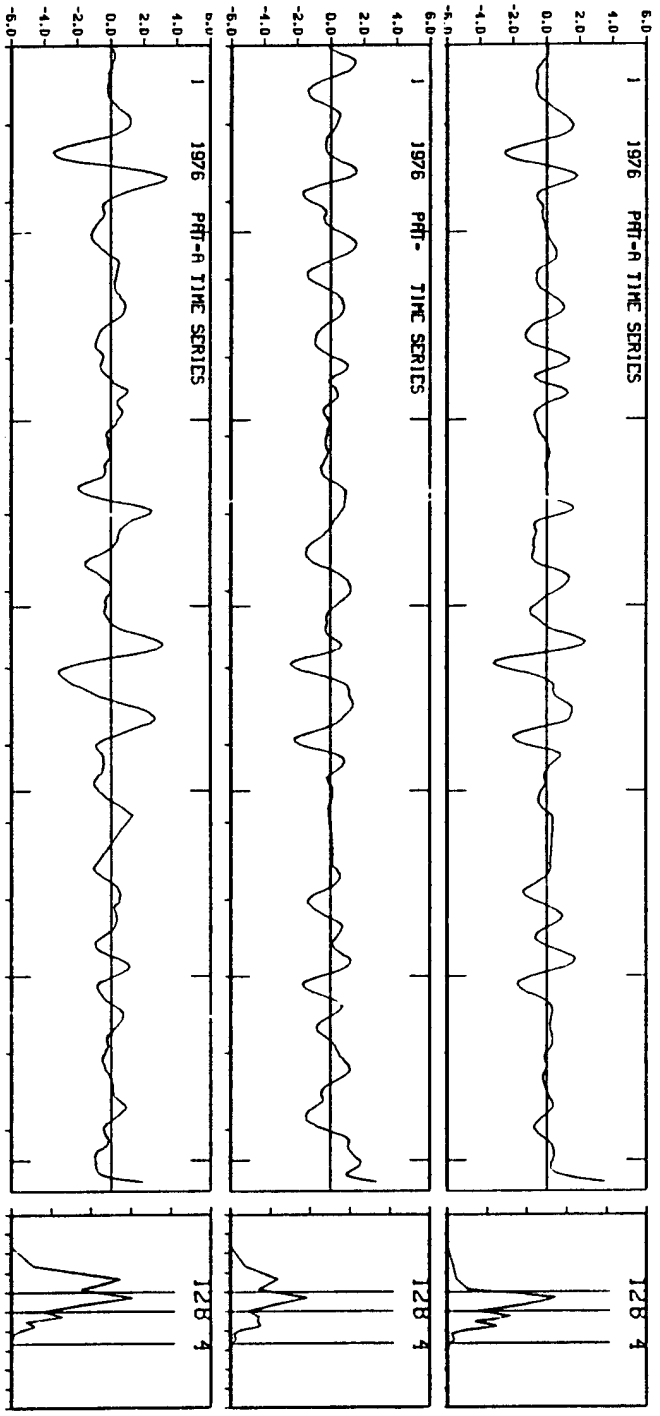

Figure 9a: Same as Figure 7 except for the year 1976

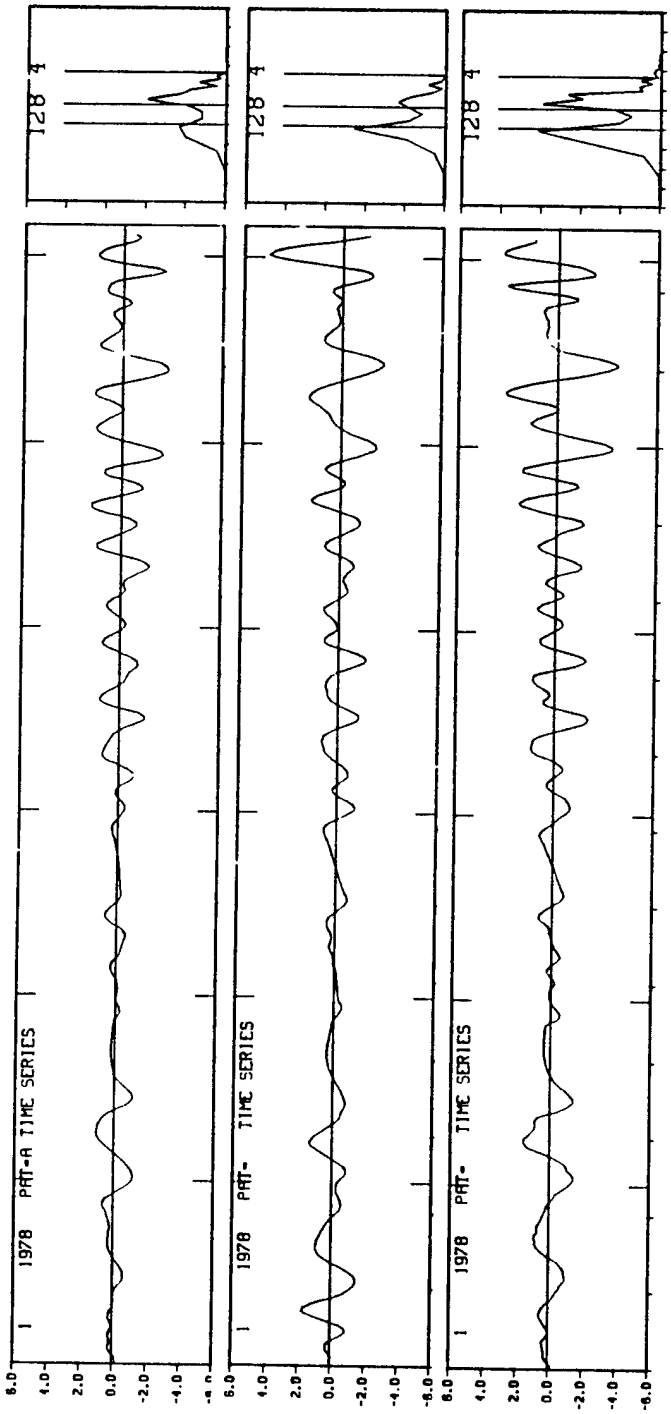

Figure 9b: Same as Figure 7 except for the year 1978

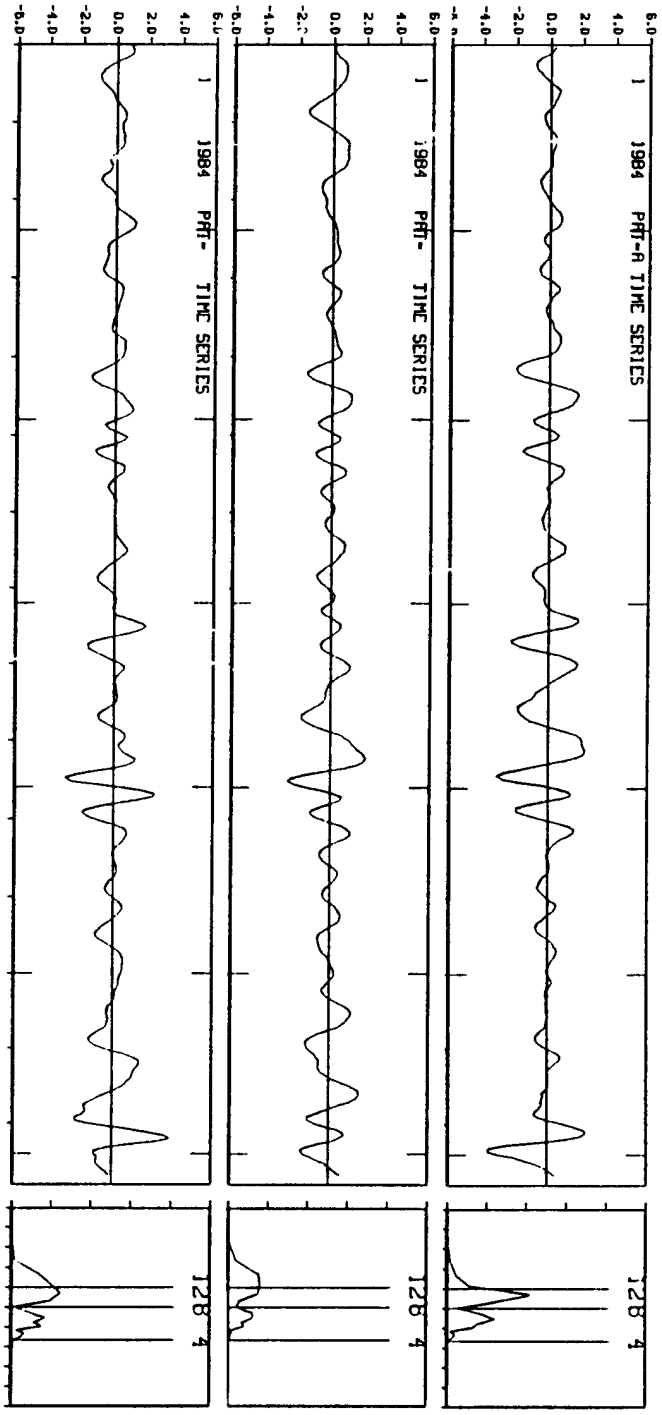

Figure 9c: Same as Figure 7 except for the year 1984

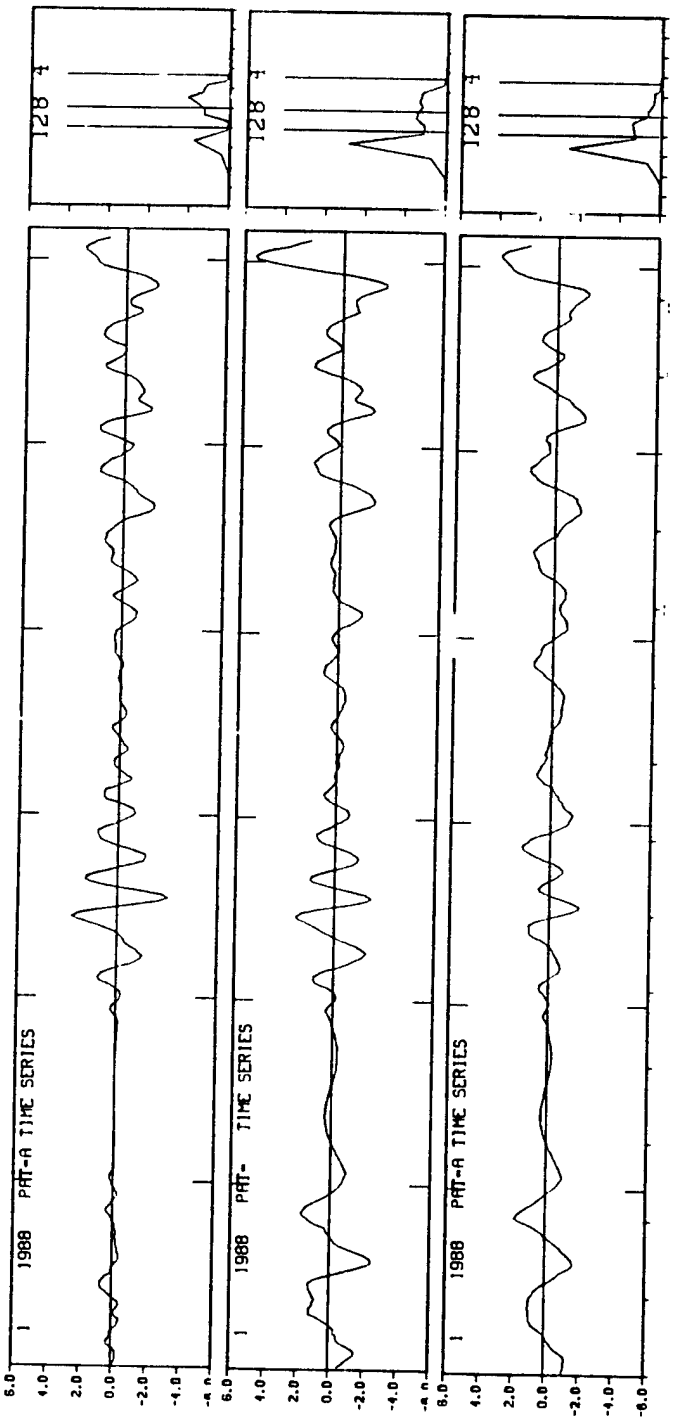

Figure 9d: Same as Figure 7 except for the year 1988

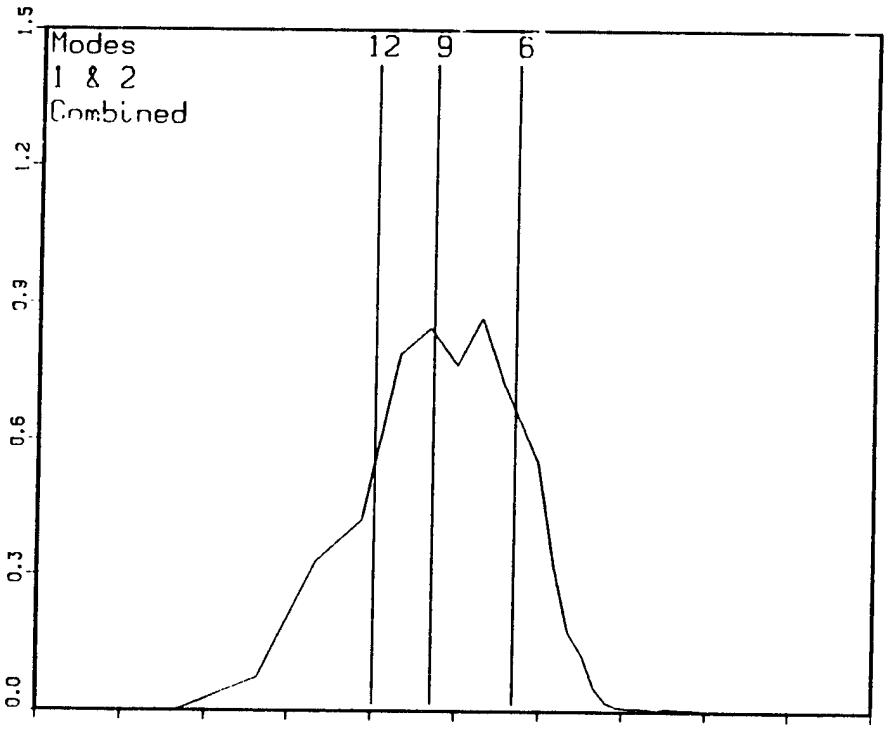

Figure 10a: Composite power spectrum for 15Y MCC mode#1 and #2 combined.

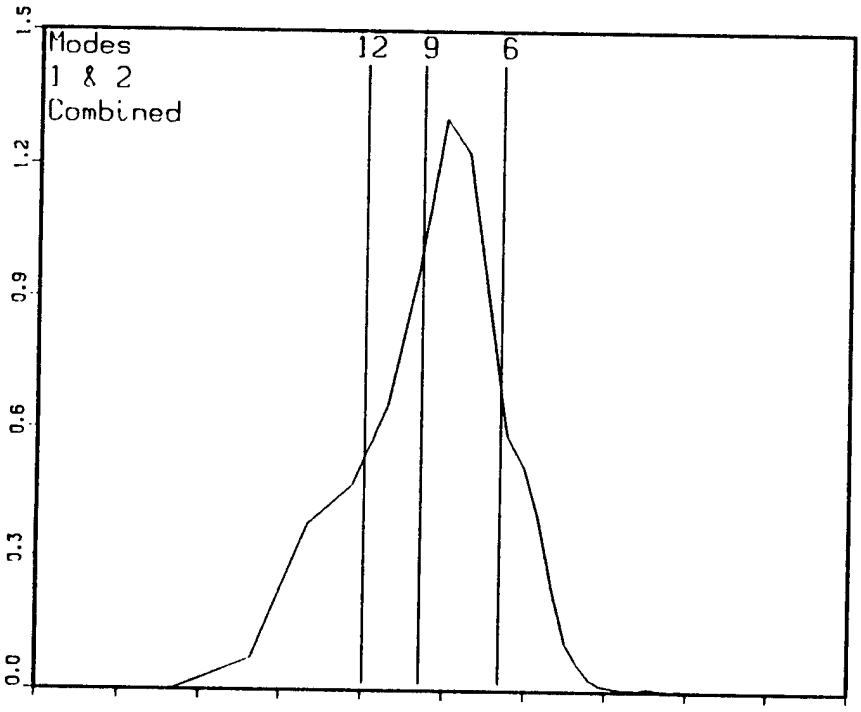

Figure 10b: Same as Figure 10a except for Group A

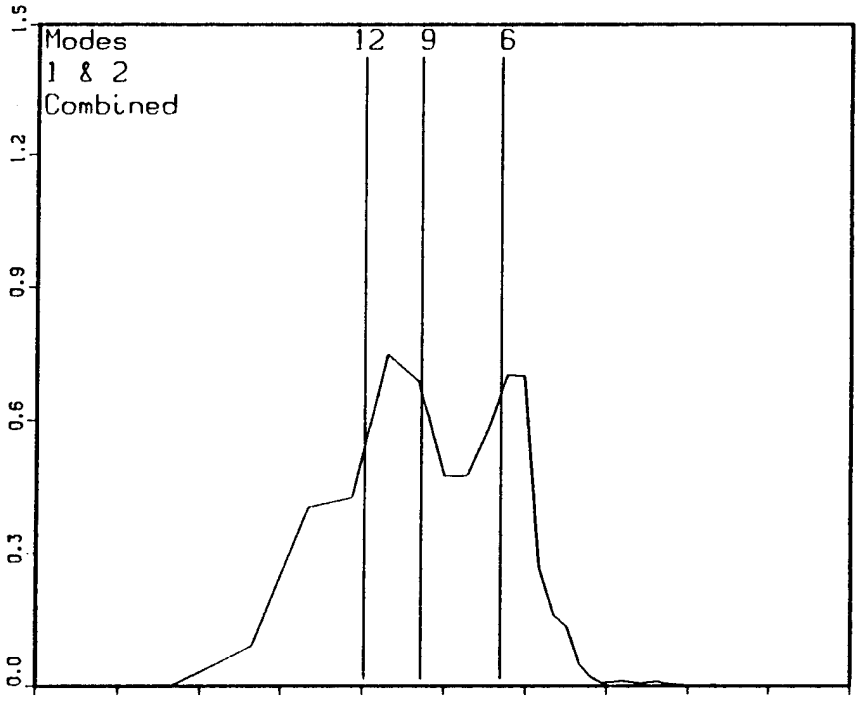

Figure 10c: Same as Figure 10a except for Group B

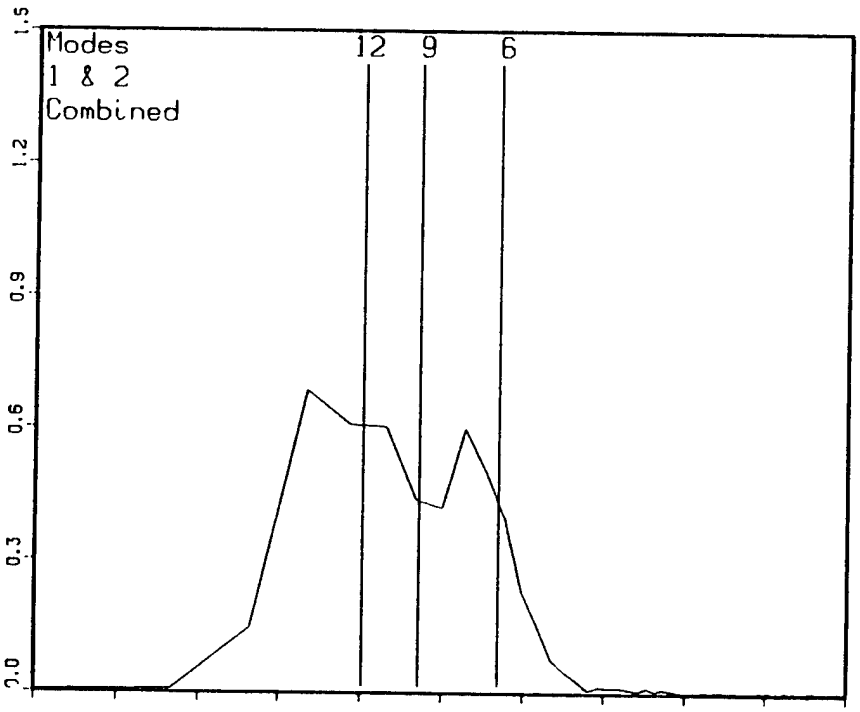

Figure 10d: Same as Figure 10a except for Group C

IV. ONE-POINT CORRELATIONS

The spatial patterns of this mode over the larger domain (70°E-180°, 20°S-40°N) in the meridional (v) and zonal (u) wind components at three levels, sfc, 700 hPa, and 200 hPa, are determined by the single-point correlation between these fields and the time-integrated amplitude coefficient of mode 1. Fig. 11 shows the correlation patterns of v_{sfc} with the 15Y mode 1, at lags 0 and 4 days, respectively. Here all 15 years of data are used. Since the MCC modes are calculated based on v_{sfc}, the correlation pattern at zero lag closely resembles the structure of mode 1 shown in Fig. 2.

Chang et al. (1995) demonstrated that the northwestward propagating wave patterns are correlated with occurrence of tropical cyclones for the 1989-1991 summers of NOGAPS data. Adopting their method, the possible relationship between the propagating waves and tropical cyclone activities may be examined by comparing the time series of the time integrated wave amplitudes and typhoon occurrences. From the top panels of Figs. 7-9, the times of large-amplitude wave activities for the 15Y mode 1 are determined to compare with tropical cyclone activities. This is done by identifying the time of the maximum and minimum points for several phases of the disturbances when the time-integrated disturbance amplitude exceeds 1.5 m/s and then correlate it with the location of tropical cyclone centers as reported by the Joint Typhoon Warning Center (JTWC), Guam. These locations of tropical cyclone centers at maximum amplitude times of mode 1 are plotted against the v_{sfc}-mode 1 correlation map at phases T0 and T4 days (Fig. 11). For each phase the majority of the cyclone centers are concentrated in a region to the west of positive cells,

where the main positive dv/dx wave axis as defined by the correlation pattern is located. The clustering of tropical cyclone centers near this axis indicates a strong relationship between the main wave pattern in the core domain and the circulations of the tropical cyclones. This relationship is clearest in the western Pacific east of the Philippines, but it also holds in the northwest corner of the core domain near the southern China coast and the northern South China Sea.

Since the tropical Global Band data contain bogussed tropical cyclone vortices at the surface, it is conceivable that the good correspondence between the tropical cyclone locations and the wave pattern is due to the bogussed data. However, the wave pattern describes a much larger spatial scale than the bogussed vortices. The bogussed tropical cyclones are not applied to other levels, and the objective analysis scheme is two-dimensional only, so the correlation map for v_{700} provides information that is independent of the bogus data. Fig. 12 shows the correlation map of v_{700} with the 15Y mode 1 phases T0 and T4, respectively, for the entire 15 years. It is readily seen that the northwestward wave pattern is approximately reproduced in this Figure, and is nearly in-phase with the v_{sfc} maps. The maximum correlation coefficient is around 0.3-0.4, which is only slightly below the v_{sfc} values. Therefore, the wave pattern is contained in the v_{700} data and not just an artifact of the bogussing procedure.

The v_{200} - 15Y mode 1 correlation patterns for T0 and T4 are shown in Fig. 13. The maximum correlation values of around 0.1 are very small. Nevertheless, the correlation pattern appears to be organized and consistent with the low-level patterns. The T0 phase (Fig. 13a) appears to be one quarter cycle out of phase with the v_{sfc} (Fig. 11a), with

the cells tilted forward (northwestward). The T1 phase (Fig. 13b) appears to be half a cycle out of phase with the v_{sfc} (Fig. 11b). The weak correlation and somewhat different phase differences from v_{sfc} makes the v_{200} correlation patterns only marginally useful, indicating only a possibility that there is an out-of-phase structure contained in the v_{200} data.

The 15Y correlation patterns and the tropical cyclone location relationships suggest that the 8-day northwestward wave patterns, during large amplitude fluctuations, appear to be a manifestation of the tropical cyclone activities. It would be interesting to see how this organization of the wave pattern may appear in the different groups that were categorized according to the single-year MCC modes. In the ensuing Figures, we compare the tropical cyclone locations with the timing of the large amplitude group MCC mode 1, and plot them on the v_{sfc} correlation maps for each of the three groups. For each group, only the data within the years belonging to that group are used.

Fig. 14 shows the v_{sfc} - group A mode 1 correlation patterns, with the tropical cyclone locations plotted in the phase T0 and T4 maps, respectively. Here the tropical cyclone locations are also lined up in the positive dv/dx axis in the western Pacific, although for the cell near the northwestern corner of the core domain, which partially covers the southern China coast, the distribution of the tropical cyclones is more scattered within the positive cell. The maximum correlation at v_{sfc} is between 0.4-0.5, which is slightly higher than the 15Y results shown in Fig. 11. The group A v_{700} correlation patterns are shown in Fig. 15. There is again a nearly in-phase relationship with the v_{sfc}, and the maximum correlations of between 0.4-0.5 are again slightly higher than the 15Y results. The group A v_{200}

correlation map (Fig. 16) also shows a weak but organized pattern, in this case both T0 and T4 are half a cycle out-of-phase with v_{sfc}. The maximum correlation values are 0.1-0.2, again slightly higher than those shown for 15Y. As group A includes the six years with the most organized wave pattern, it is not surprising that the correlation values are slightly higher and that the v_{200} patterns are more consistent.

Fig. 17 shows the v_{sfc} - group B mode 1 correlation patterns, with the tropical cyclone locations plotted in the phase T0 and T4 maps, respectively. The results are similar to those of group A, with maximum correlation around 0.4-0.5, and tropical cyclone locations concentrated in the positive dv/dx axis in the western Pacific. Near the northwestern corner of the core domain the tropical cyclone centers are again more scattered. The v_{700} correlation patterns (Fig. 18) are again in-phase with v_{sfc}, with maximum correlation values around 0.3-0.4, slightly less than group A and comparable to 15Y. The v_{200} correlation maps (Fig. 19) still show a weak but organized pattern with maximum values between 0.1-0.2. This pattern is roughly out-of-phase with low levels in the vicinity of the maximum correlation. Therefore, the five years in group B show the same organized wave patterns as group A.

The v_{sfc} correlation patterns for group C are shown in Fig. 20. The patterns are not as organized as the other two groups and resemble the 15Y patterns the least. At phase T0 (Fig. 20a), the maximum correlation is only 0.2, significantly lower than other groups. The distribution of tropical cyclone centers are also more scattered, although there is still some indication of preferred locations near the positive dv/dx axis. At phase T4, the maximum correlation reaches 0.4, which is comparable to 15Y, but the

tropical cyclone centers deviate more from the positive dv/dx axis, and are mostly scattered within the positive cell in the core domain. As found with other groups, the v_{700} correlation patterns (Fig. 21) show a nearly in-phase relationship with the major cells of v_{sfc}, but the maximum correlation drops to between 0.2-0.3. The v_{200} correlation patterns, shown in Fig. 22, completely lack organized wave cell patterns with randomly low correlations. Therefore, group C years show the least organized wave patterns.

We have previously noted that within group C, the 1978 single-year MCC modes 1-2 contain only 8% of the total variance, significantly below the 24-40% range of other years (Table 1). In order to find out whether the poor organization of the wave pattern in group C is mainly due to this anomalous year, the correlation maps are plotted for group CC, which excludes 1978 from group C. Figs. 23-25 show the group CC correlation maps for v_{sfc}, v_{700}, and v_{200}, respectively. In general, the organization (or lack of) of the patterns are similar to the group C results and are inferior to the other groups. The only significant difference occurs in v_{200} (Fig. 25). Here the northwestward propagating wave pattern is still missing, but along and north of 25°N (the northern boundary of the core domain) there appears to be a wave pattern with alternating signs. However, this looks distinctively unrelated to the low-level patterns and the correlations are very weak (0.1). Therefore, we can conclude that the four group C years are anomalous years, which do not show the clearly-organized wave patterns, and corresponding tropical cyclone activities, that appear in other years of the 15-year data set.

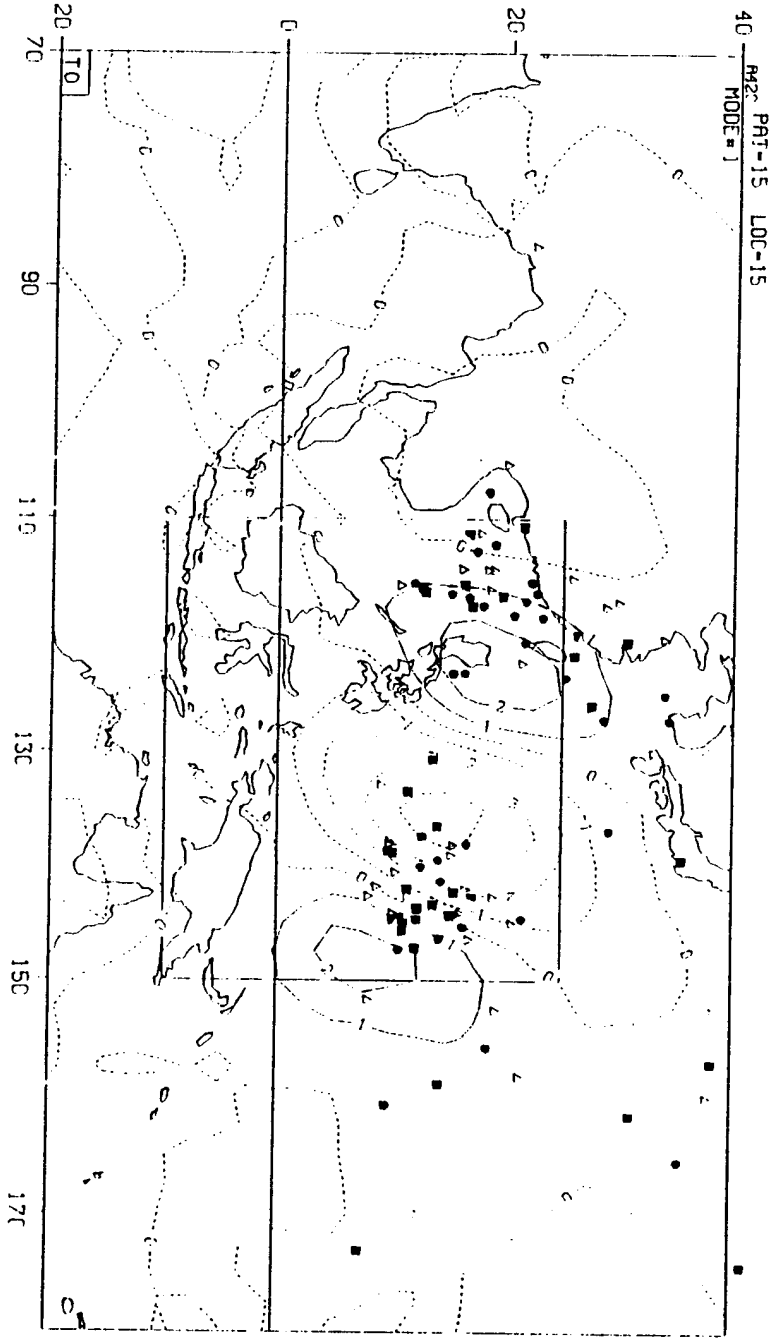

Figure 11a: Single point correlation patterns of vsfc with MCC mode#1, at lag 0 days and with the tropical cyclone position ploted. Contour interval is 0.1 and negative values are dashed

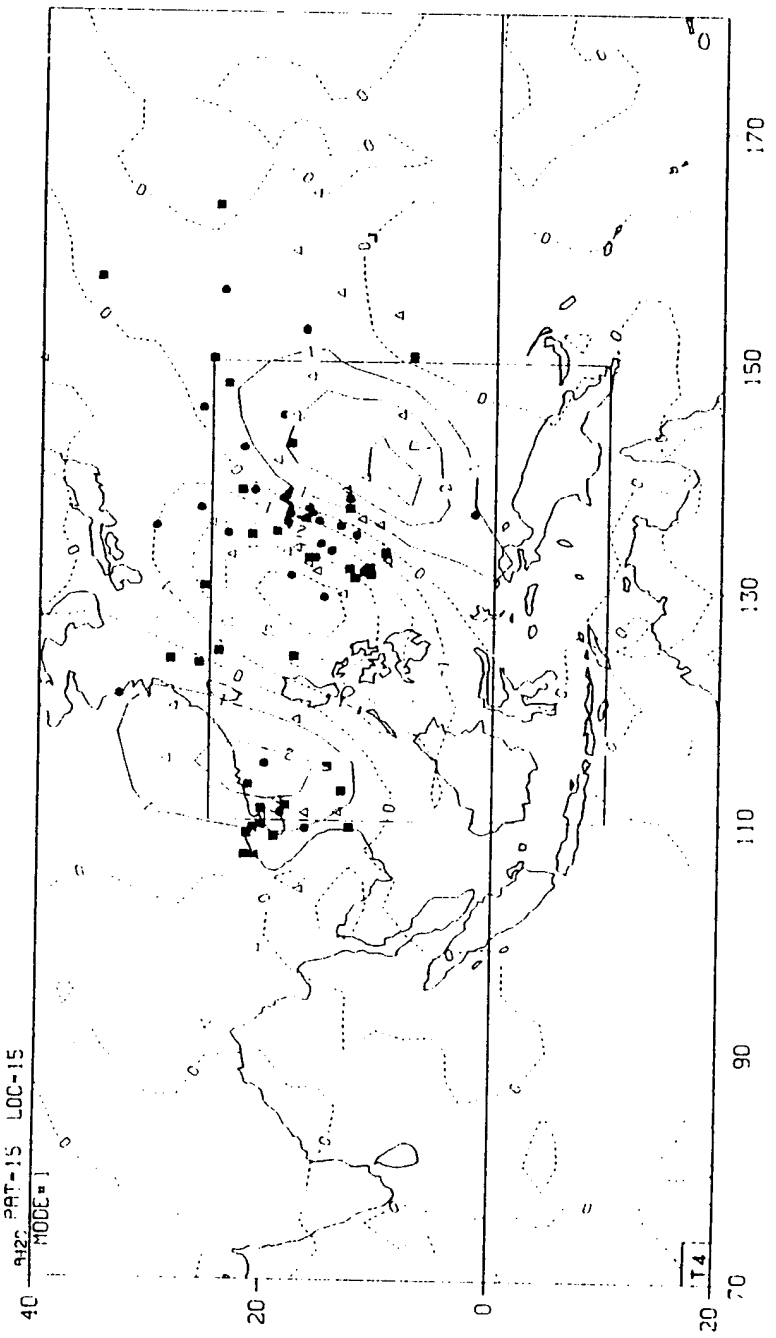

Figure 11b: Single point correlation patterns of vsfc with MJO mode#1, at lag 2 days. Contour interval is 0.1 and negative values are dashed

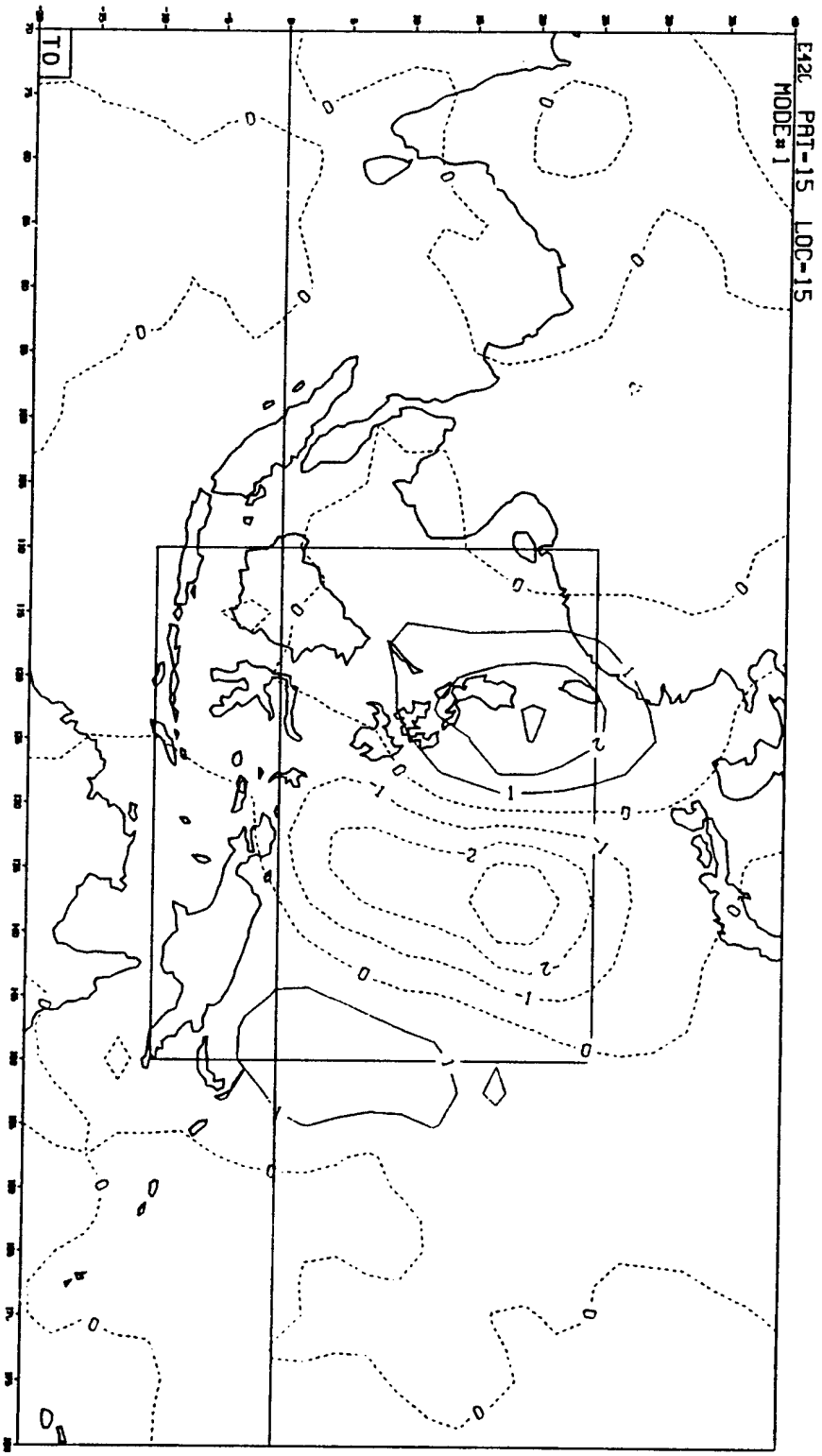

Figure 12a: Same as Figure 11a except for v700

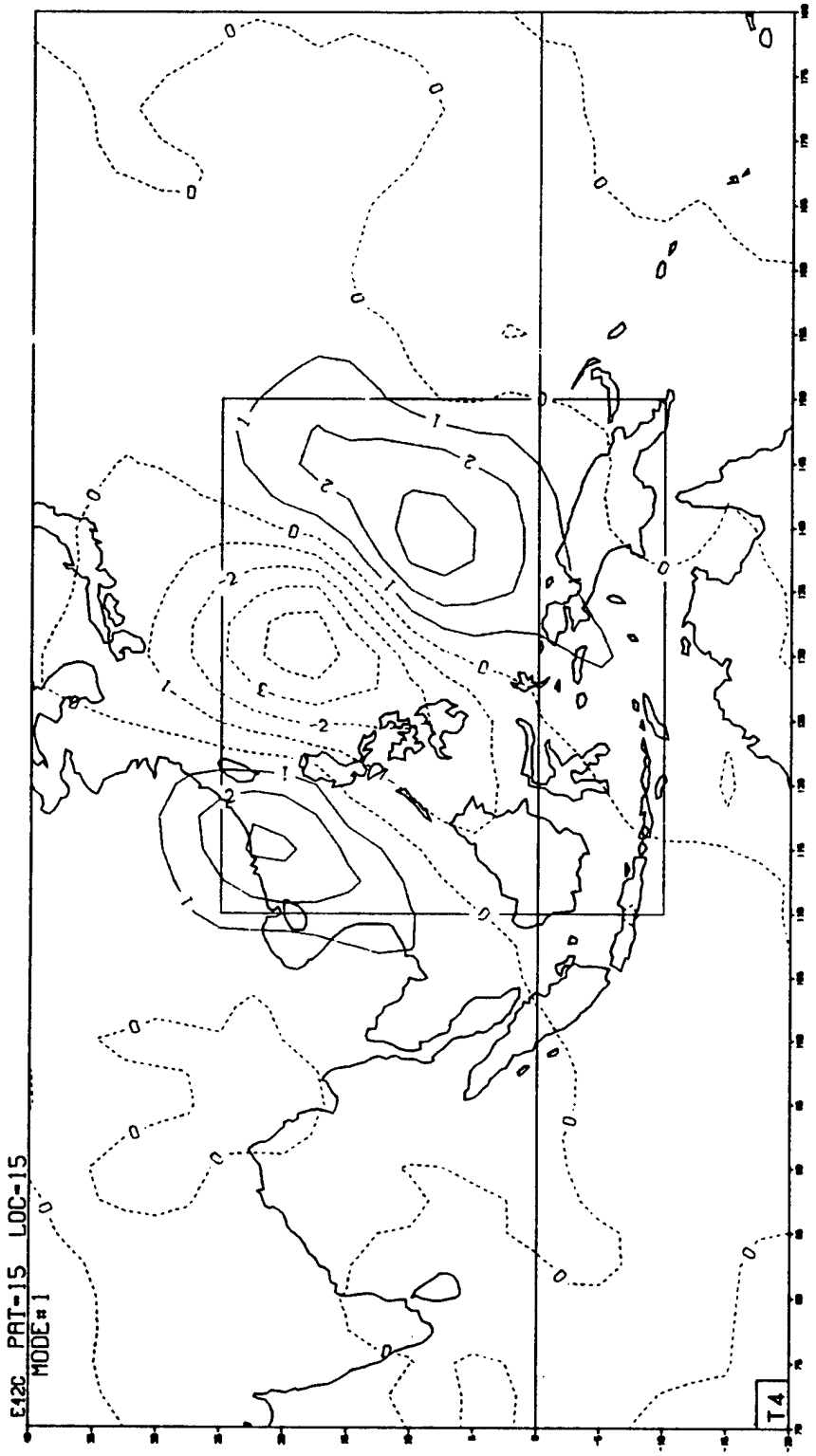

Figure 12b: Same as Figure 11b except for v700

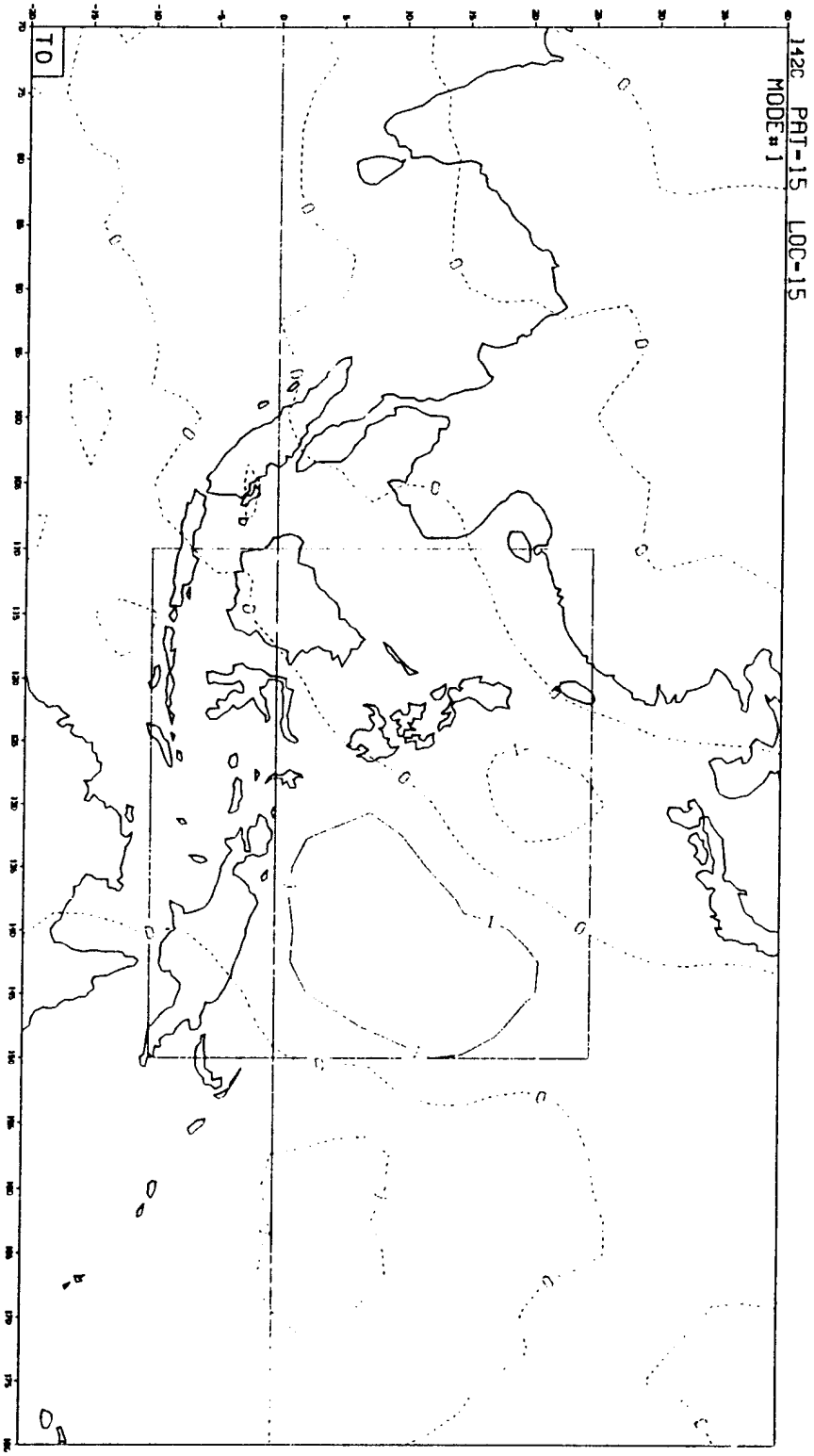

Figure 13a: Same as Figure 11a except for v200

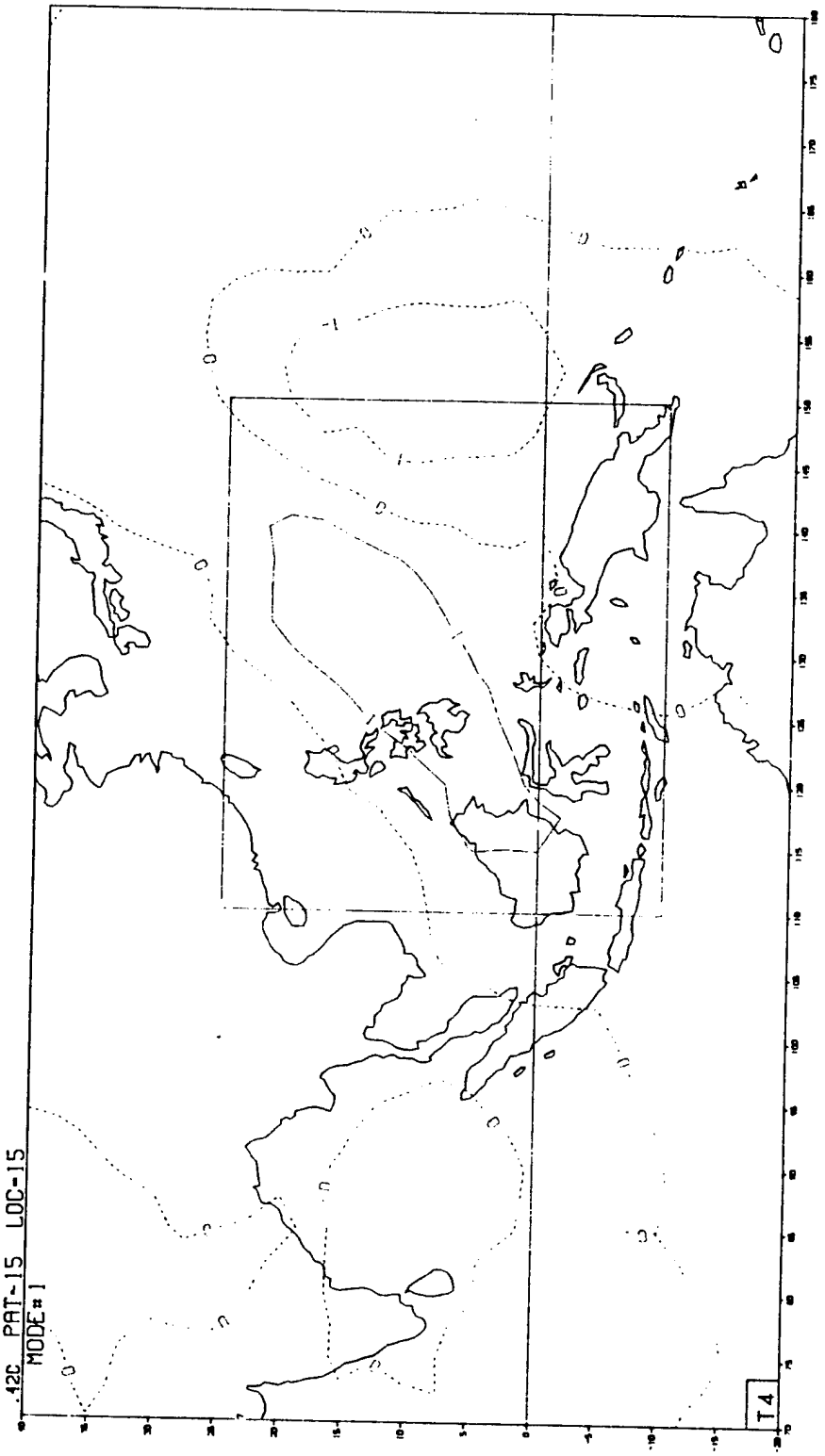

Figure 13b: Same as Figure 11b except for v200

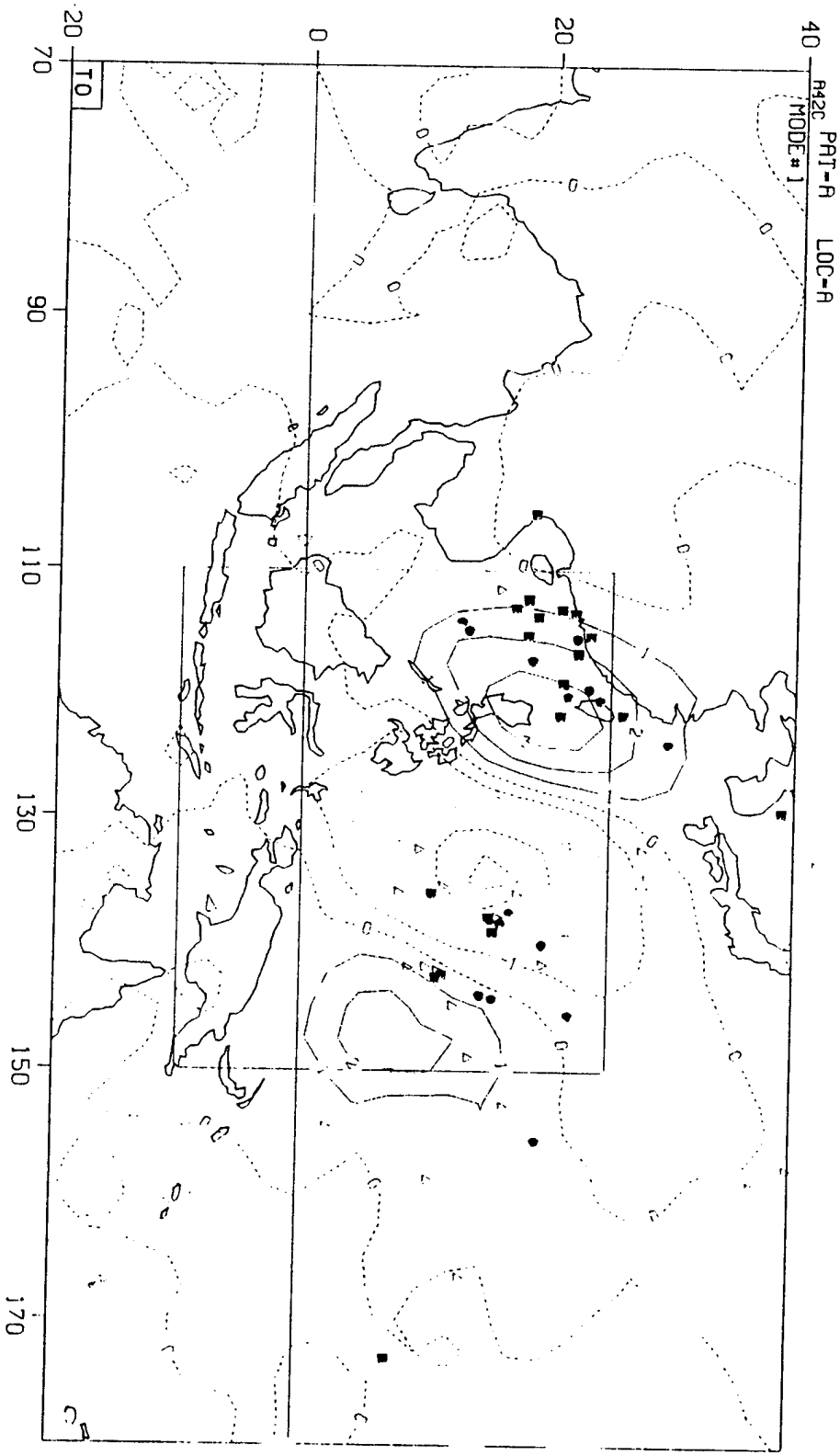

Figure 14a: Same as Figure 11a except for Group A vsfc

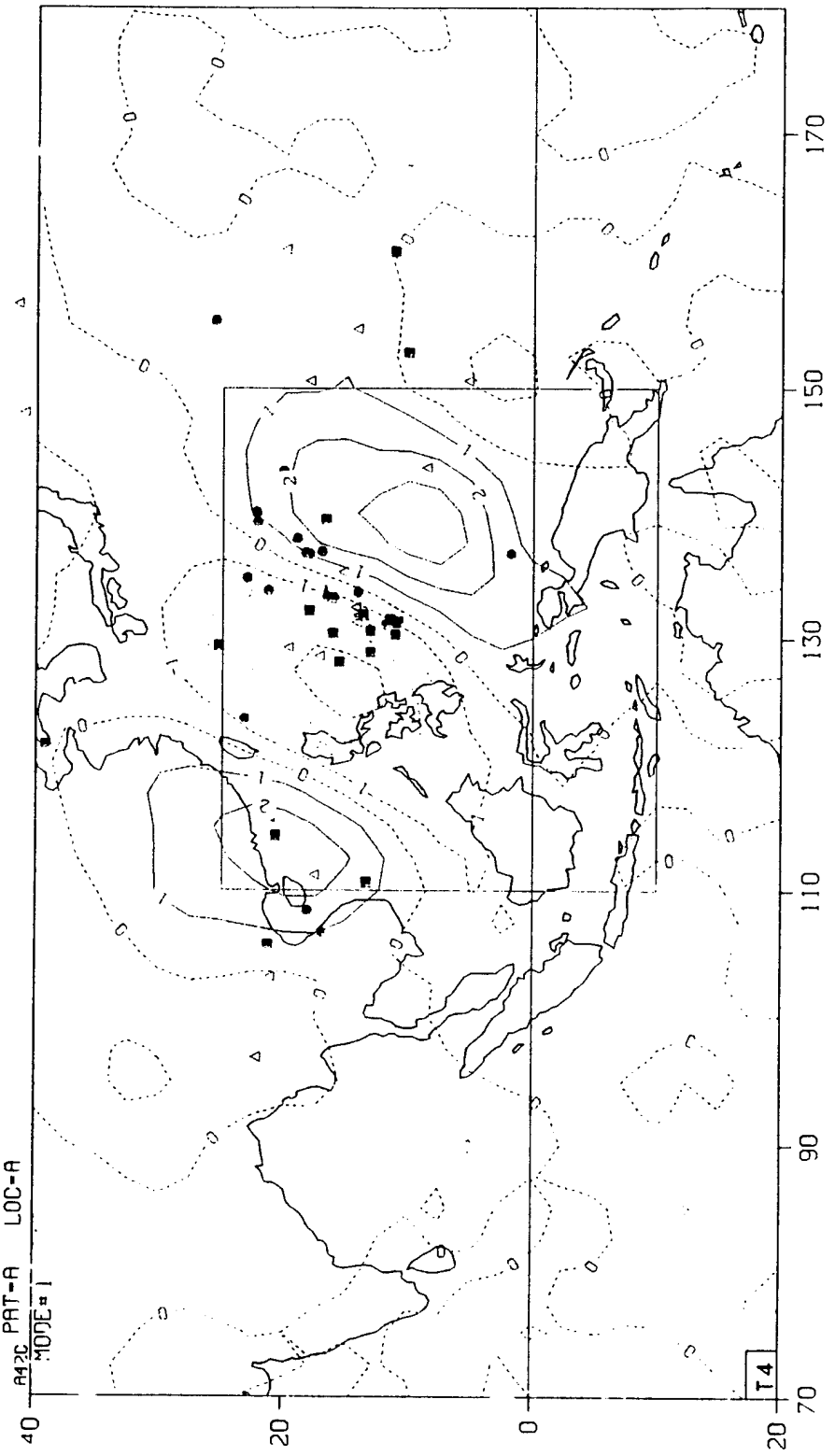

Figure 14b: Same as Figure 11b except for Group A Vsfc

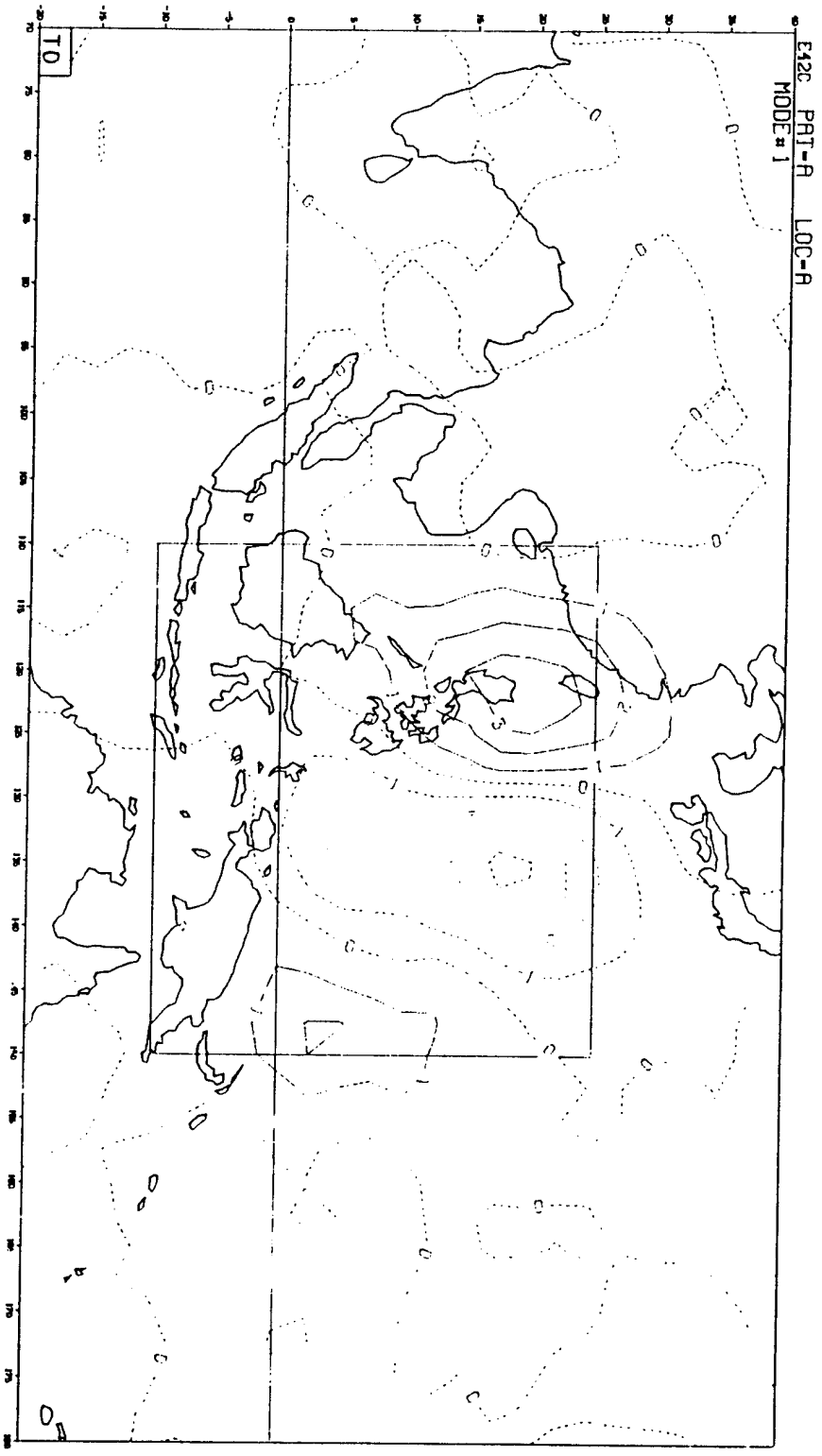

Figure 15a: Same as Figure 11a except for Group A v700

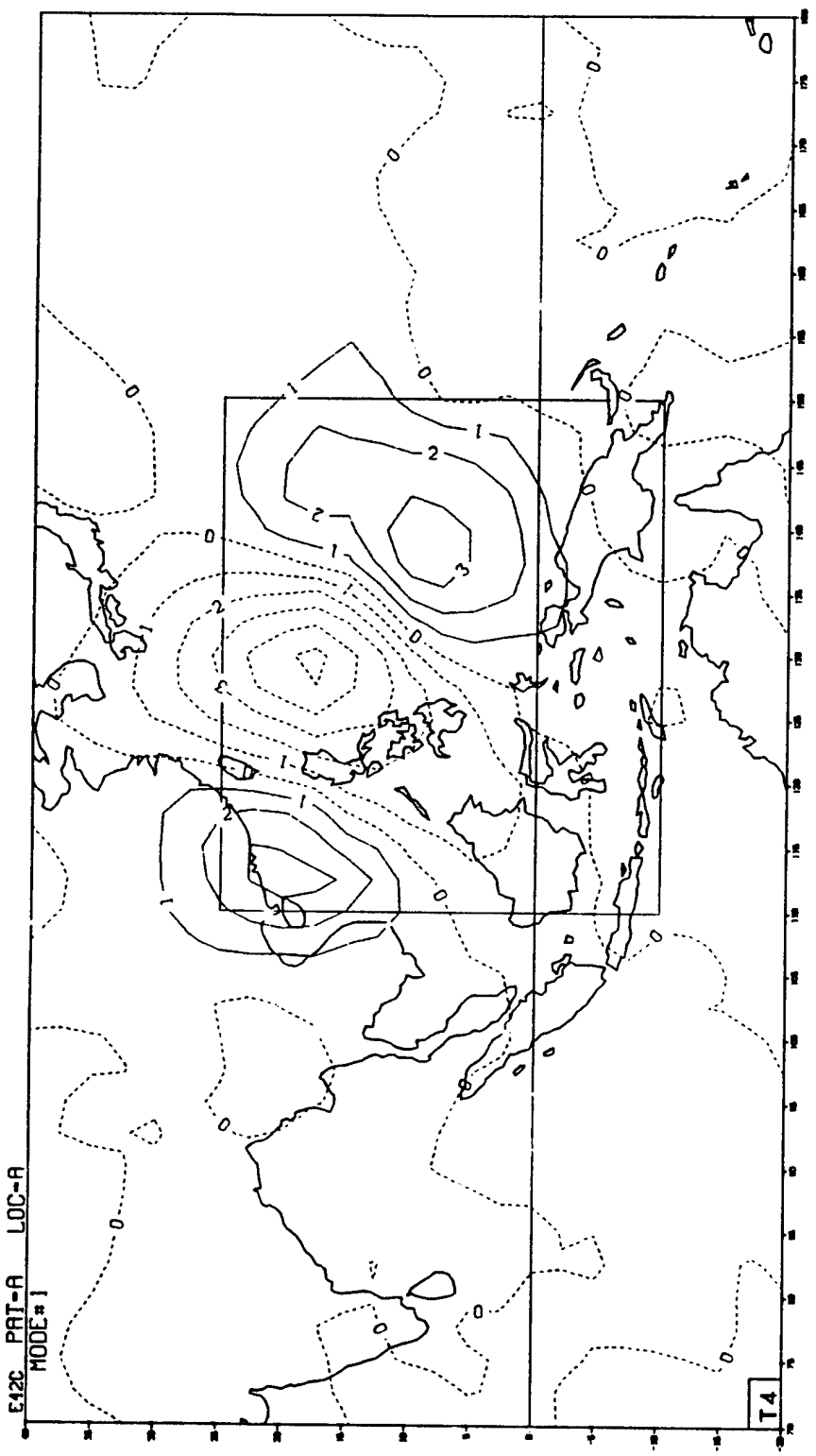

Figure 15b: Same as Figure 11b except for Group A v700

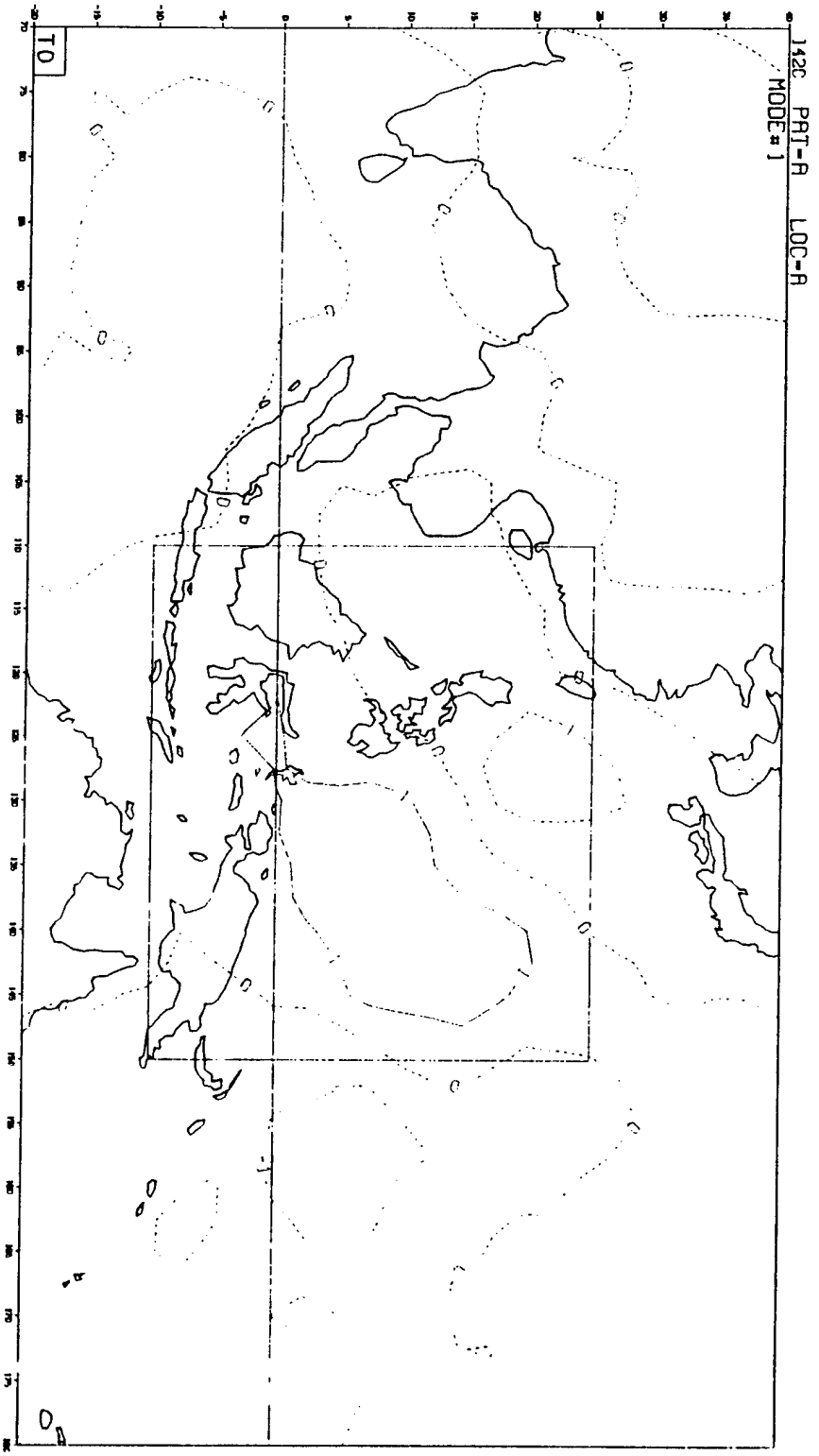

Figure 16a: Same as Figure 11a except for Group A v200

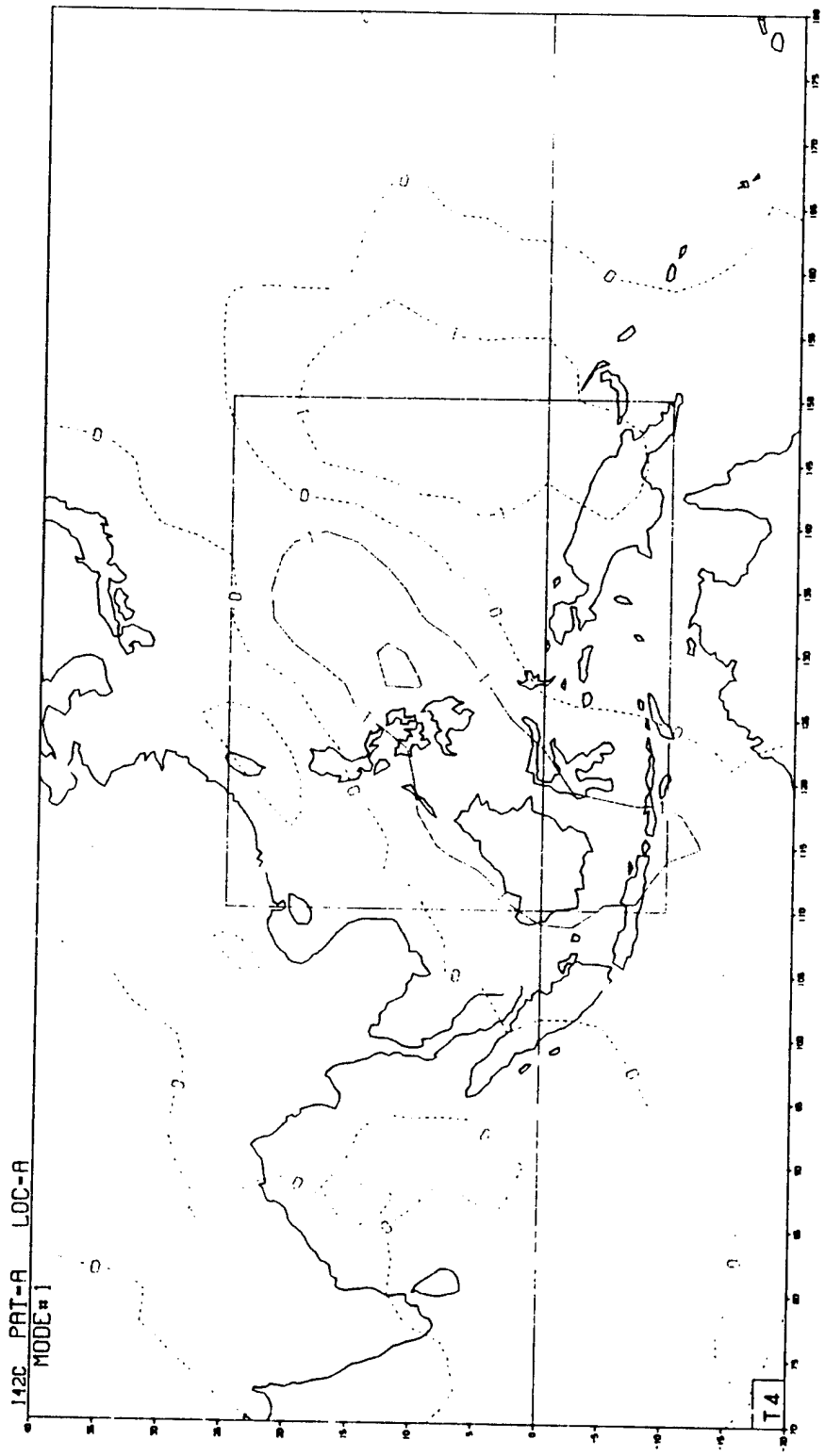

Figure 16b: Same as Figure 11b except for Group A v200

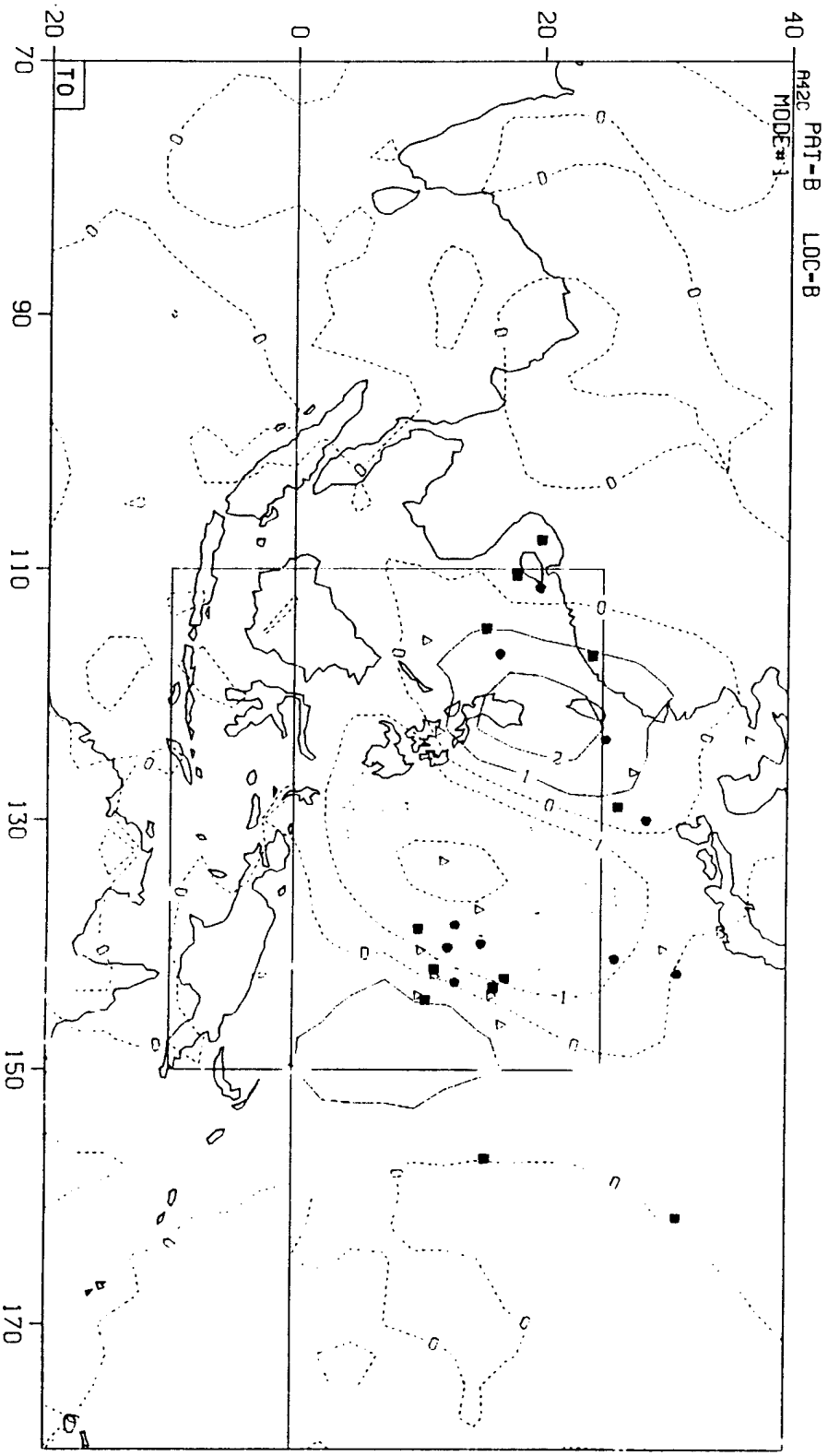

Figure 17a: Same as Figure 11a except for Group B vsfc

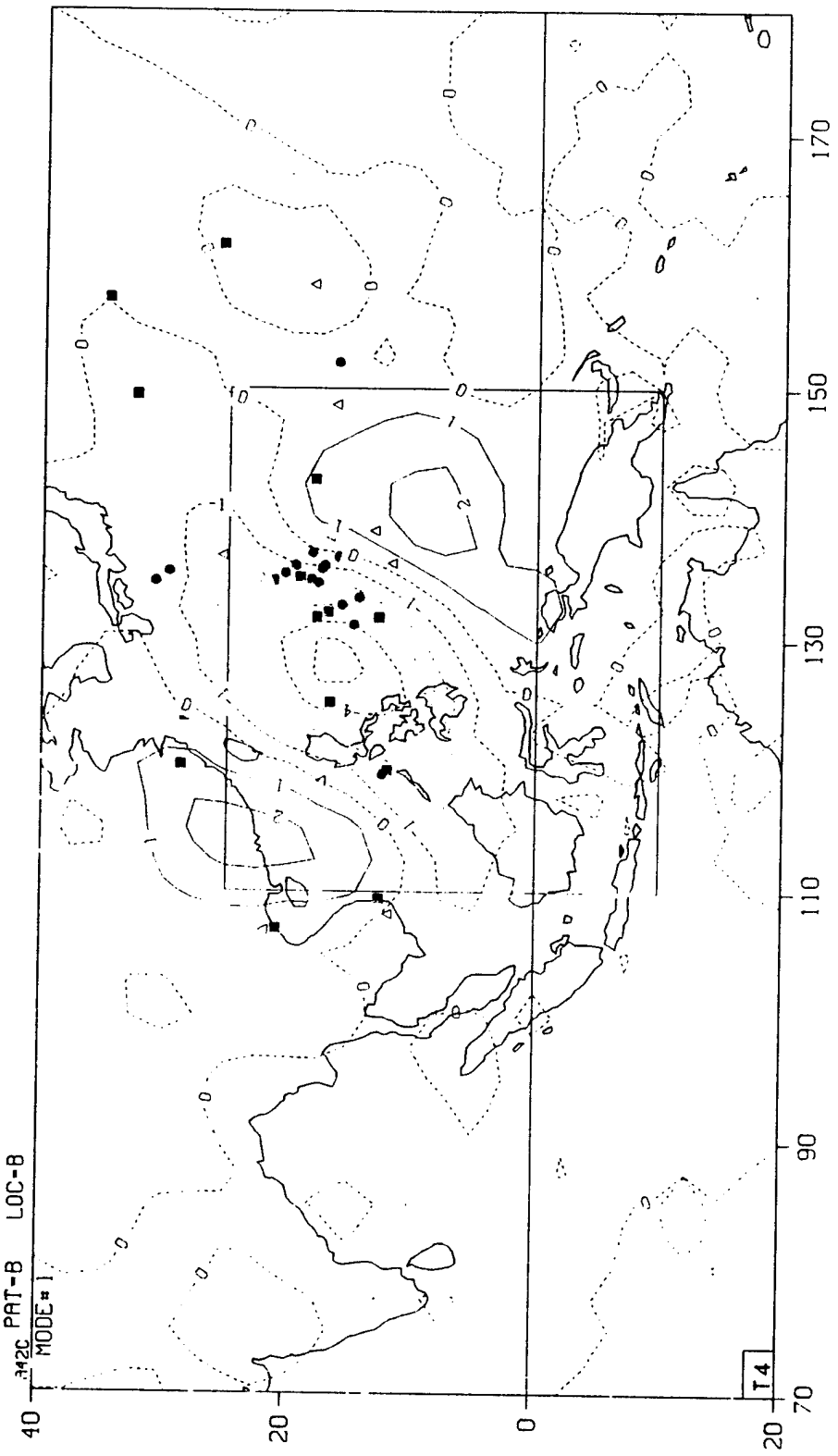

Figure 17b: Same as Figure 11b except for Group B vsfc

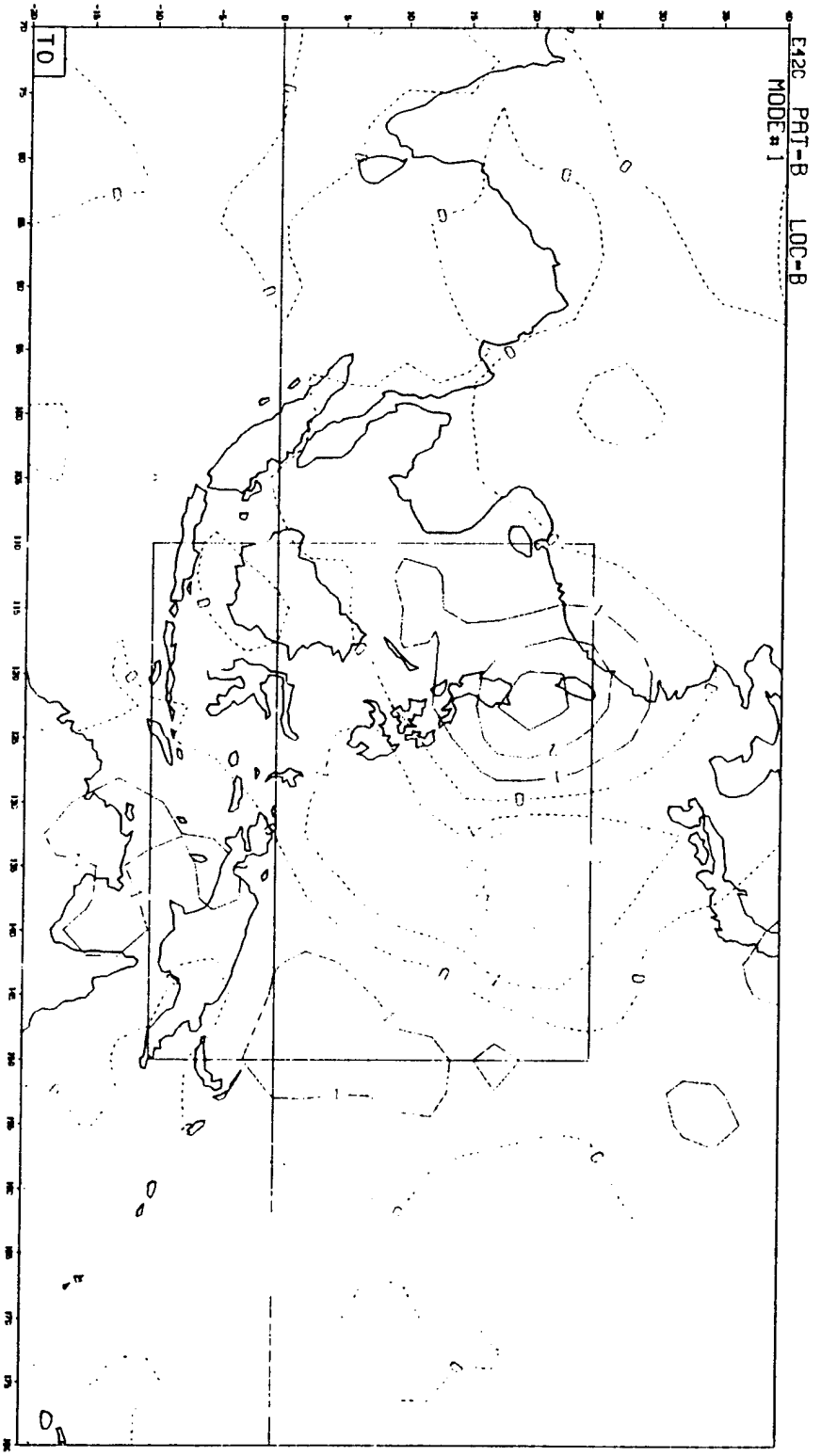

Figure 18a: Same as Figure 11a except for Group B v700

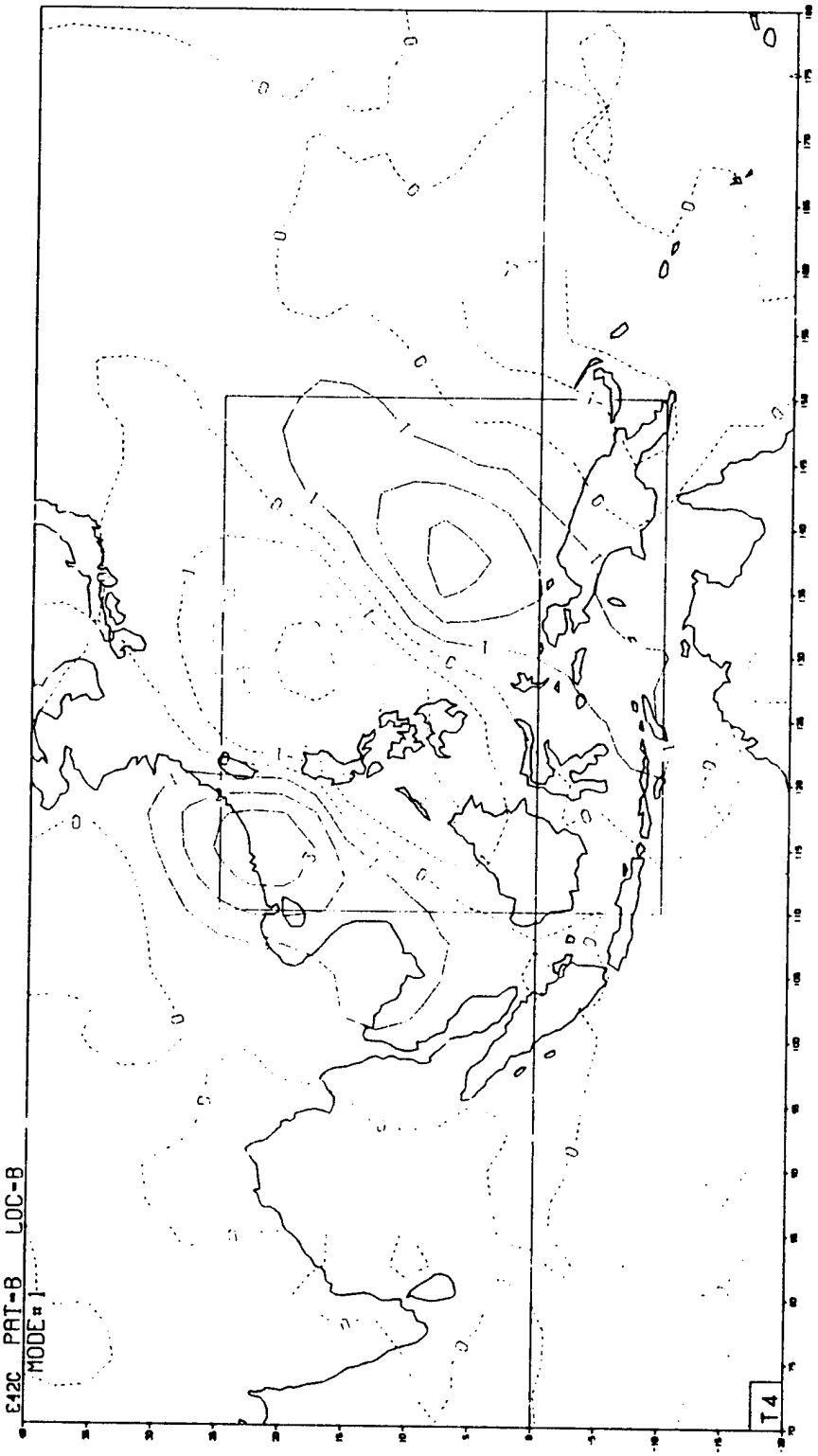

Figure 18b: Same as Figure 11b except for Group B v700

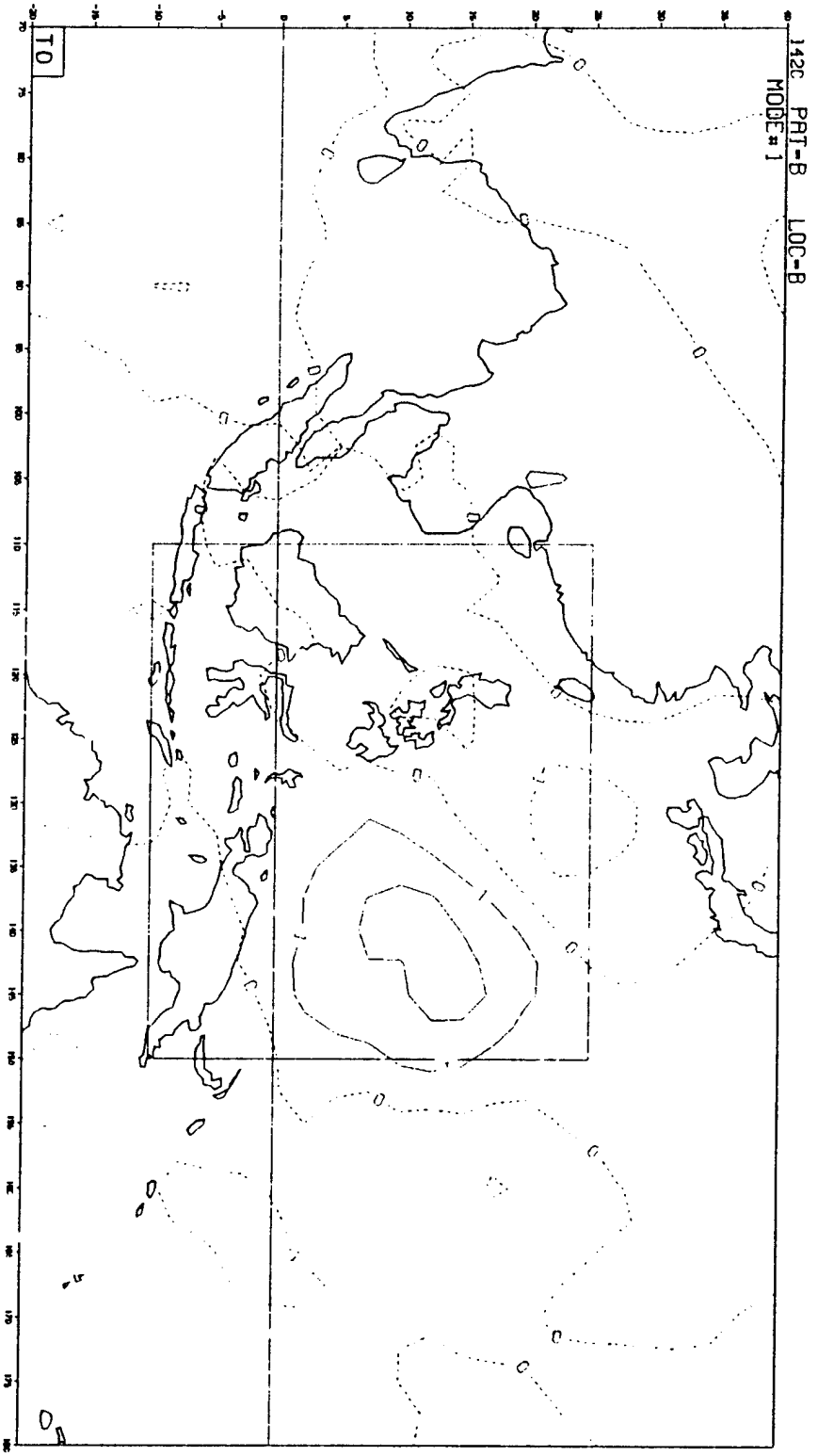

Figure 19a: Same as Figure 11a except for Group B v200

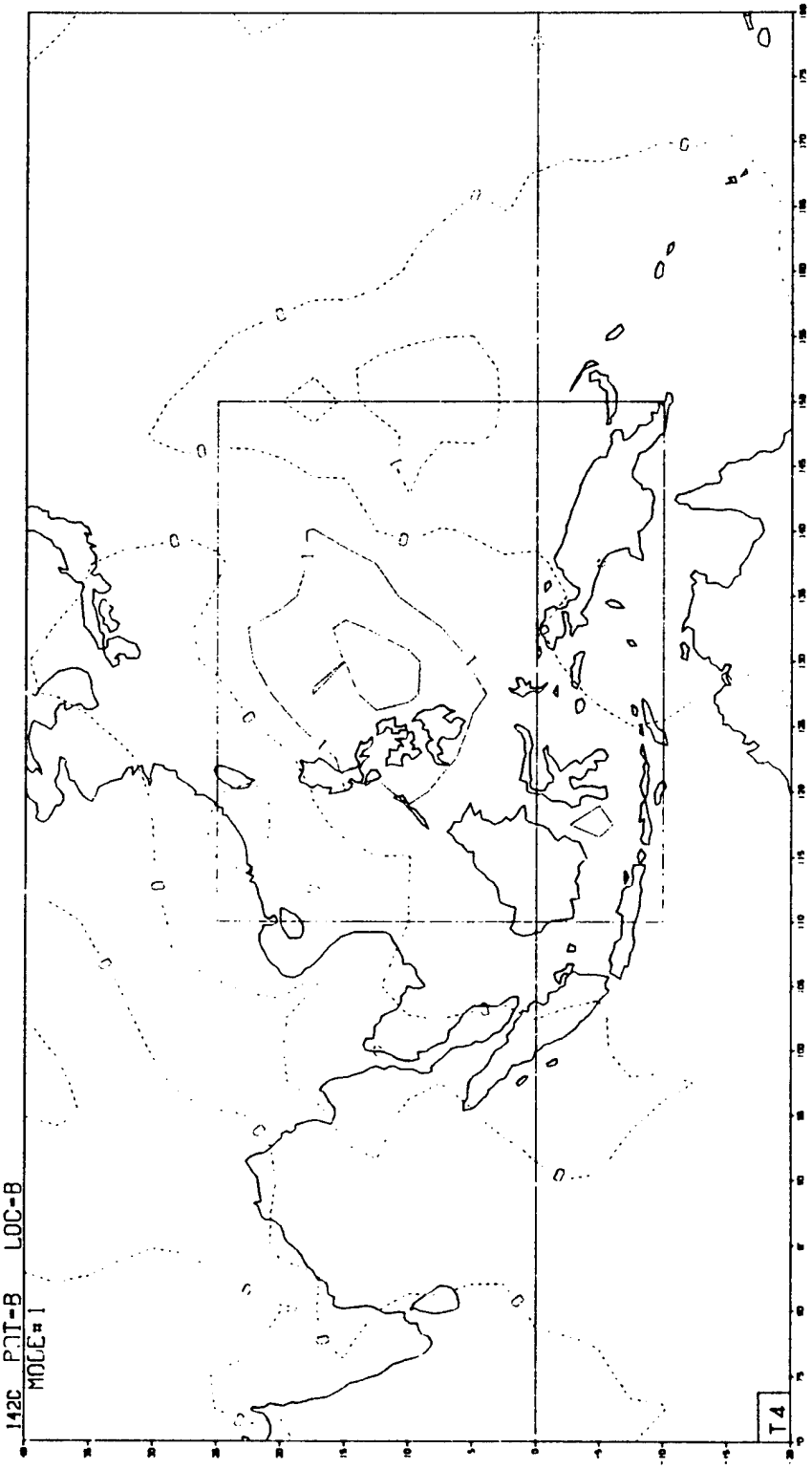

Figure 19b: Same as Figure 11b except for Group B v200

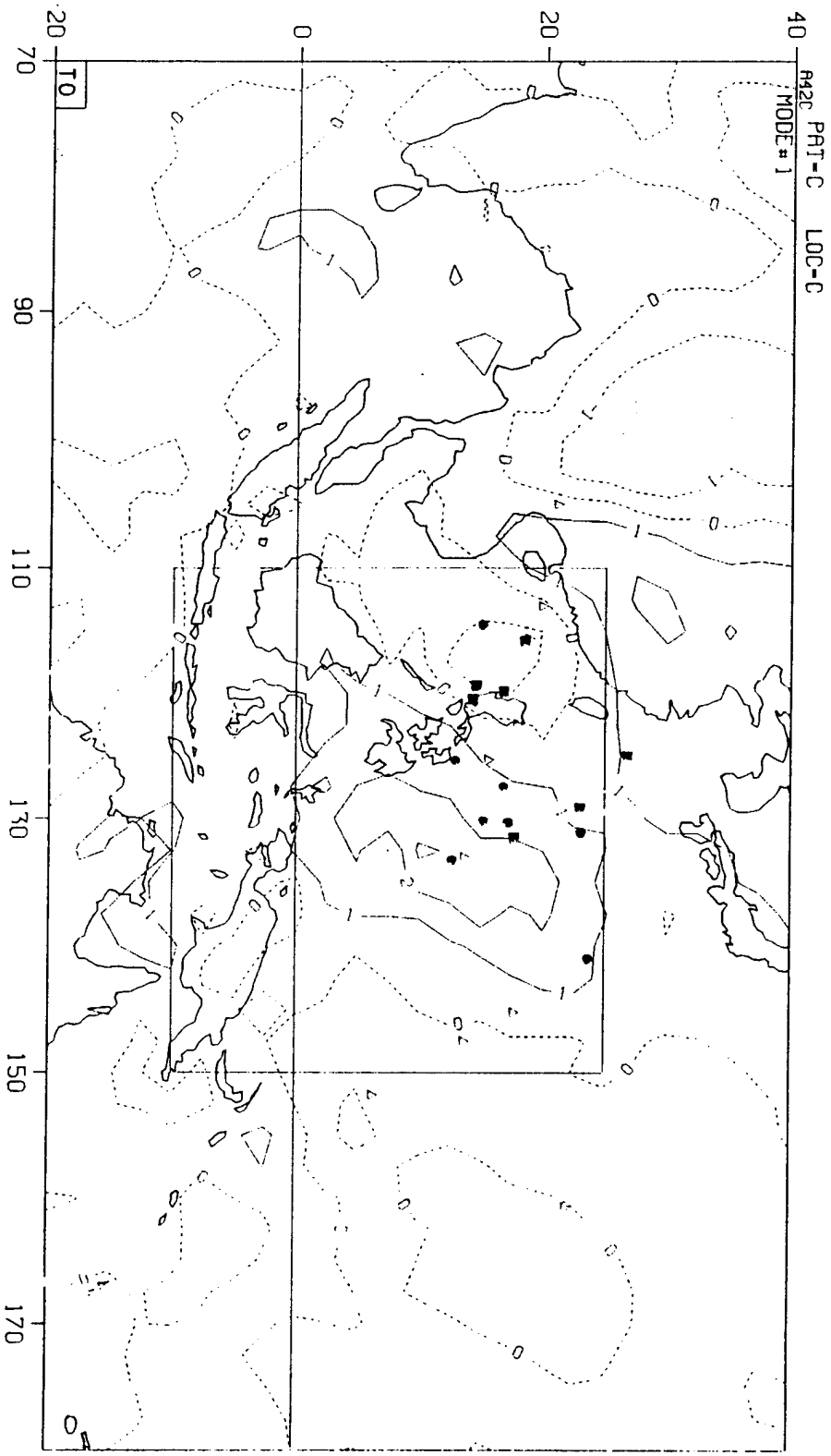

Figure 20a: Same as Figure 11a except for Group C vsfc

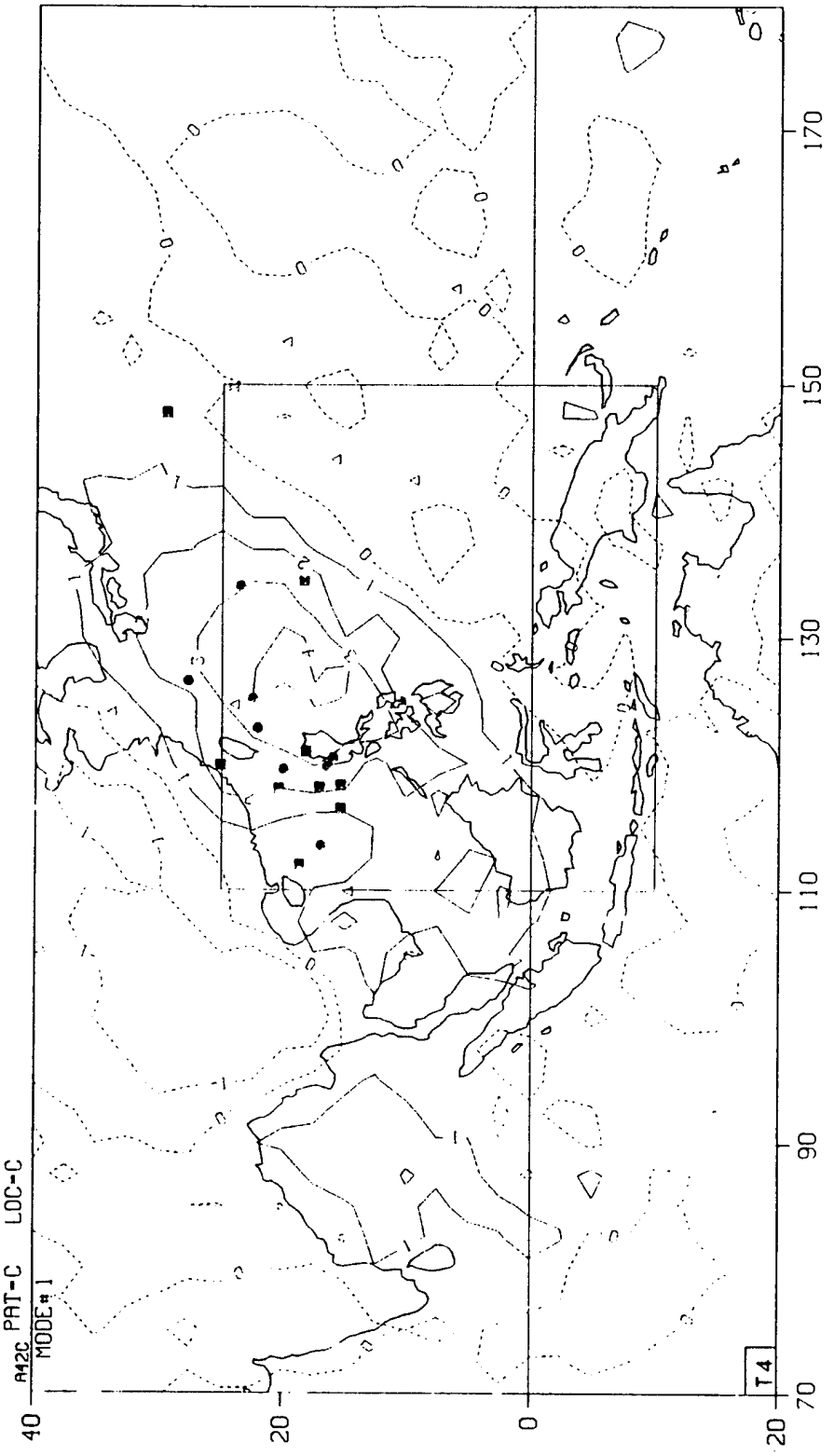

Figure 20b: Same as Figure 11b except for Group C vsfc

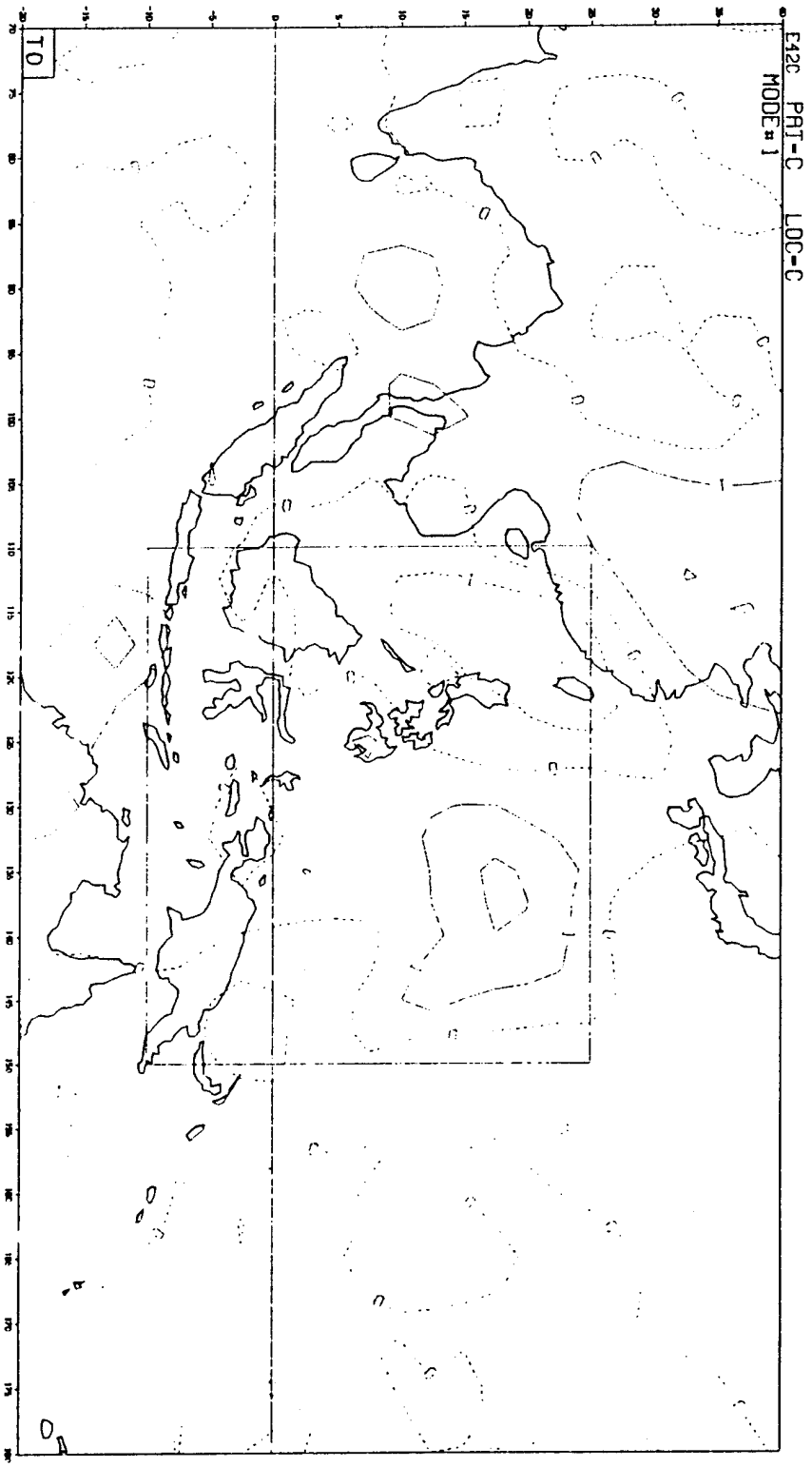

Figure 21: Same as Figure 11a except for Group C v700

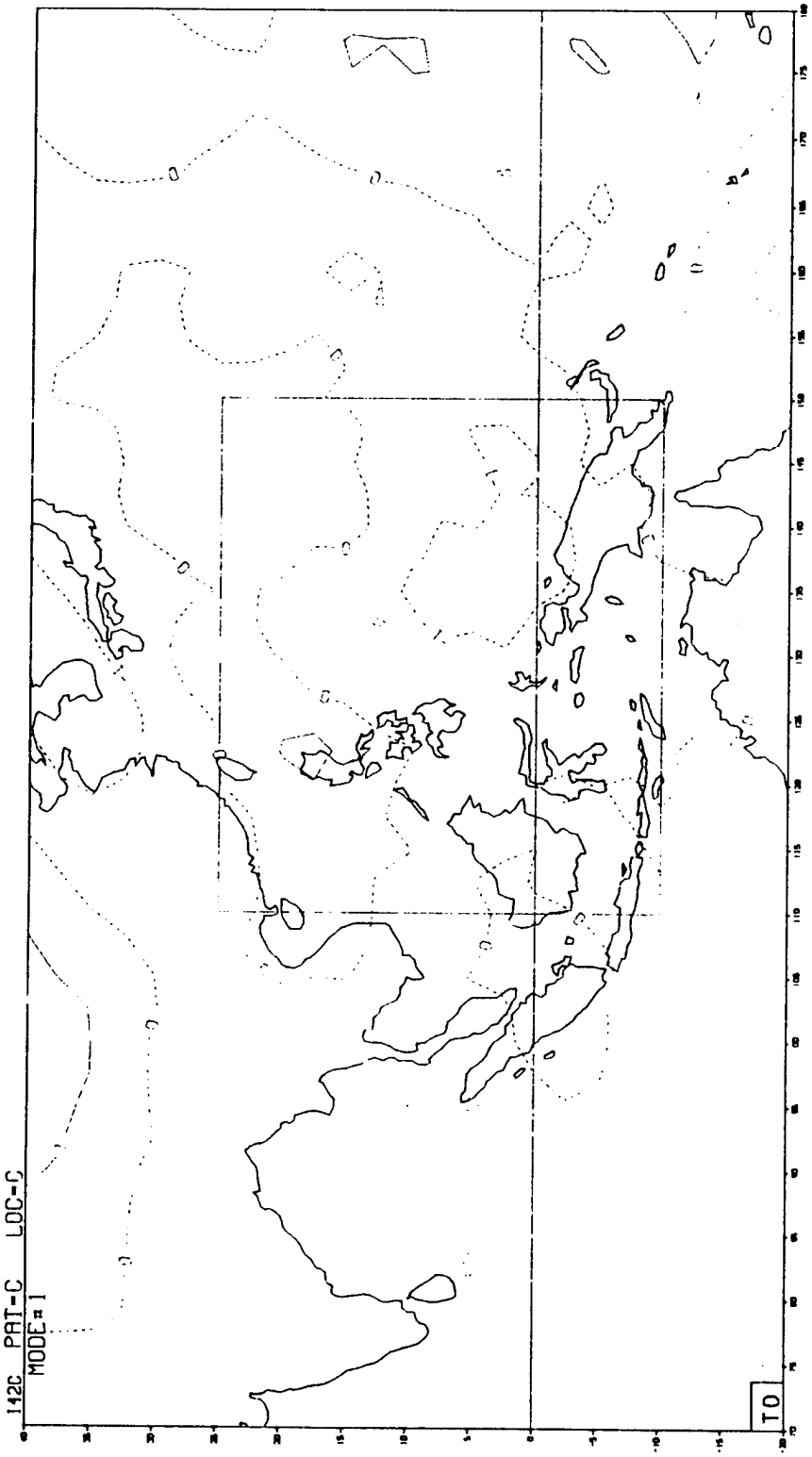

Figure 22: Same as Figure 11a except for Group C v200

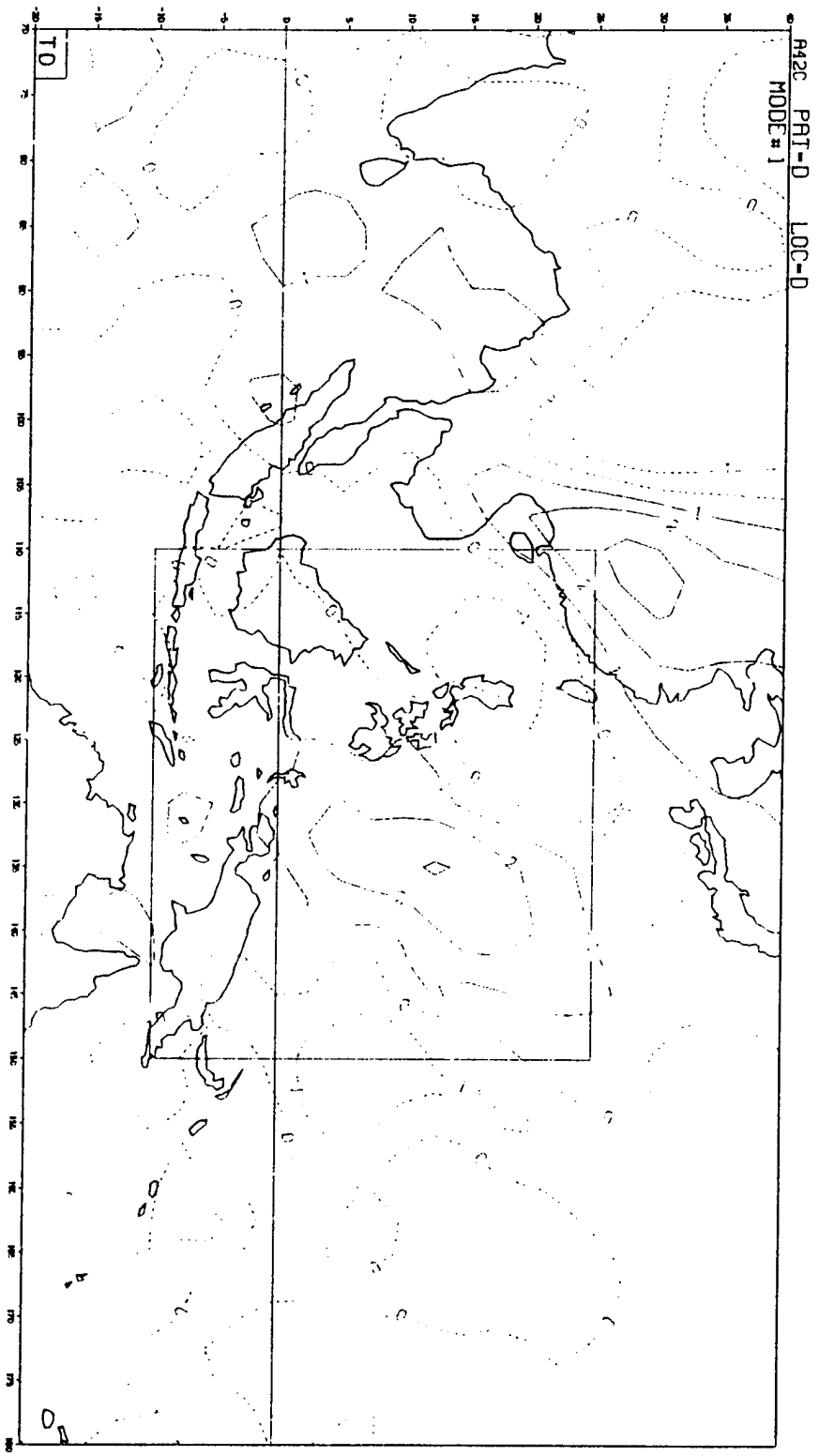

Figure 23: Same as Figure 11a except for Group CC vsfc.

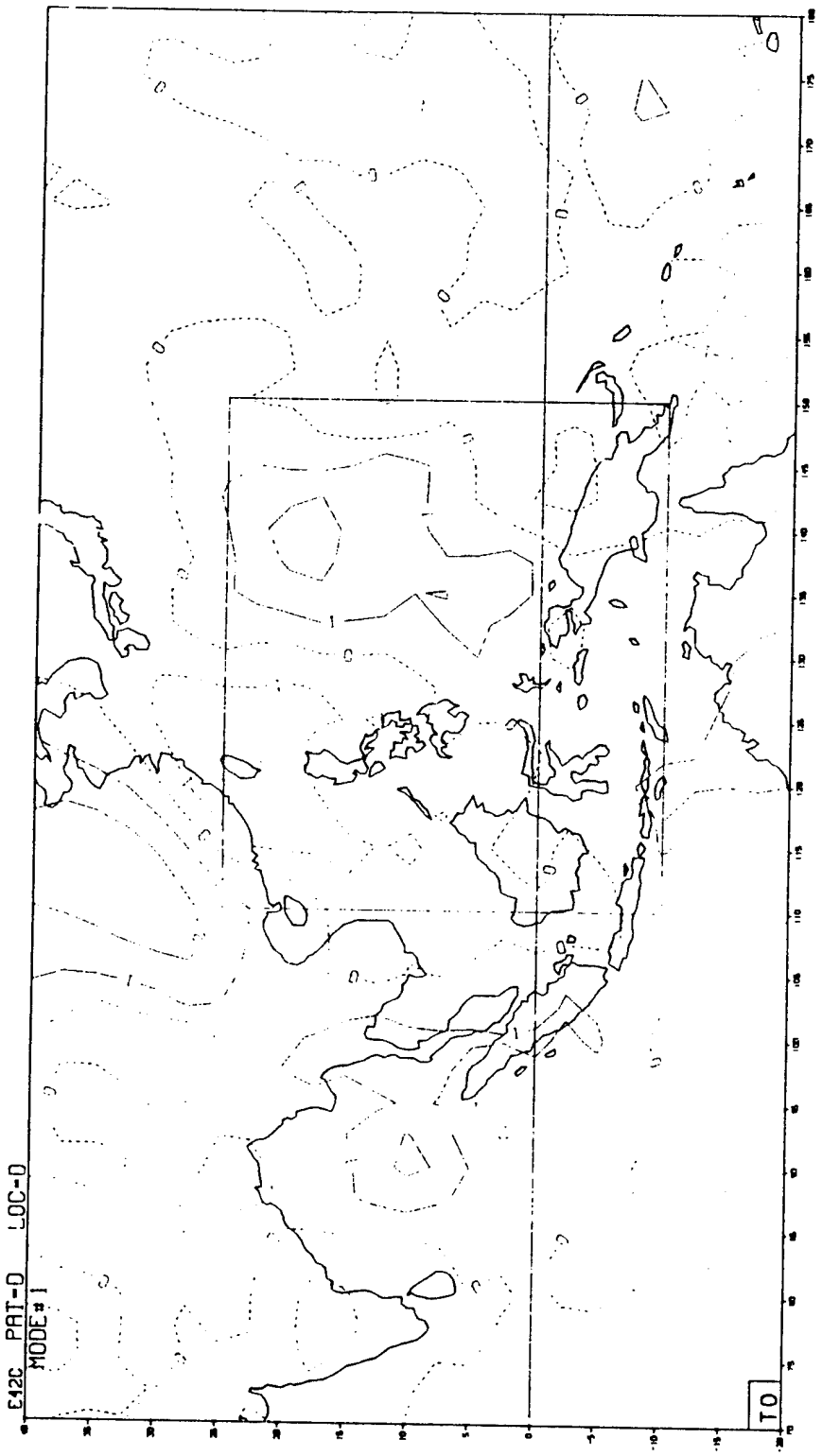

Figure 24: Same as Figure 11a except for Group CC v700

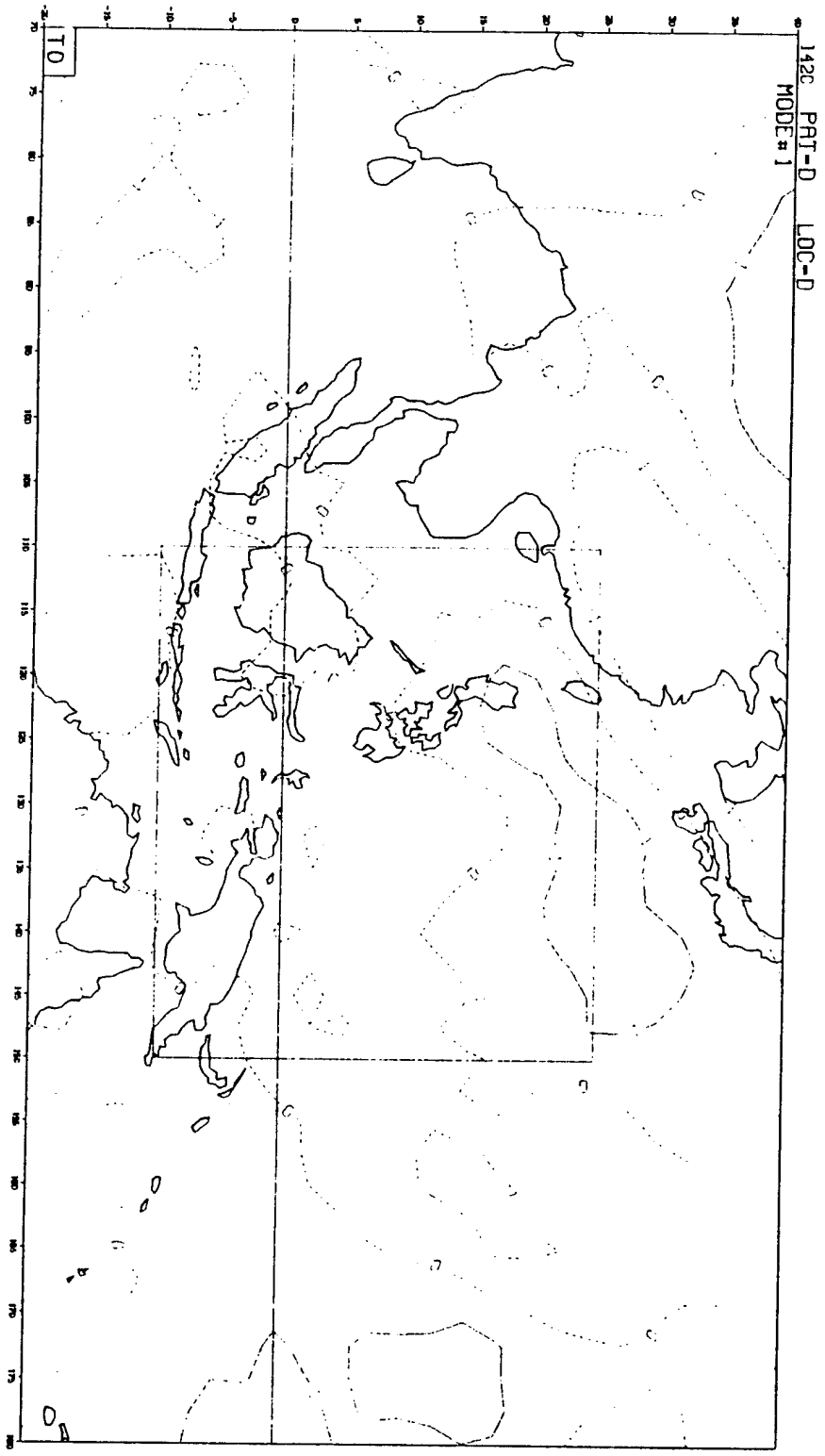

Figure 25: Same as Figure 11a except for Group CC v200

V. COMPOSITE ANALYSIS

Another approach to reveal the three-dimensional and time patterns of the leading MCC modes is to composite the motion fields according to the phases of oscillations in the MCC mode time series. This is carried out by identifying oscillations in the time-integrated amplitude time series whose signals are considered strong. For each case selected the timing of maximum amplitude is assigned to be time T0. The time variation of all wind fields are then composited with respect to the time lag, at 12 h intervals, from T0, for all selected cases. The time-mean background flow is removed from the composite charts in order to make the anomaly patterns standing out. The selection of strong signal cases are identical to that done in comparing tropical cyclone locations with the v_{sfc} correlated pattern carried out in the previous section. Here, the timing of each large-amplitude occurrence for the MCC mode 1 is now a case for T0. This procedure gives 90 T0 cases for the 15Y mode. (It should be noted that not all 90 cases have corresponding tropical cyclone locations in Fig. 11, some cases have none and some have more than one.) As will be shown in Table III, these 15Y cases include 37 cases from group A years, 33 from group B, and 20 from group C.

	15Y	GROUP	COINCIDING
A	37	42	32
B	33	32	30
C	20	19	0

Table III:Composite case in 15Y, Group A,B and C

Fig. 26 shows the v_{sfc} composite. As expected, the main T0 and T4 patterns resemble closely the 15Y v_{sfc} - mode 1 T0 and T4 correlation patterns (Fig. 11). During the first 24 h

(T0-T2) there is an indication of an northwestward extension of the wave pattern into the Asian continent, which is not found in the correlation pattern. The northwest extension of the wave pattern disappears as the time lag increases beyond T2, but the main wave pattern inside and near the core domain stays organized and propagates northwestward throughout the 5.5 days (T0-T11) of the composite. Fig. 27 is a vector plot of the composite v_{sfc} and u_{sfc}. The wave pattern is dominated by a cyclone-anticyclone couplet that propagates through the core domain. The 15Y v_{700} composite and corresponding wind vector plots are shown in Figs. 28 and 29, respectively. The patterns are consistent with the correlation pattern (Fig. 12) and are approximately in-phase with the surface plots. In addition to the main wave pattern, during T8-T11 there appears to be a cyclonic vortex in the midlatitude western Pacific east of Japan (Fig. 29). Although there is some indication of a similar signal at the surface, this system does not appear to be consistently present or move through the entire series, and there is no corresponding correlation in Fig. 12 to suggest any significance.

The 15Y 200 hPa v and wind vector composites are shown in Figs. 30 and 31. The v_{200} composite shows a noisier picture than the low levels, but the propagating wave pattern inside the core domain can readily be seen. The structure shows more northeast-southwest elongation than circular cell features. In general, the propagating patterns are more conspicuous than those indicated by the 15Y v_{200} correlation (Fig. 13). The wind vector composite (Fig. 31) appears noisy, but significant large-scale divergent and convergent patterns are noticeable. In Fig. 31 the main areas of divergence and convergence in and near the core domain are marked. We can see a general pattern of

northwestward propagation of these divergence/convergence areas and also the propagation of anticyclonic and cyclonic features. The divergence pattern suggests that the wave mode is associated with strong convection, which is consistent with the observed association with tropical cyclone activities.

The composite analysis is also carried out for each of the three groups. For group A, 42 cases are selected. Table 3 shows that 32 of these cases are also selected in the 15Y analysis. The surface v and wind vector composites (Figs. 32) are very similar to the corresponding 15Y composites, showing clearly organized northwestward propagating wave patterns. In fact, the group A patterns are more clearly defined than the 15Y, which is not surprising as group A contains the six most organized years. In addition, the northwest extension of the wave pattern over the Asian continent noticed during T0-T2 at the 15Y v_{sfc} composite (Fig. 26) is also detectable in group A. In fact, the signal of this extension shows up slightly at T0-T1 then disappears, t0 reappear after T6 and becomes quite visible during T9-T11. Thus, the group A composite suggests the possibility that the wave pattern can continue to propagate beyond the core domain into the region of Tibetan. This downstream propagation is also visible in the wind vector composite (Fig. 33). The 700 hPa group A composites (Figs. 34-35) also clearly depicts the wave pattern and resemble the 15Y pattern. The 200 hPa group A composites are shown in Figs. 36-37. The wind vectors indicate a similar northwestward propagating divergence/convergence pattern to that found in the 15Y group. The strong wind speeds in the Group A pattern reconfirms that the group A years are the strongest, most organized years for this wave.

The group B composites contain 32 cases, of which 30

are included in the 15Y composites. In general, group B composites at the surface (Figs. 38-39) and 700 hPa (Figs. 40-41) show clearly defined wave patterns that are comparable to the 15Y results. At 200 hPa (Figs. 42-43), the patterns also resemble the 15Y pattern with slightly stonger wind speeds.

The group C composites contain 19 cases, none of which overlaps with the 15Y cases. These are the four years with least organization, and, as is with the correlation results, the wave pattern is only detectable at the lower levels. The surface and 700 hPa composites are shown in Figs. 44-45 and 46-47, respectively. There are indications of the wave pattern but the Figures are also filled with other noisy features. The 200 hPa composites are shown in Figs. 48-49. There are a number of rotational and divergent disturbance features in each of the time panels, but there is no discernible time-continuous, organized structure in the core domain that can be related to the northwestward propagating wave pattern.

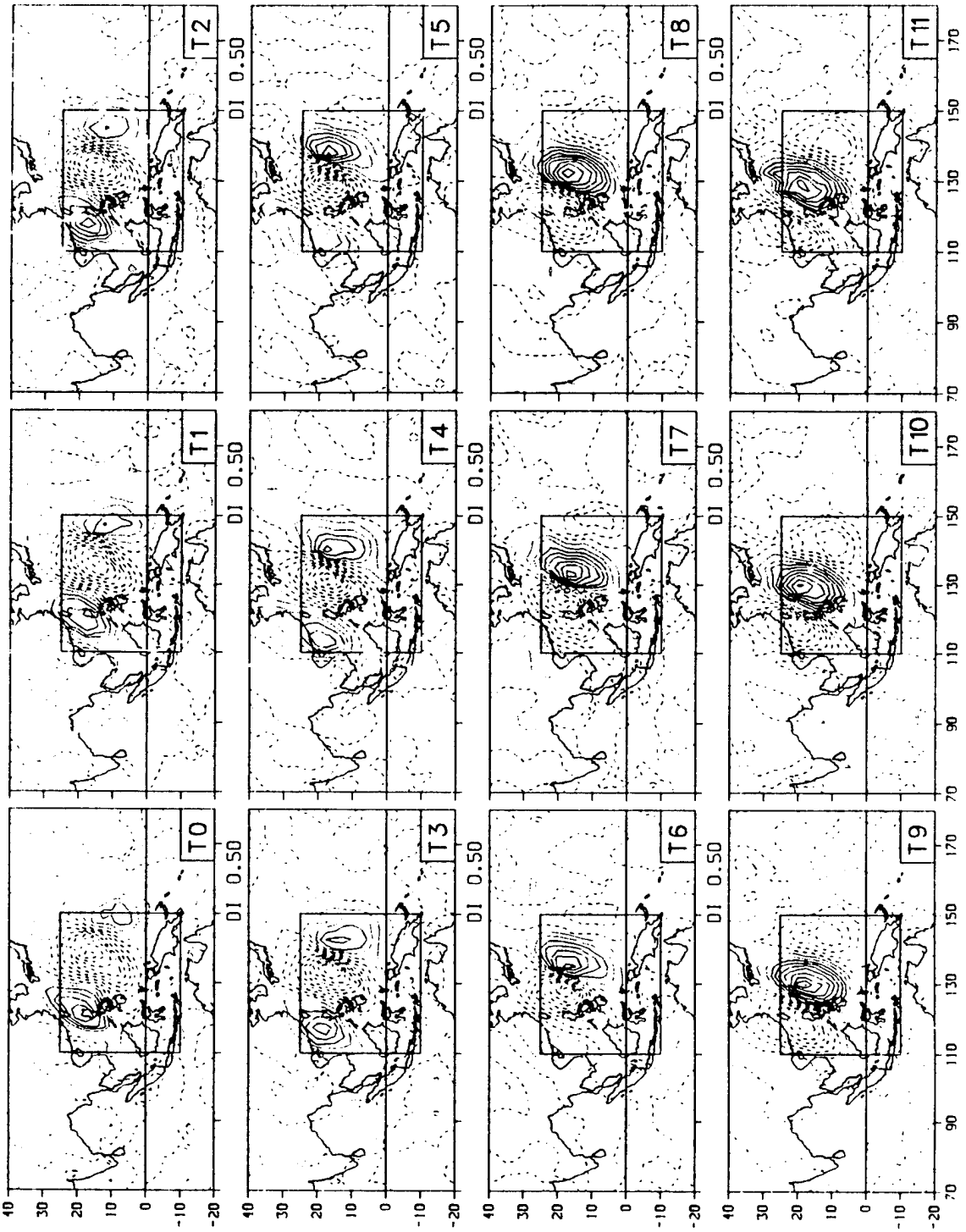

Figure 26: 15Y Surface wind contour plots at 12 consecutive 12-hour time lags from T0 to T11 with the background mean removed. (surface v contour plot based on 90 case composite)

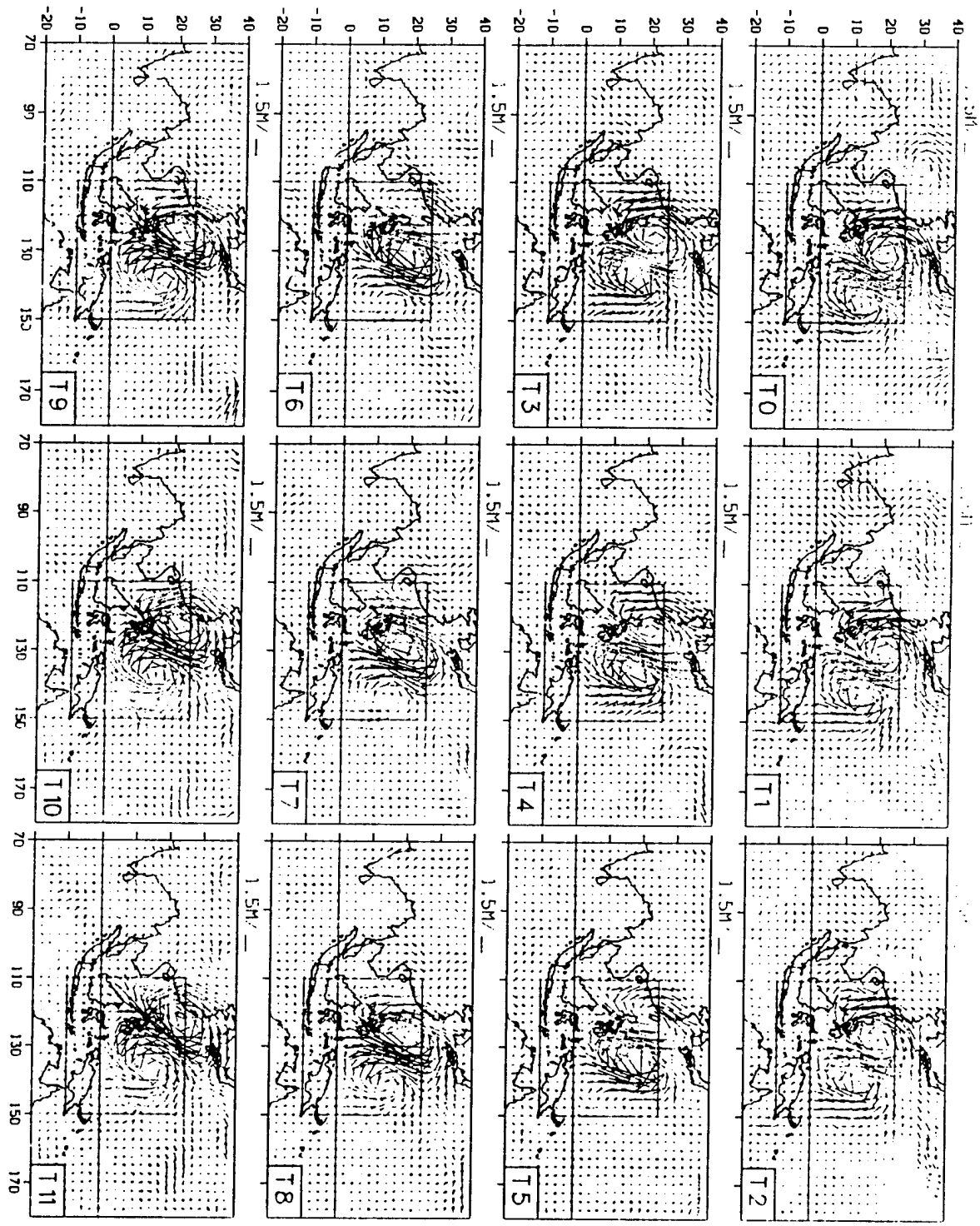

Figure 27: 15Y surface wind vector plots at 12 consecutive 12-hour time lags from T0 to T11 with the background mean removed

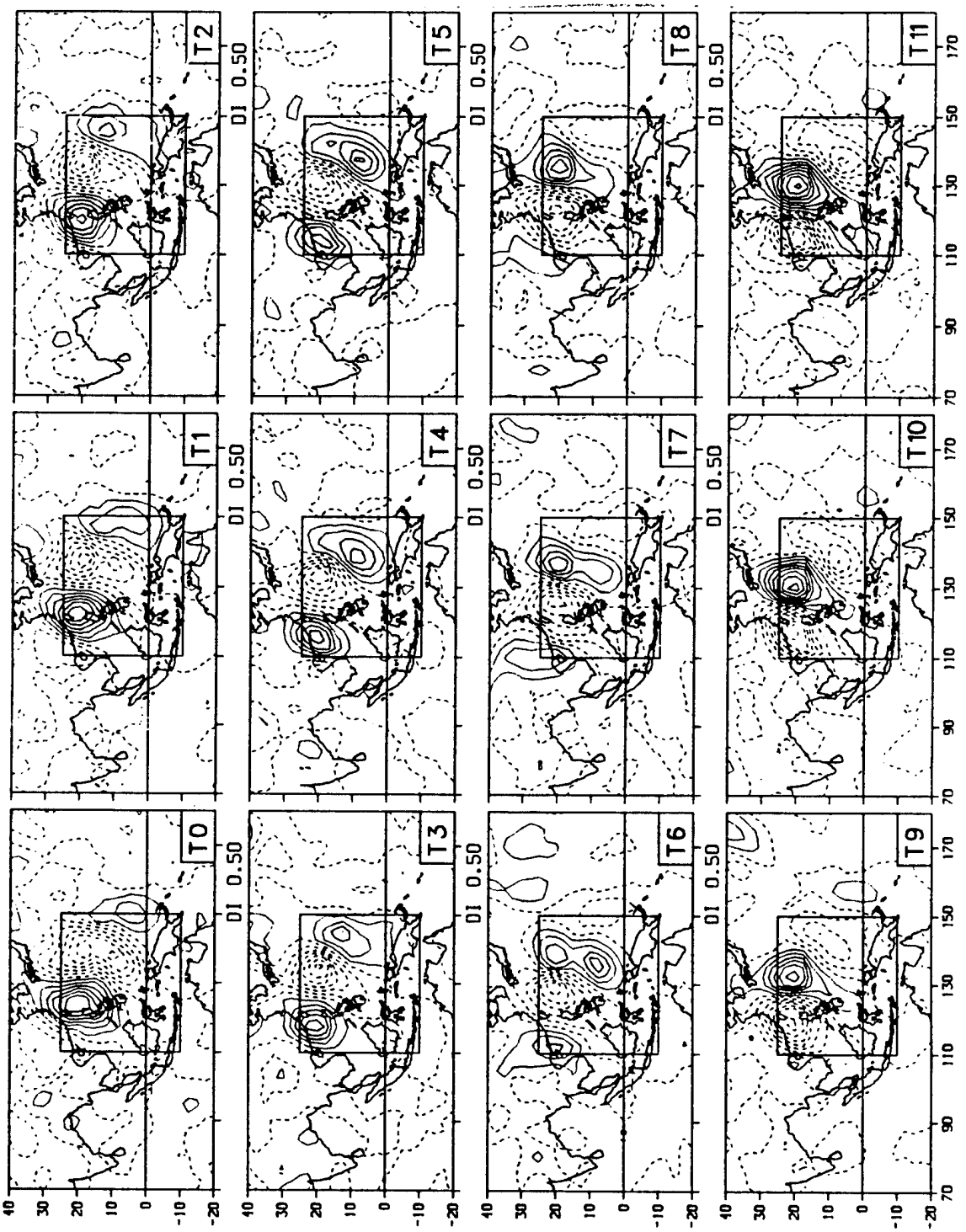

Figure 28: Same as Figure 26 except for v700

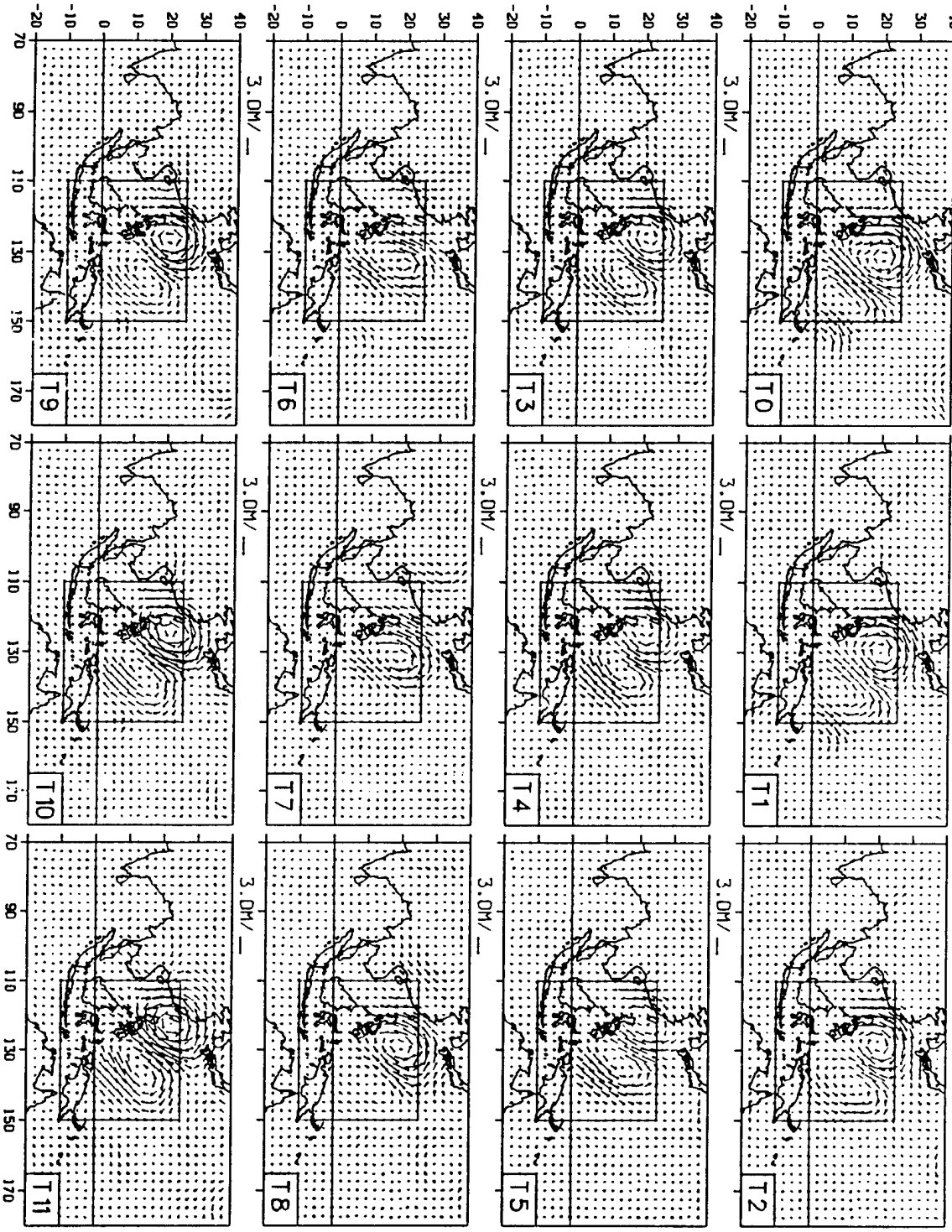

Figure 29: Same as Figure 27 except for v700

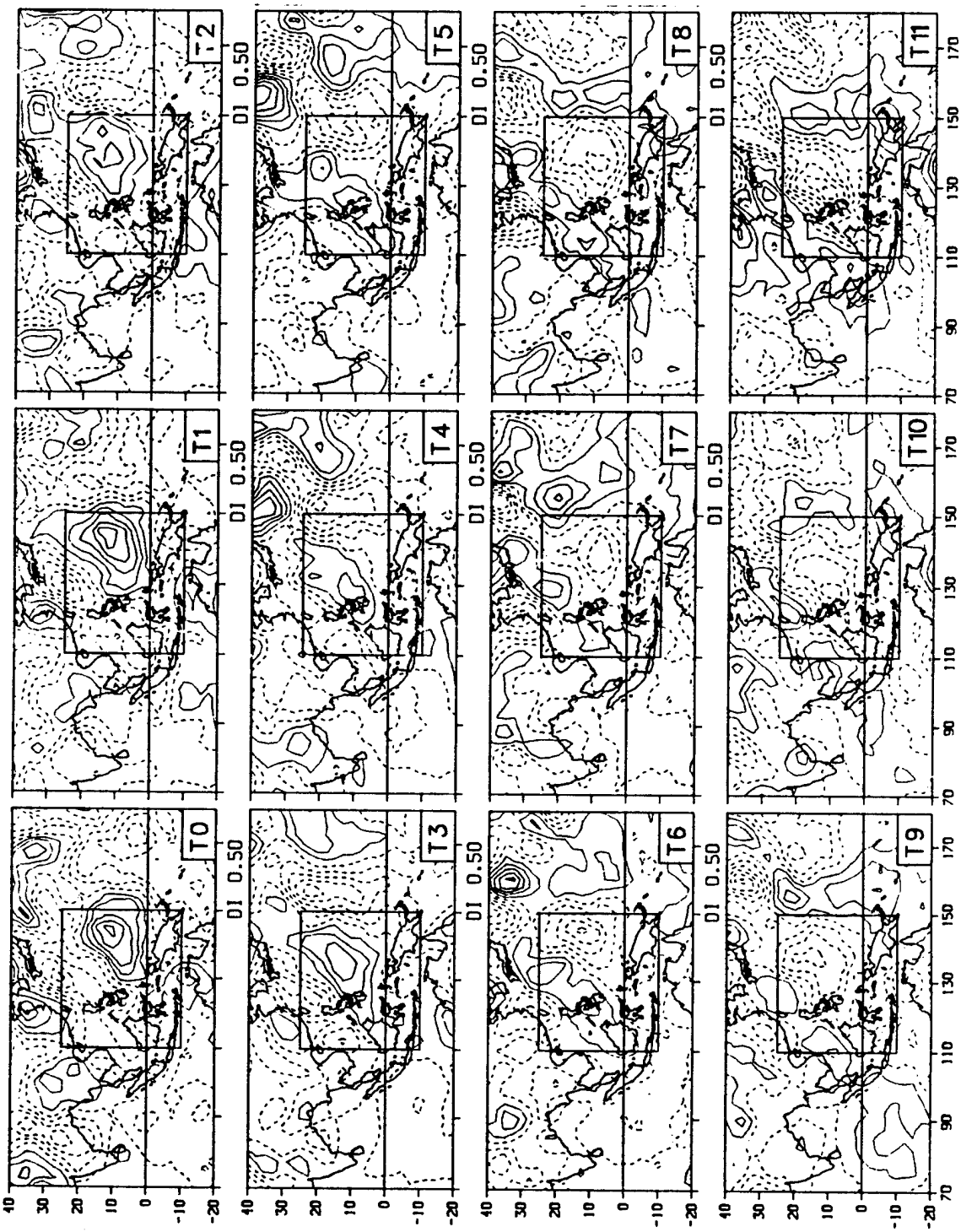

Figure 30: Same as Figure 26 except for v200

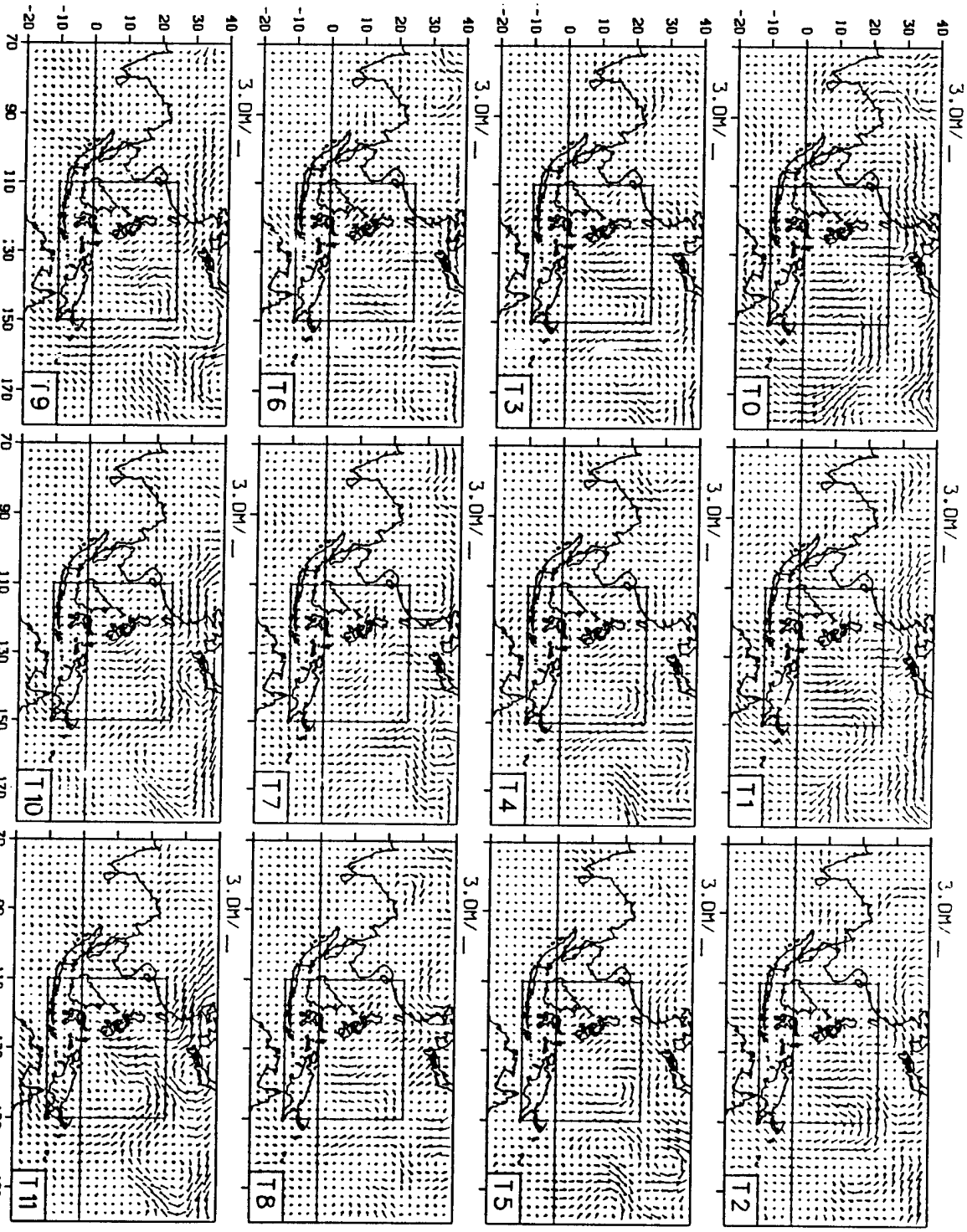

Figure 31: Same as Figure 27 except for v200

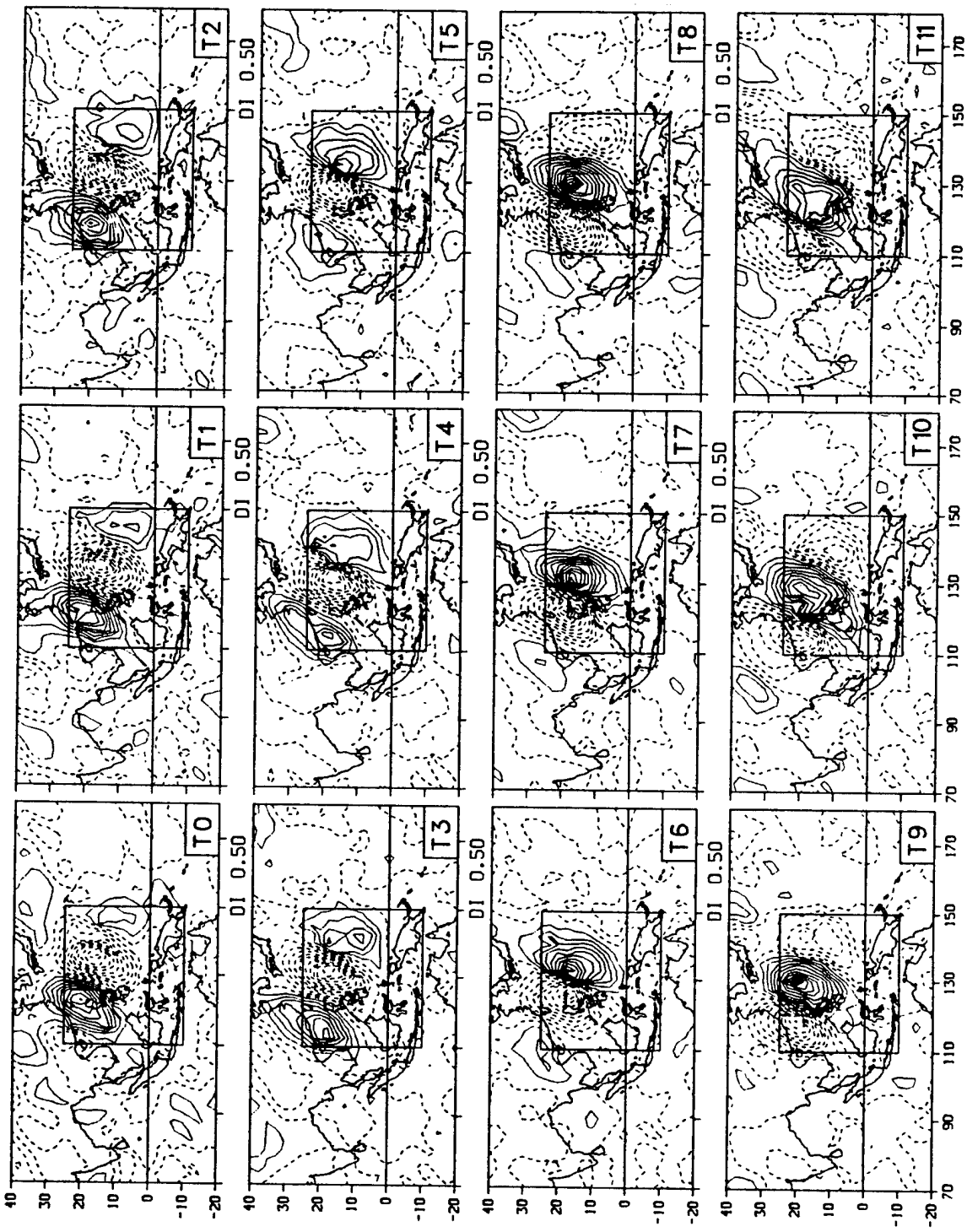

Figure 32: Same as Figure 26 except for Group A vsfc

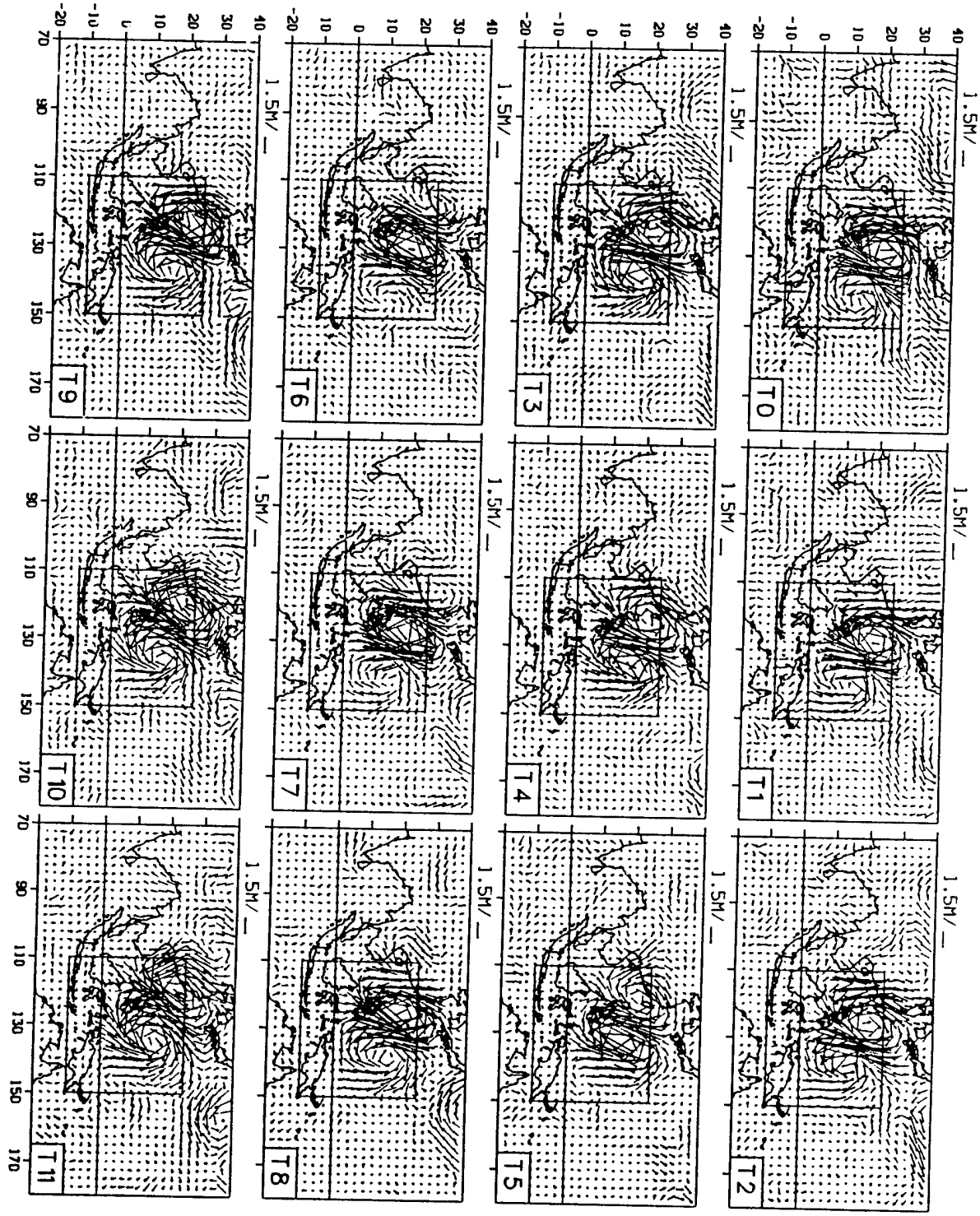

Figure 33: Same as Figure 27 except for Group A vsfc

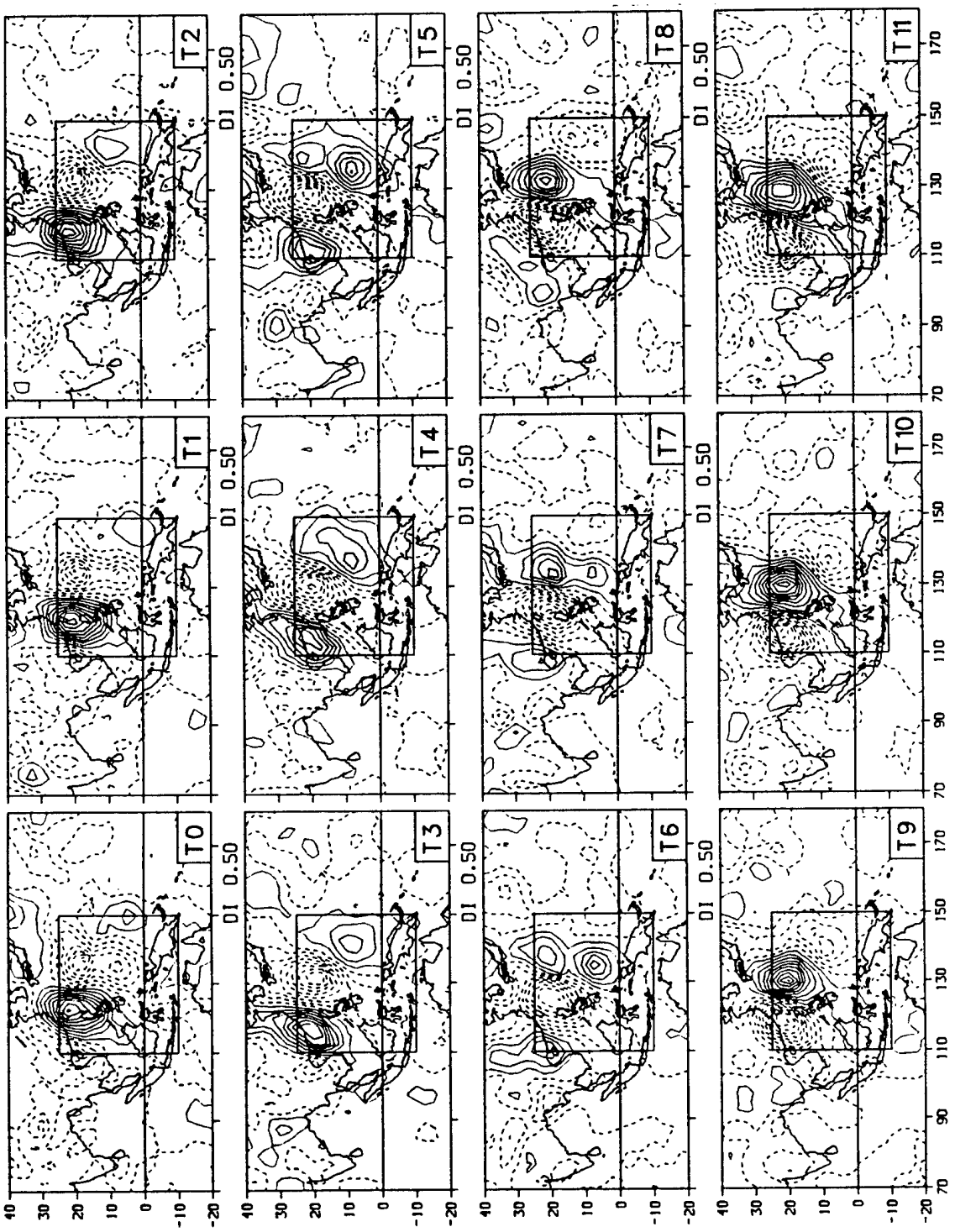

Figure 34: Same as Figure 26 except for Group A v700

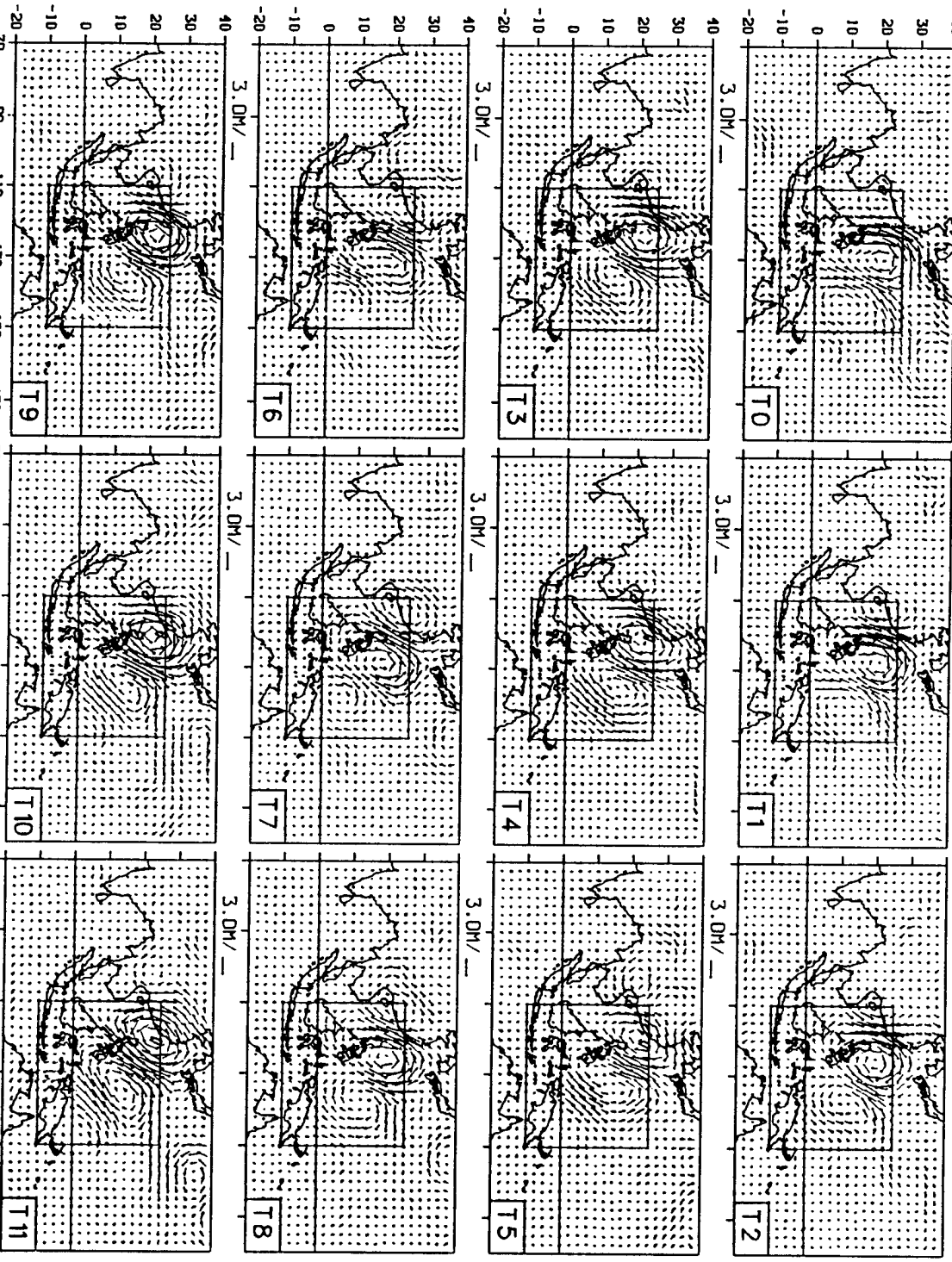

Figure 35: Same as Figure 27 except for Group A v700

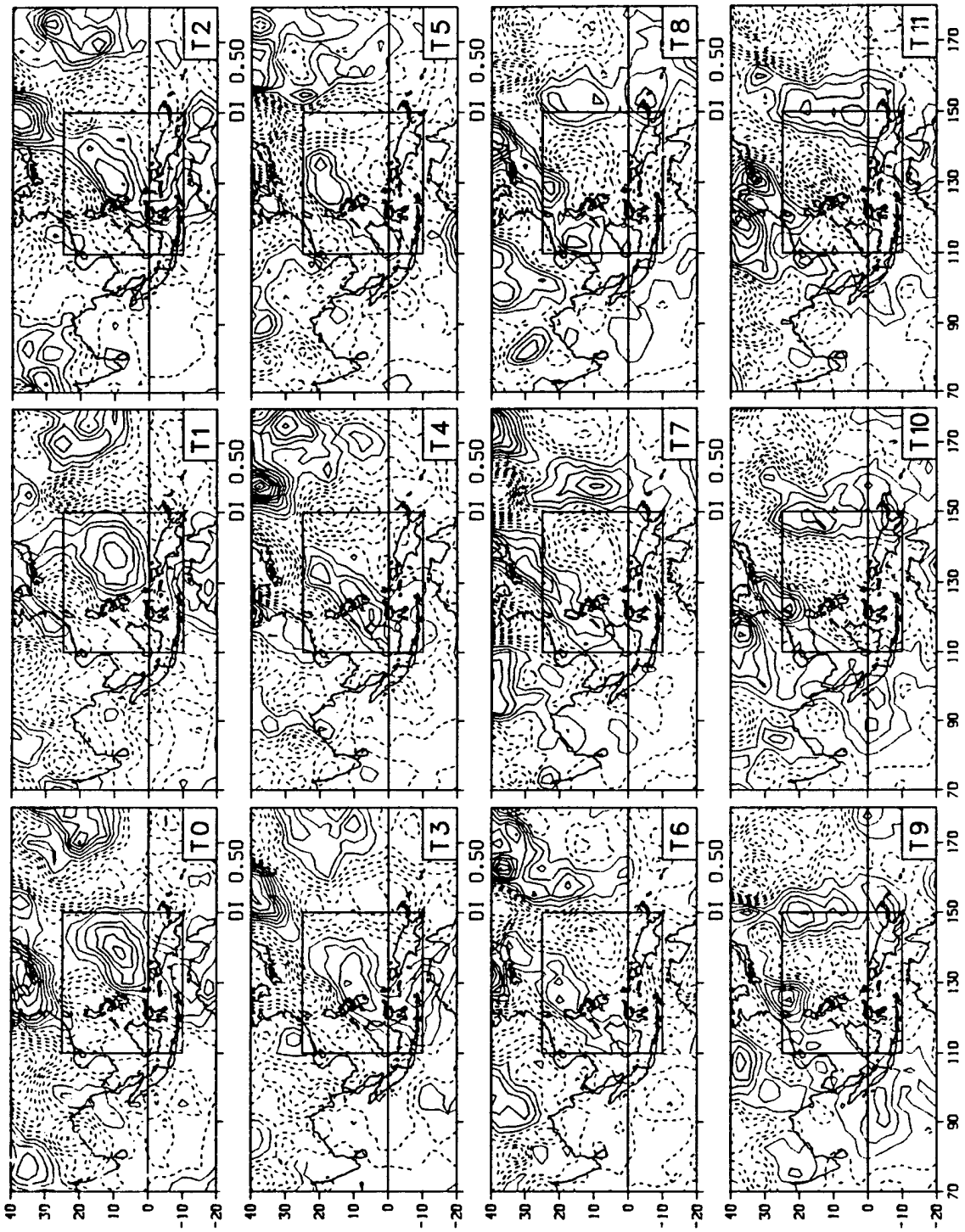

Figure 36: Same as Figure 26 except for Group A v200

Figure 37: Same as Figure 27 except for Group A v200

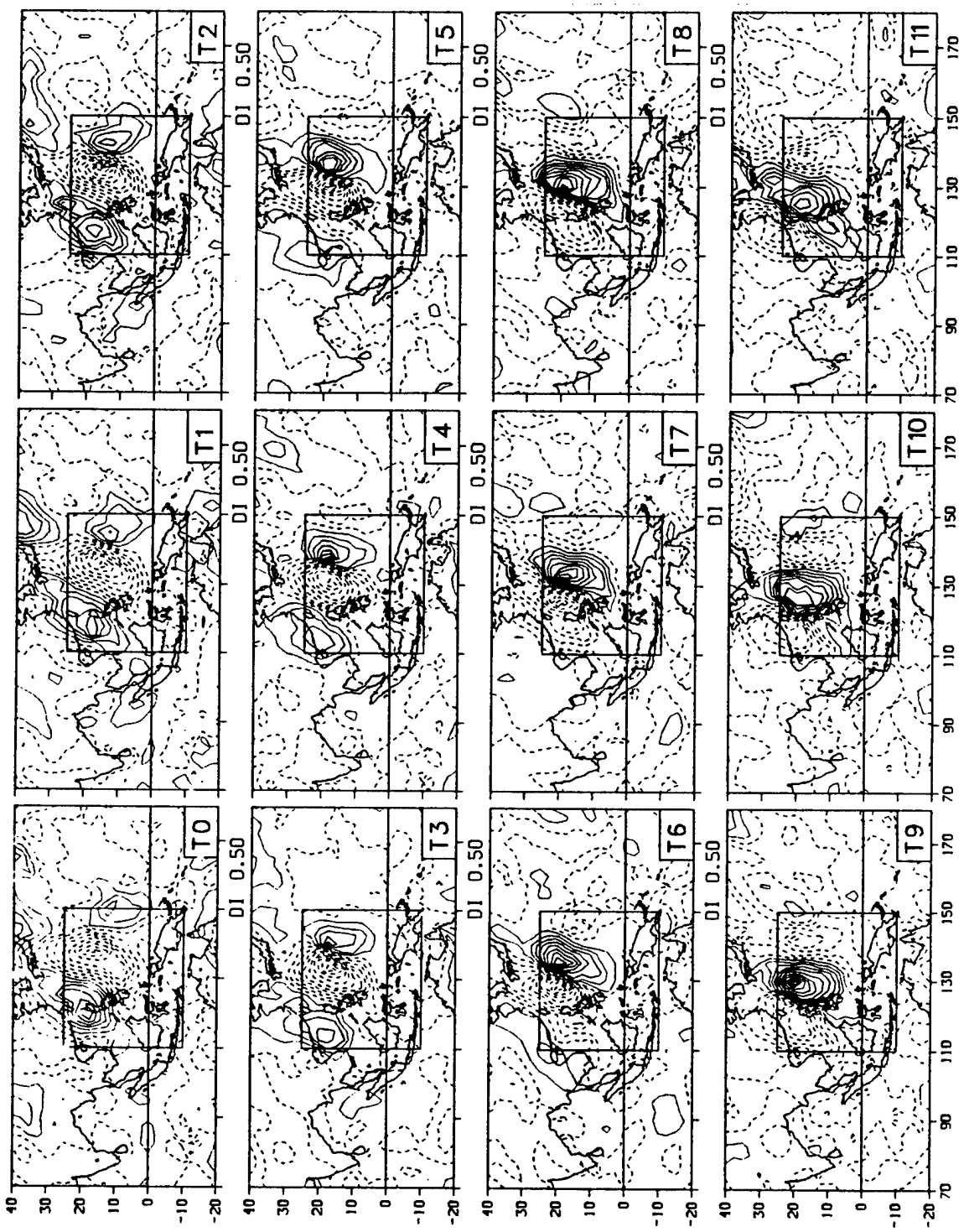

Figure 38: Same as Figure 26 except for Group B vsfc

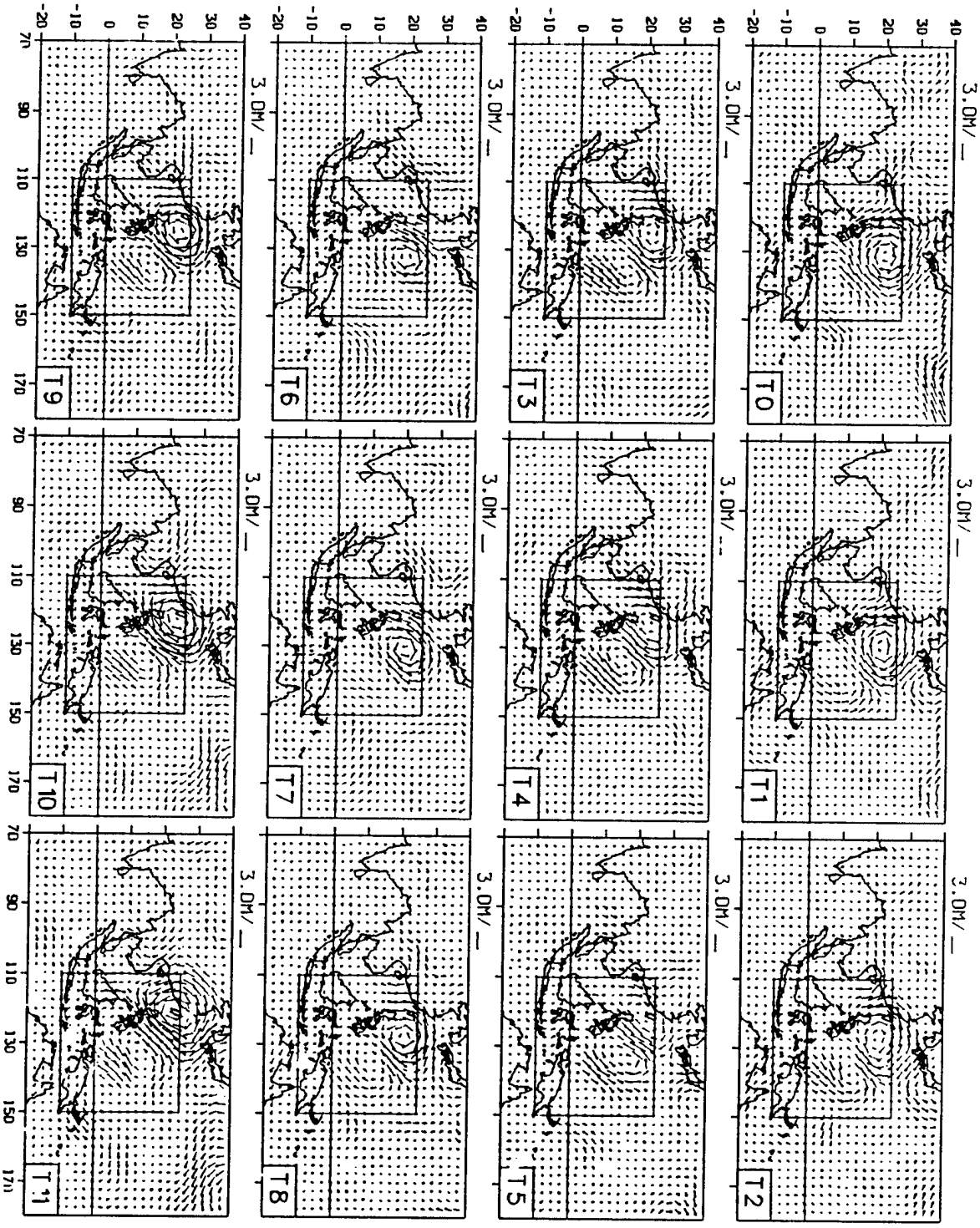

Figure 39: Same as Figure 27 except for Group B vsfc

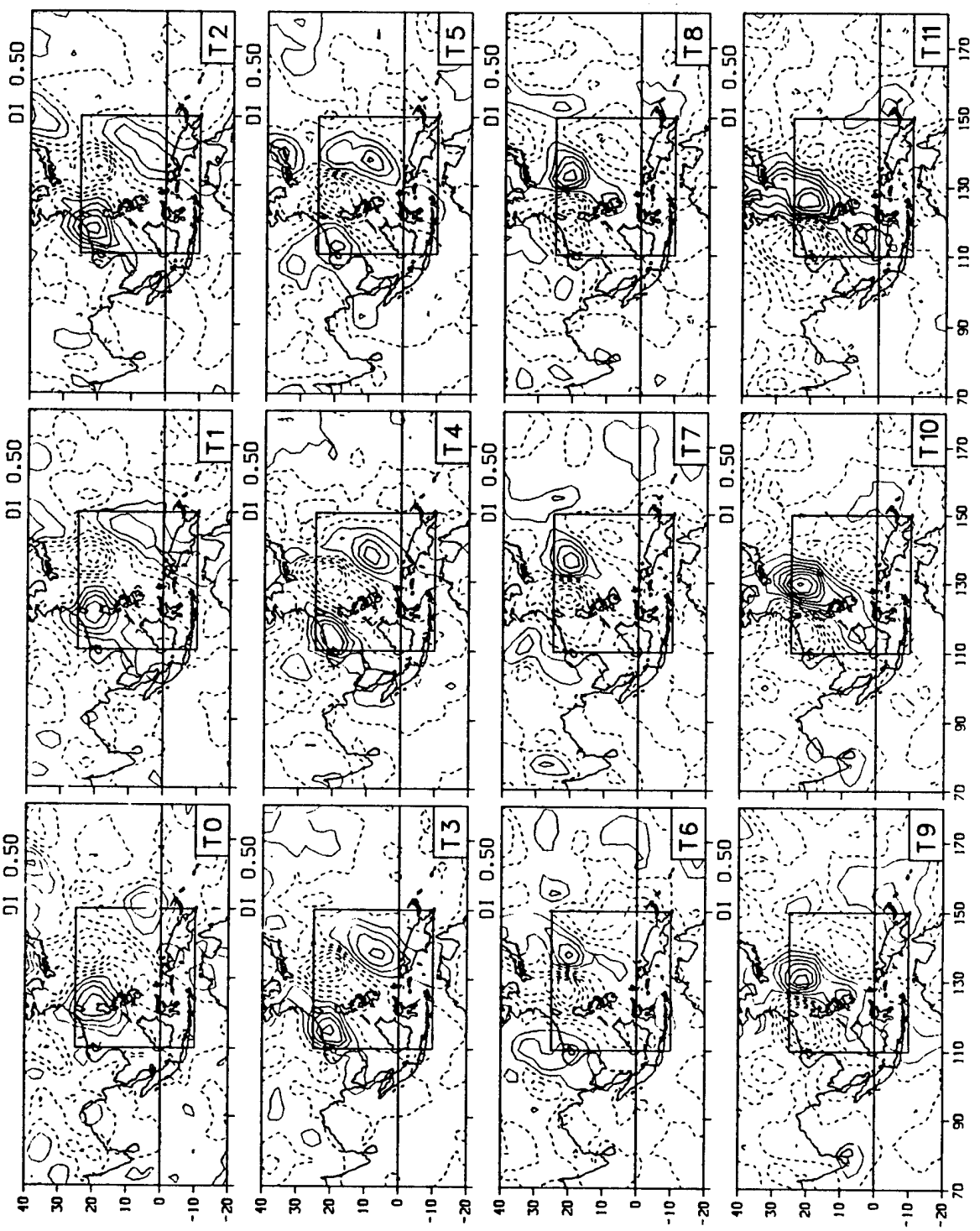

Figure 40: Same as Figure 26 except for Group B v70C

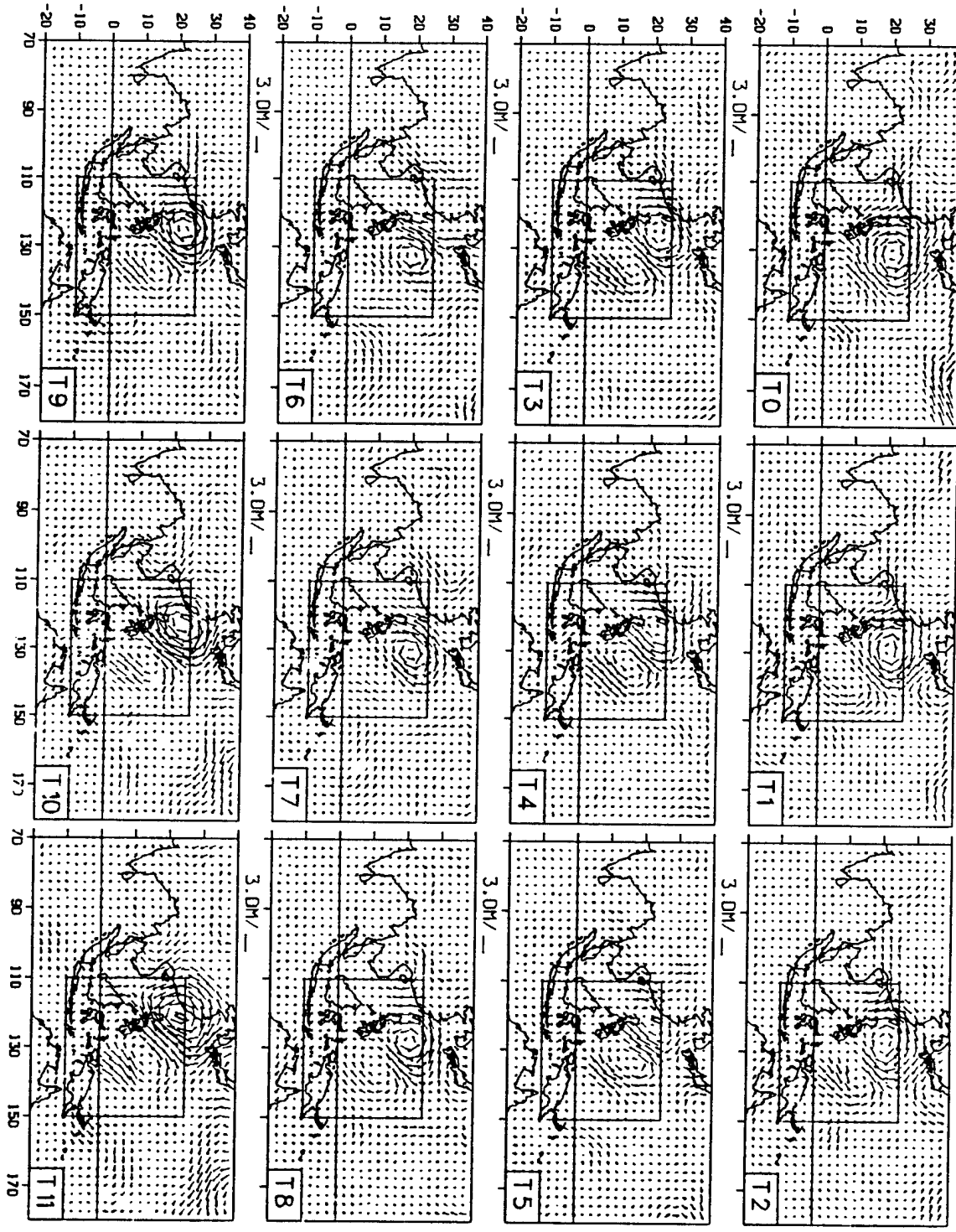

Figure 41: Same as Figure 27 except for Group B v700

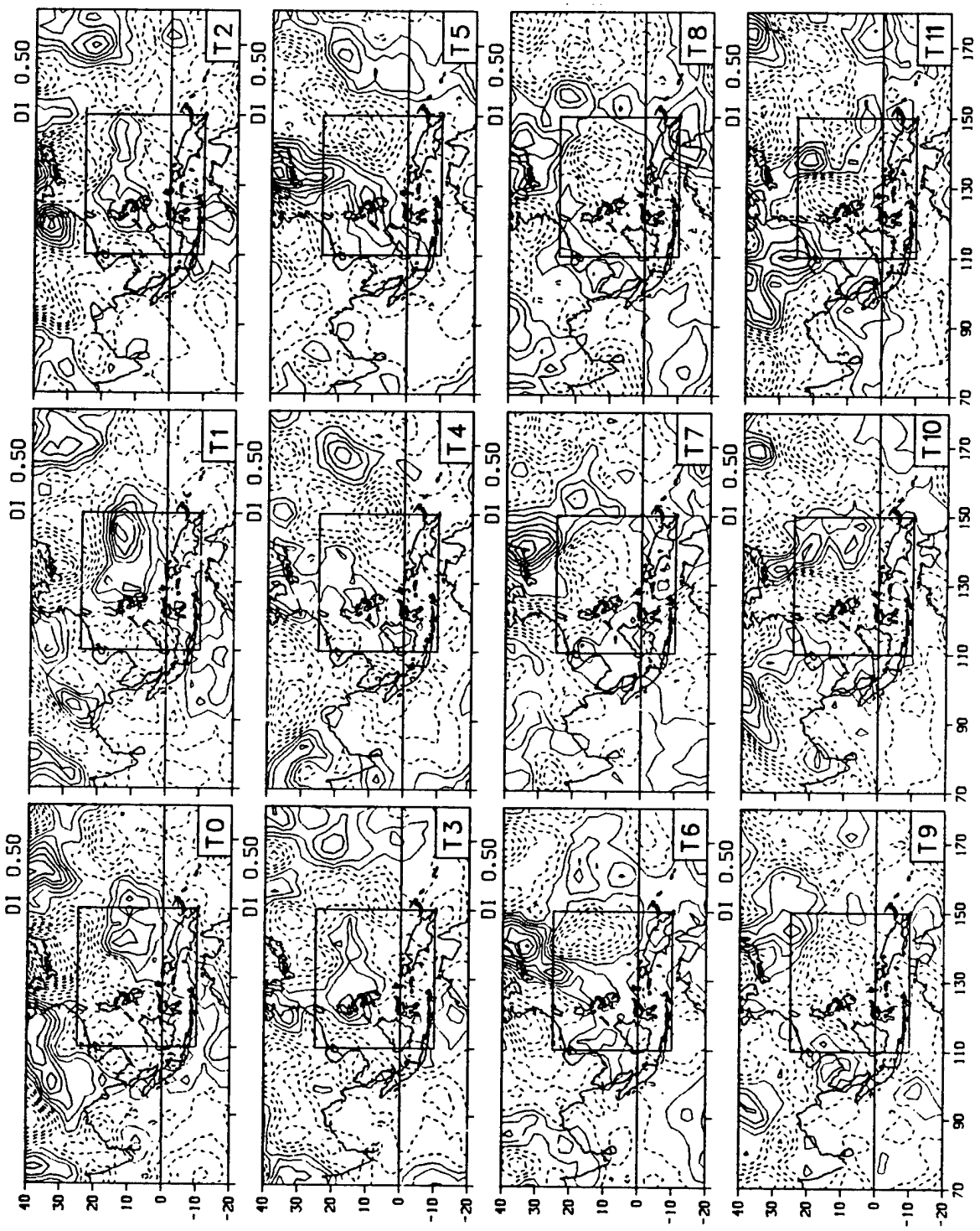

Figure 42: Same as Figure 26 except for Group B v200

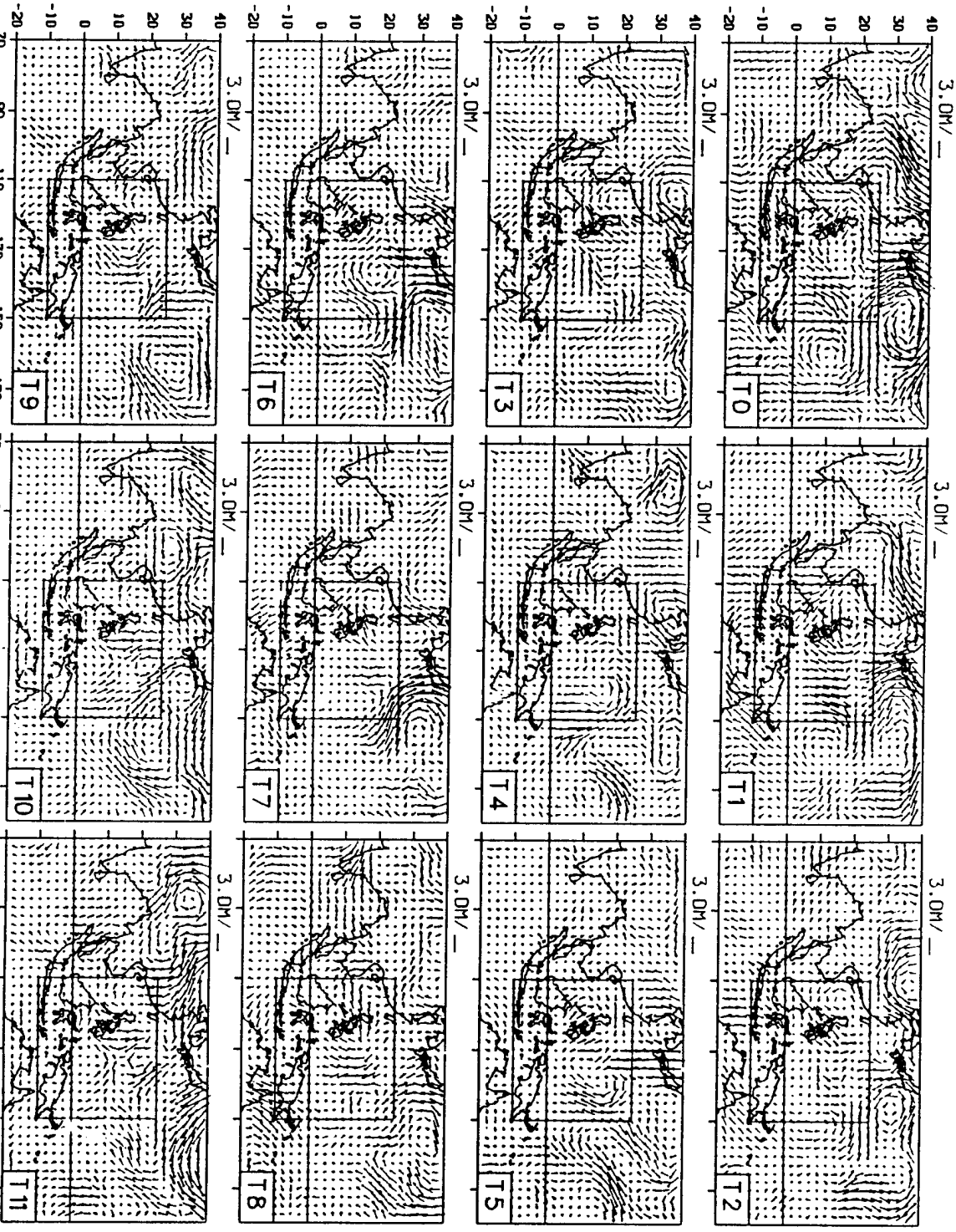

Figure 43: Same as Figure 27 except for Group B v200

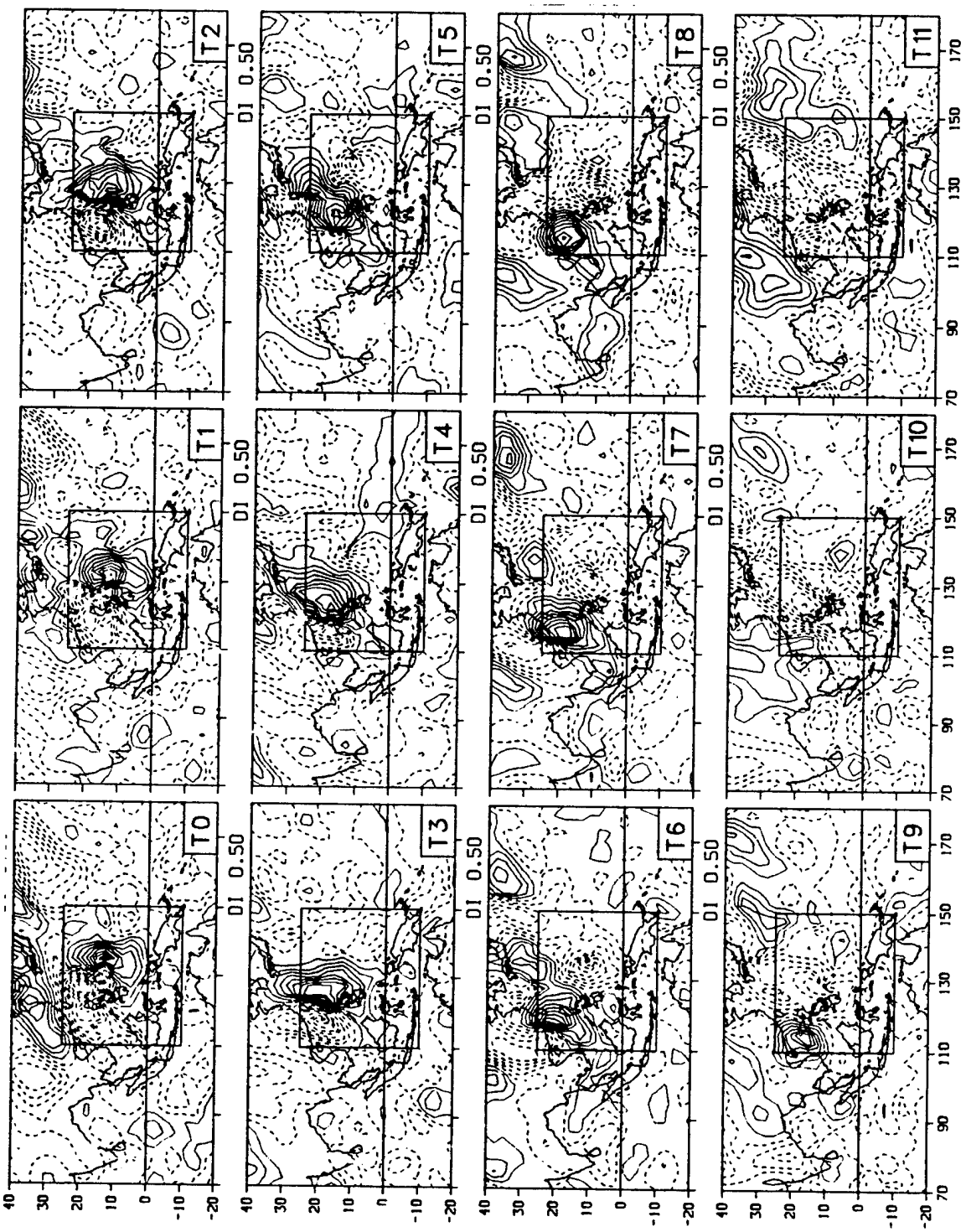

Figure 44: Same as Figure 26 except for Group C vsfc

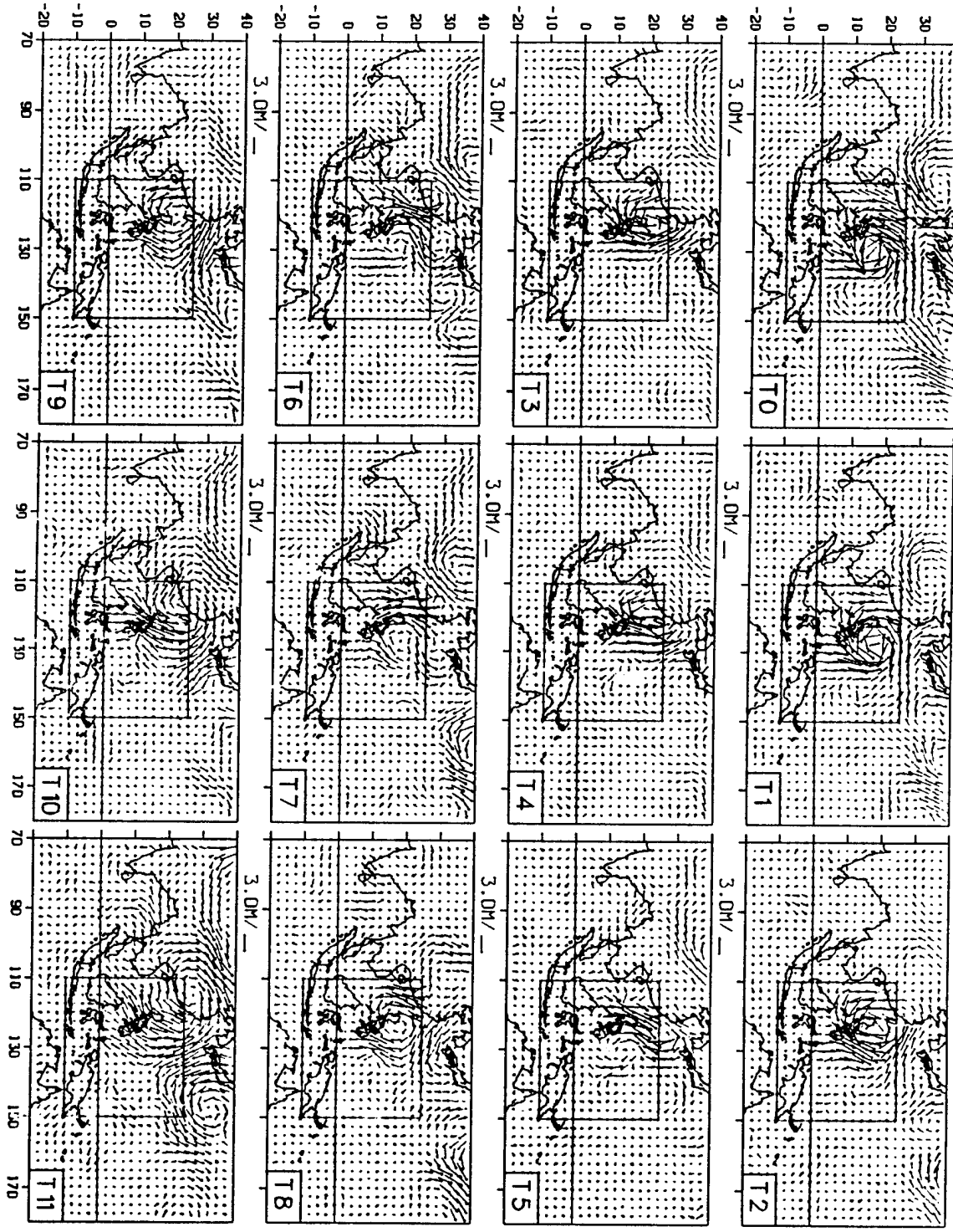

Figure 45: Same as Figure 27 except for Group C vsfc

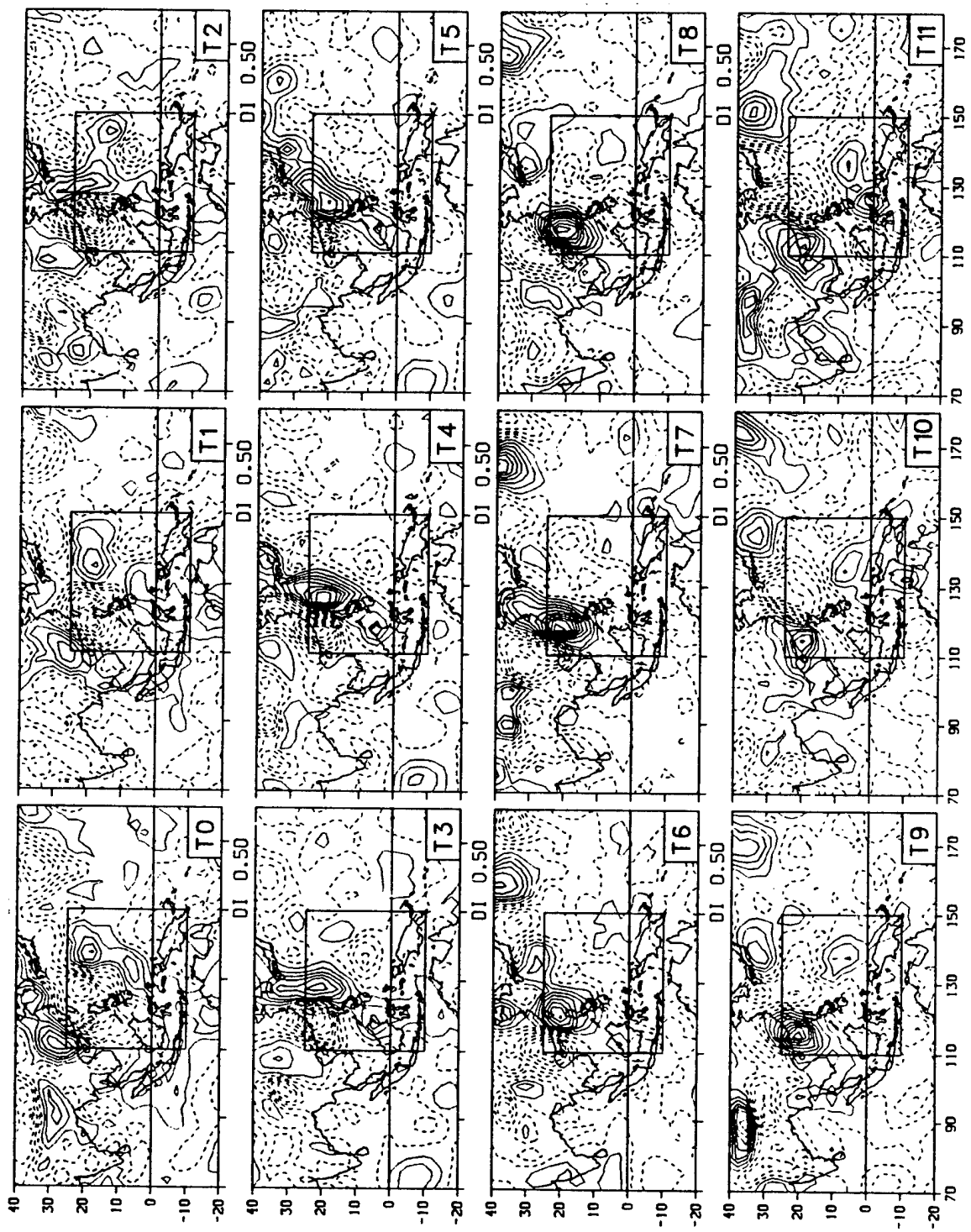

Figure 46: Same as Figure 27 except for Group C v700

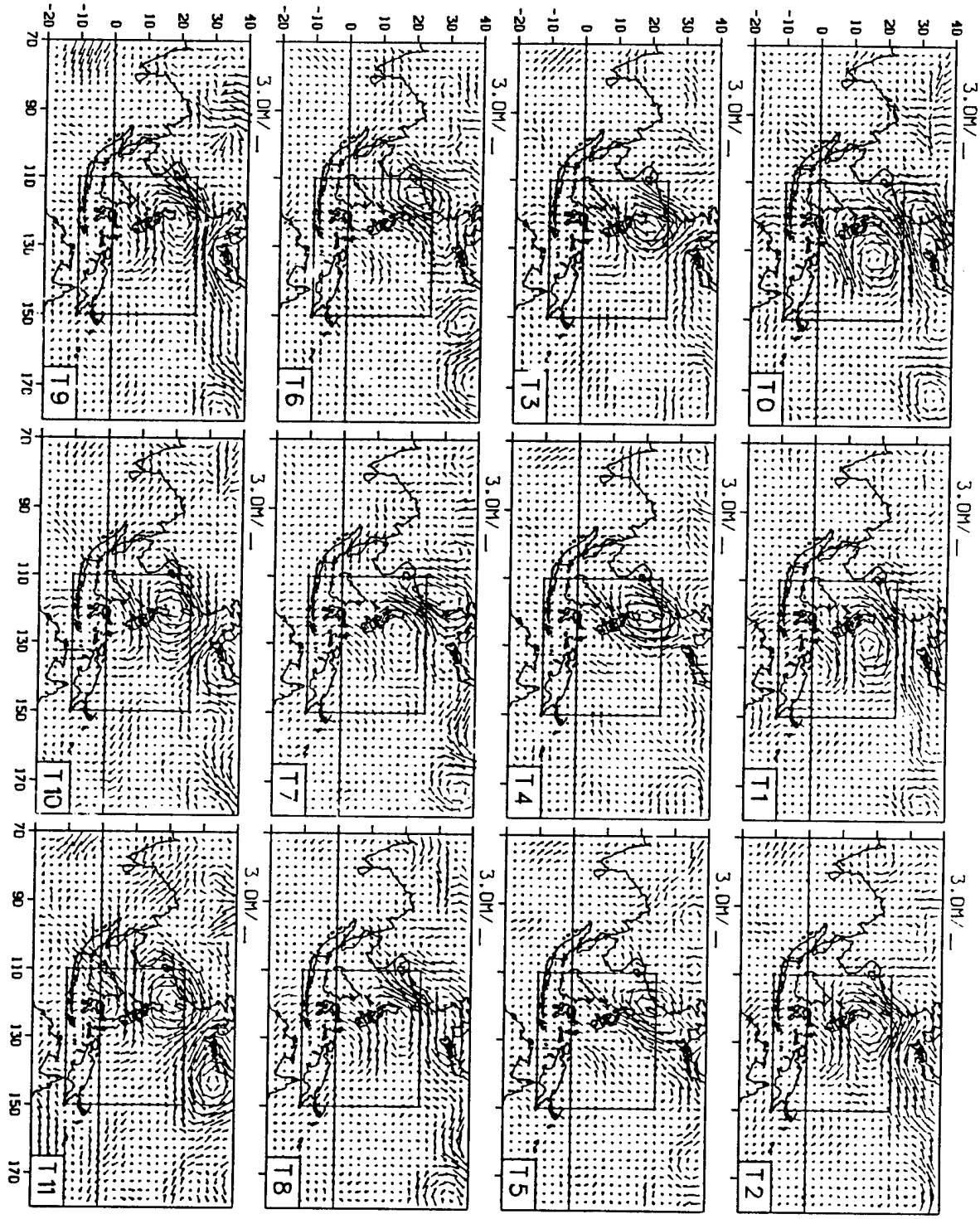

Figure 47: Same as Figure 27 except for Group C v700

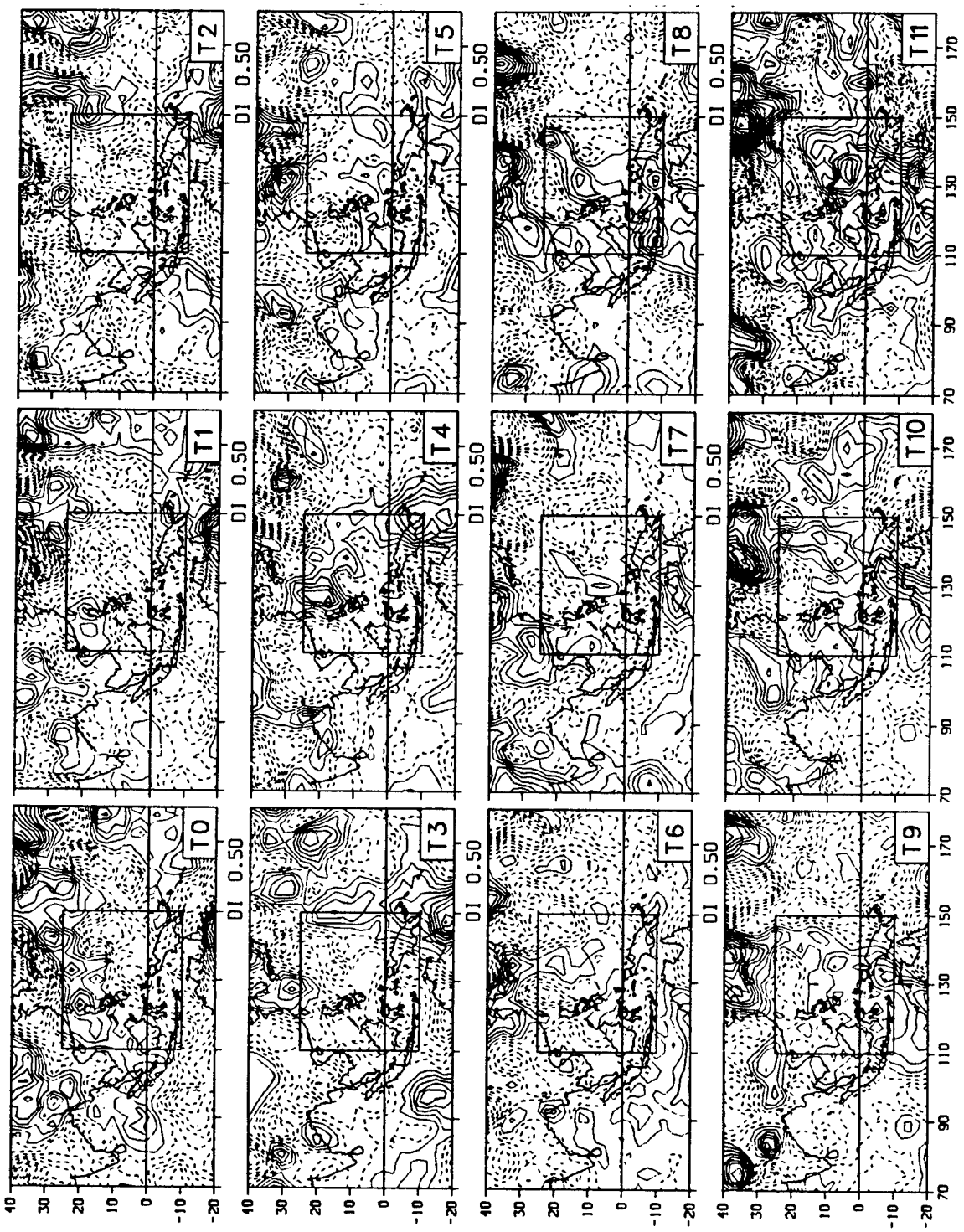

Figure 48: Same as Figure 26 except for Group C v200

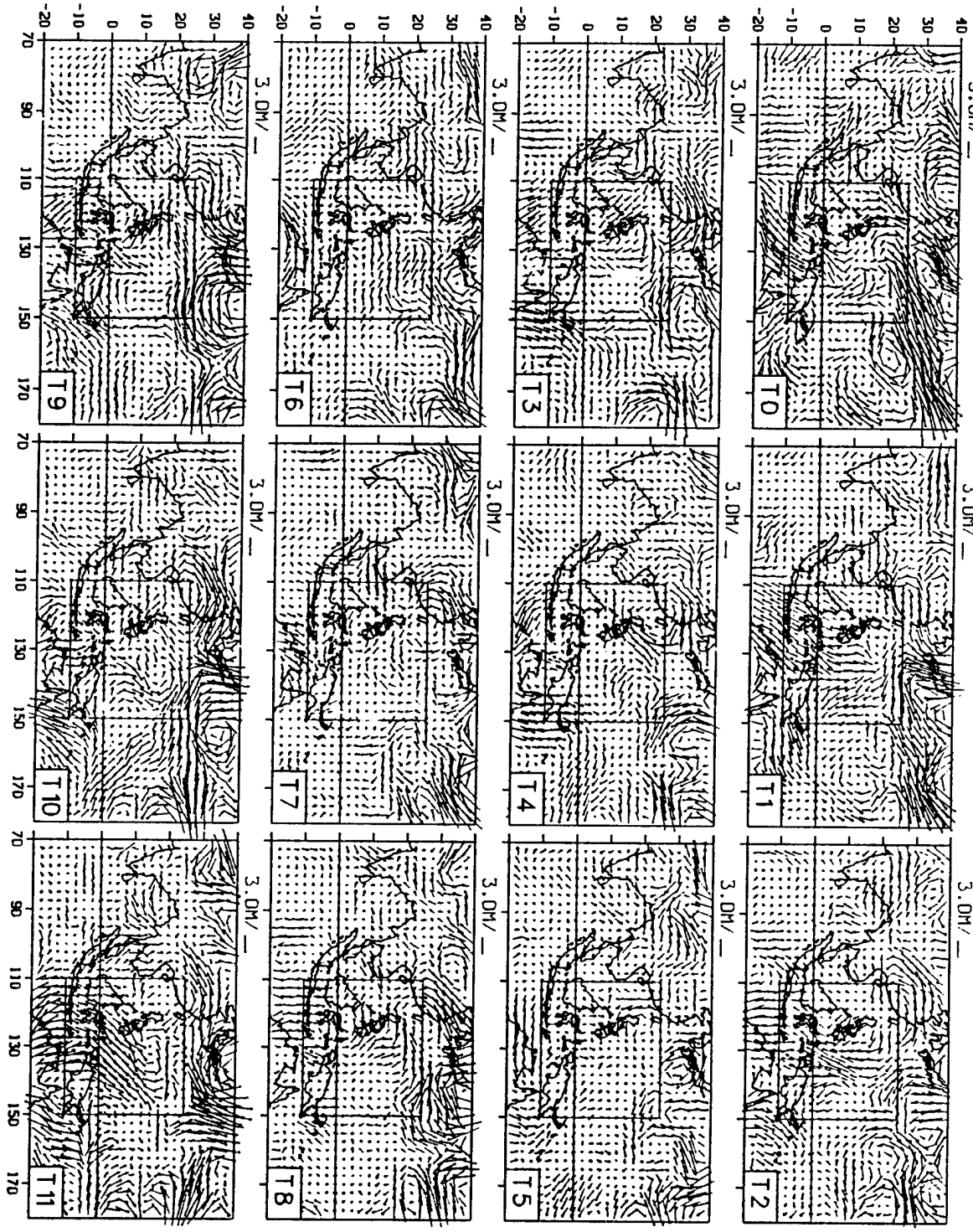

Figure 49: Same as Figure 27 except for Group C v200

VI. SUMMARY AND CONCLUSIONS

This research used the MCCA method to study the tropical summertime synoptic-scale disturbances over the northwestern Pacific that were contained in the 1974-1988 Navy tropical global band data. Two filters were applied to the data: 1) A high-pass filter with a harmonic cutoff at 20-days, which was applied to remove the strong influence of the persistence first guess, and 2) only the first 18 principal components (EOF's) over a core domain between 10°S-25°N, 110°-150°E, were kept for the MCCA. These 18 EOF's contain approximately 79% of the total variance. The two leading MCC modes of the surface meridional wind component over the core domain describe a northwestward propagating wave pattern with a northeast-southwest tilt, a wavelength of approximately 2500-3000 km and a period in the range of 6-12 days. These modes appear to be the associated with the same wave pattern that was observed by Chang et al (1995) in the northern summer 1989-1991 NOGAPS data using the same MCCA method. The averaged fractional variance for this leading mode pair is about 25% of the first 18 EOF's (20% of total high-pass variance), and the average correlation between consecutive 12-hour time fields is 0.87.

Single-year MCCA was performed on each of the 15 summers and the resulting leading mode structures are compared with the 15-year (15Y) modes. In six of the 15 years(Group A) the single-year mode resembles closely the 15Y mode with well-defined structure. The composite power spectrum of the Group A amplitude time series shows a sharp spectral peak at 8 days, which is similar to the 8-9 day peak found by Chang et al (1995). In another five years(Group B) the single-year MCC mode resembles the 15Y mode partially, with much of the same spatial scale. The

Group B composite power spectrum shows a broad range of high power between 6-12 days with peaks at 6 and 11 days, respectively. The last four years(Group C) have leading MCC modes that differ noticeably from the structure of the 15Y mode and from each other. The MCC modes computed from each of the three groups were compared to the 15Y modes. Group A shows the clearest defined wave pattern, Group B also shows a pattern that is more clearly defined than the individual-year modes of group B years. Even group C modes reveal patterns that are similar to the 15Y wave structure. Thus, the longer data sets apparently brings out better defined structures than the individual year data.

The wind structure over a larger domain encompassing the western Pacific and eastern Indian Ocean between 20°S-40°N, 70°E-180° was then computed using both a one-point correlation analysis and a composite analysis based on selected cases. Both were done for the 15-year data set as well as the three groups. The correlation pattern for the 15Y mode at the surface shows that the influence of the mode structure covers a larger area than the core domain, particularly up and downstream of the northwestward propagation track. As was done by Chang et al (1995), a search of the locations of tropical cyclone centers during times of moderate to large 15Y mode amplitudes were conducted and the locations were plotted in the correlation maps according to the phases of the leading MCC modes. Chang et al. conclud that these tropical cyclone centers tend to align along the cyclonic axis of the wave mode pattern. The same results were observed for the 15Y, and groups A and B modes, and, to a lesser degree, the group C modes.

For the 15Y mode as well as the group A and B modes, the wave structure is also reflected, to various degrees, in

the 700 and 200 hPa v-correlation maps. The 700 hPa structure is nearly in-phase with the surface v, and the 200 hPa, with lower correlation values, is approximately 1/4- to 1/2-cycle out of phase with the low levels. For group C the correlation at 700 hPa is weaker, and at 200 hPa it is ill organized.

The composite u,v-vectors for 15Y and the three groups were done by selecting moderate to strong cases based on the amplitude time series, in the same way as the search for tropical cyclone locations for the surface v correlation plots. The composite was with respect to the time lag from the large amplitude time points. For the 15Y and group A and B modes, the surface and 700 hPa show couplets of cyclonic-anticyclonic circulations that propagate northwestward through the core domain. At 200 hPa the propagation pattern contains alternating divergence and convergence zones that tilt northeast-southwest. These patterns indicate that the wave motions are associated with strong convective activity, which is consistence with the frequent presence of tropical cyclones. Both group A and B composites show stronger velocities on the 200 hPa than the 15Y composite. Group C, as expected, did not show consistent organized patterns at 200 hPa.

The different characteristics between the 11 years of groups A and B, and the four years of group C, also transpire in the comparison of case selections between the 15Y modes and the group modes shown in Table 3. The majority of the groups A and B cases (62 out of 74) coincide (T0 within ±12 h) with the 15Y cases (62 out of 70) selected in the A-B years. On the other hand, none of the 19 group C cases coincide with any of the 20 15Y cases selected in the Group C years. It is therefore apparent that the 11 A-B years possess strong signals of the northwestward

propagating mode, while the 4 C-years do not.

A strong correlation between tropical cyclone location and the leading 15Y mode was found. Tropical cyclone track characteristics are known to vary significantly between different flow regimes. The tracks in the northwestern Pacific may be classified as straight-movers, recurvers, or erratic (Harr and Elsberry, 1995). The climatological straight track is more or less along the northwestward propagating wave track. It may be conceivable that during years of mainly straight tracks, signals of the northwestward propagating pattern is stronger, and during years of mainly non-straight tracks the signals will be weaker. Thus, during years of substantial erratic-track tropical cyclone activity the organization of the wave mode may be expected to be the weakest. In order to see whether the interannual variation in the manifestation of the northwestward propagating wave pattern may be related to the track characteristics, we compare the tropical cyclone forecast errors with the wave mode characteristics each year. The hypothesis here is that erratic tropical cyclone tracks are the most difficult to forecast. Therefore, large 72-h forecast error indicates more erratic behavior.

Table IV lists this comparison where the 72h official forecast errors are extracted from the Annual Tropical Cyclone Report of JTWC. It is immediately apparent that there is no systematic trend for the group A years to have smaller errors or group C years to have larger errors. The only possible indication of a relation is 1978, which has the smallest variance in it single-year leading MCC modes (whose 8% variance is 1/3 to 1/5 of the other 14 years' values). The 1978's mean 72-h error for typhoons was 459 n. mi, which is the largest among the 15 years. The JTWC annual report for 1978 also pointed out that it was a year

YEAR	GROUP	72-HOUR	
		ALL	TYPHOON
1974	B	348	357
1975	A	450	442
1976	C	338	336
1977	A	407	390
1978	C	410	459
1979	A	316	319
1980	B	389	362
1981	B	334	342
1982	B	341	337
1983	B	405	384
1984	C	363	361
1985	A	367	355
1986	A	394	403
1987	A	303	318
1988	C	315	327

Table IV:Annual mean forecast errors (NM)

Western North Pacific

with unusual, erratic typhoon tracks. However, for 1978 the mean 72-h error for all tropical cyclones (410 n. mi) is less than 1975 (450 n. mi), which is a group A year. The 1978 mean error is also comparable to 1977 (407 n. mi), which is another group A year. Therefore, the organization of the northwestward propagating wave pattern does not seem to be related to 72-h mean forecast errors. On the other hand, the mean forecast error could be affected significantly by a few bad forecasts. In future studies, detailed evaluation and comparison of the tropical cyclone

track characteristics for the different groups are desirable.

The present data set uses persistence as the first guess and therefore its quality is questionable in data-sparse areas. New numerical weather prediction (NWP)-based, four-dimensional data assimilation datasets have the advantage of model forecasts as the first guess, but the length of available data sets is relatively short. Major NWP centers are now producing reanalyzed data fields that start in the late 1970's. Future investigations of the northwestward propagating wave pattern may be conducted with these improved climatological datasets when they become available. In these reanalyzed fields all variables at all standard levels are available for a detailed analysis, and the results will not be affected by the operational bogus procedures. Hopefully, more understanding of the nature of the northwestward propagating waves and their relationships with the tropical cyclones can be obtained.

APPENDIX. INDIVIDUAL YEAR MCC MODE #1 STRUCTURE

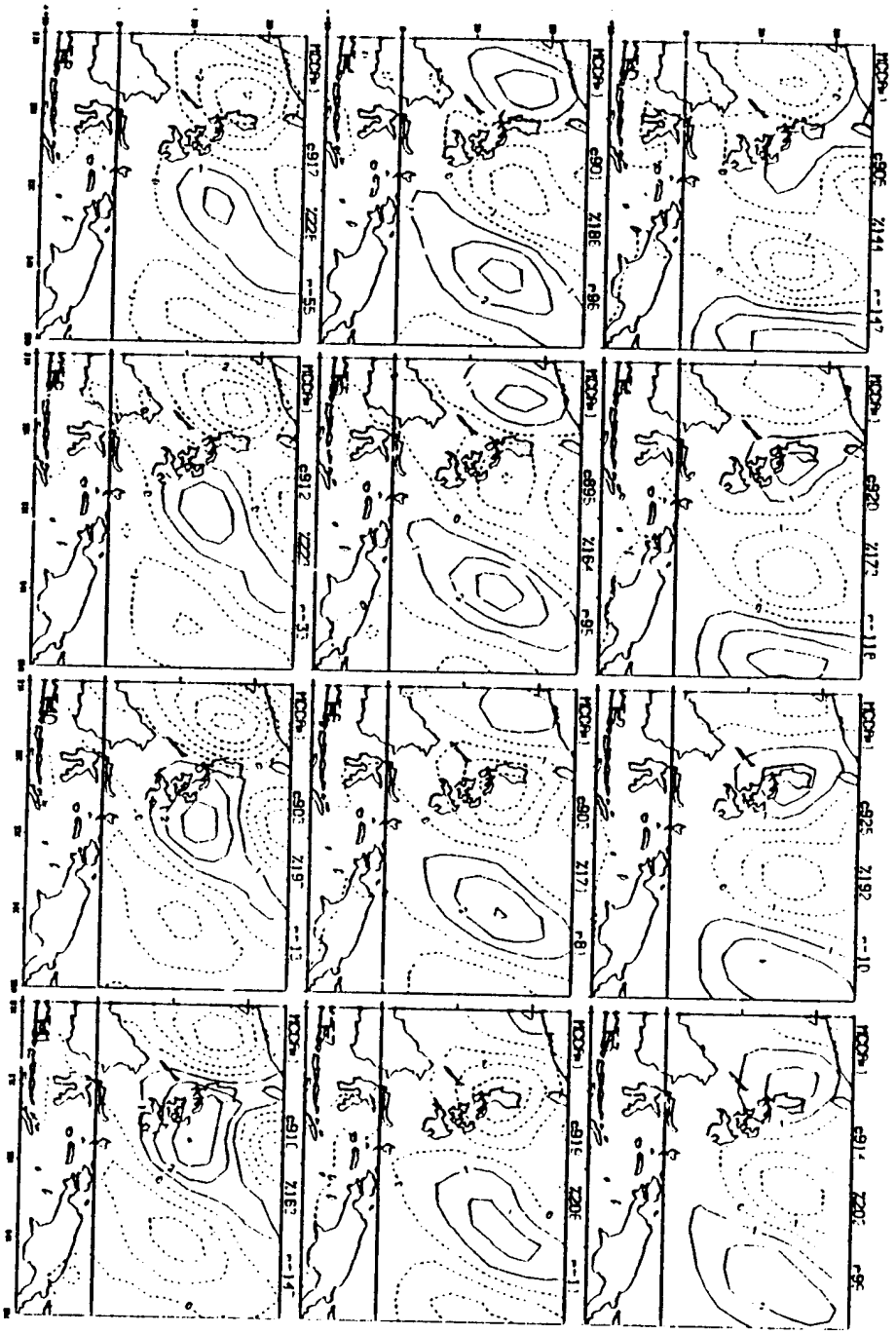

Figure A1: Weighting function for individual years(1974) MCC mode#1(equivalent to MCC mode#1 structure) of surface meridional wind(v) for 12 consecutive 12-hour frames from 00h to 132h(5.5 day). Contour interval is 0.06 and dashed lines correspond to northerly winds when MCC mode#1 amplitude is positive.

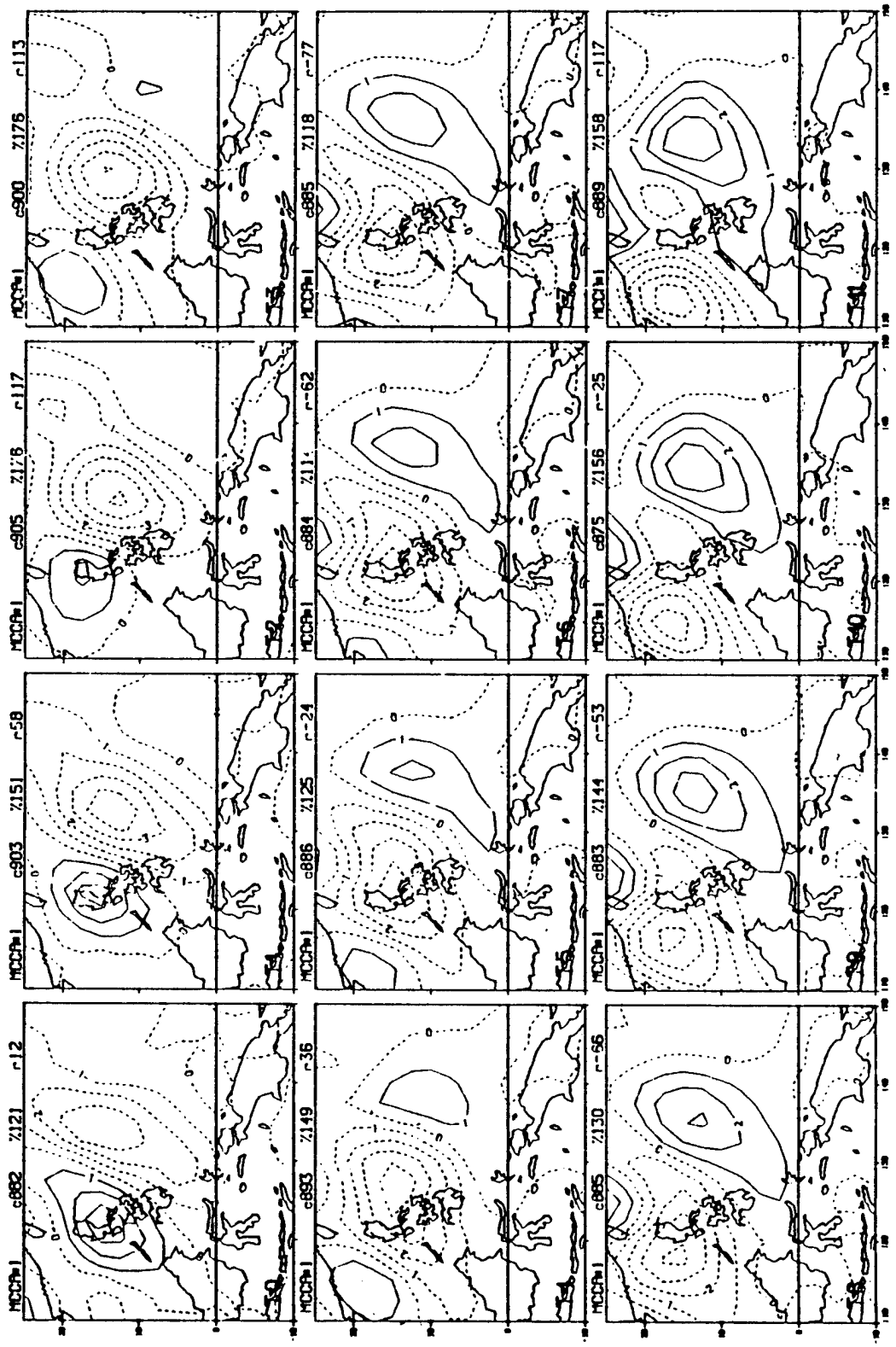

Figure A2: Same as Figure A1 except for year 1974

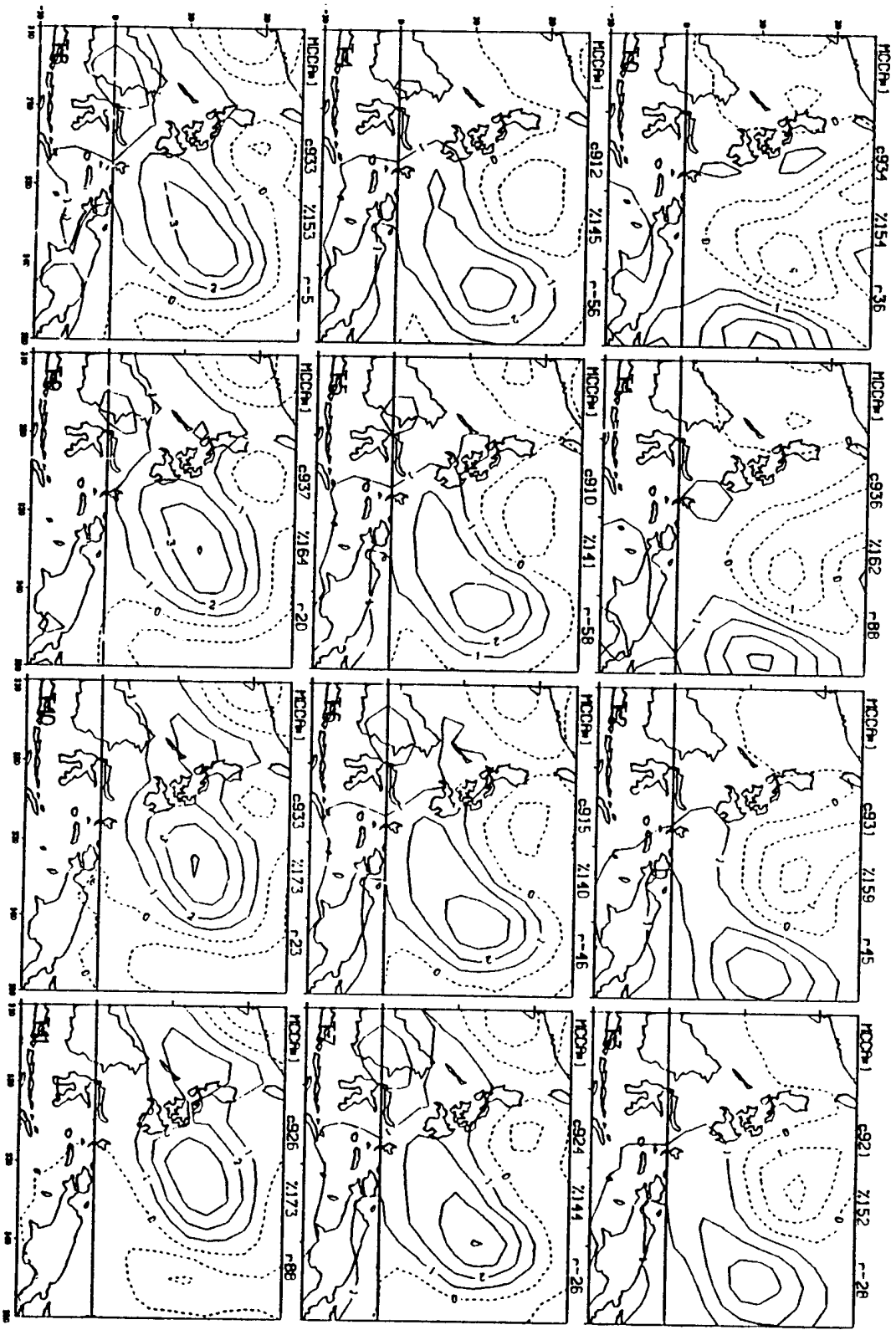

Figure A3: Same as Figure A1 except for year 1976

Figure A4: same as Figure A1 except for year 1977

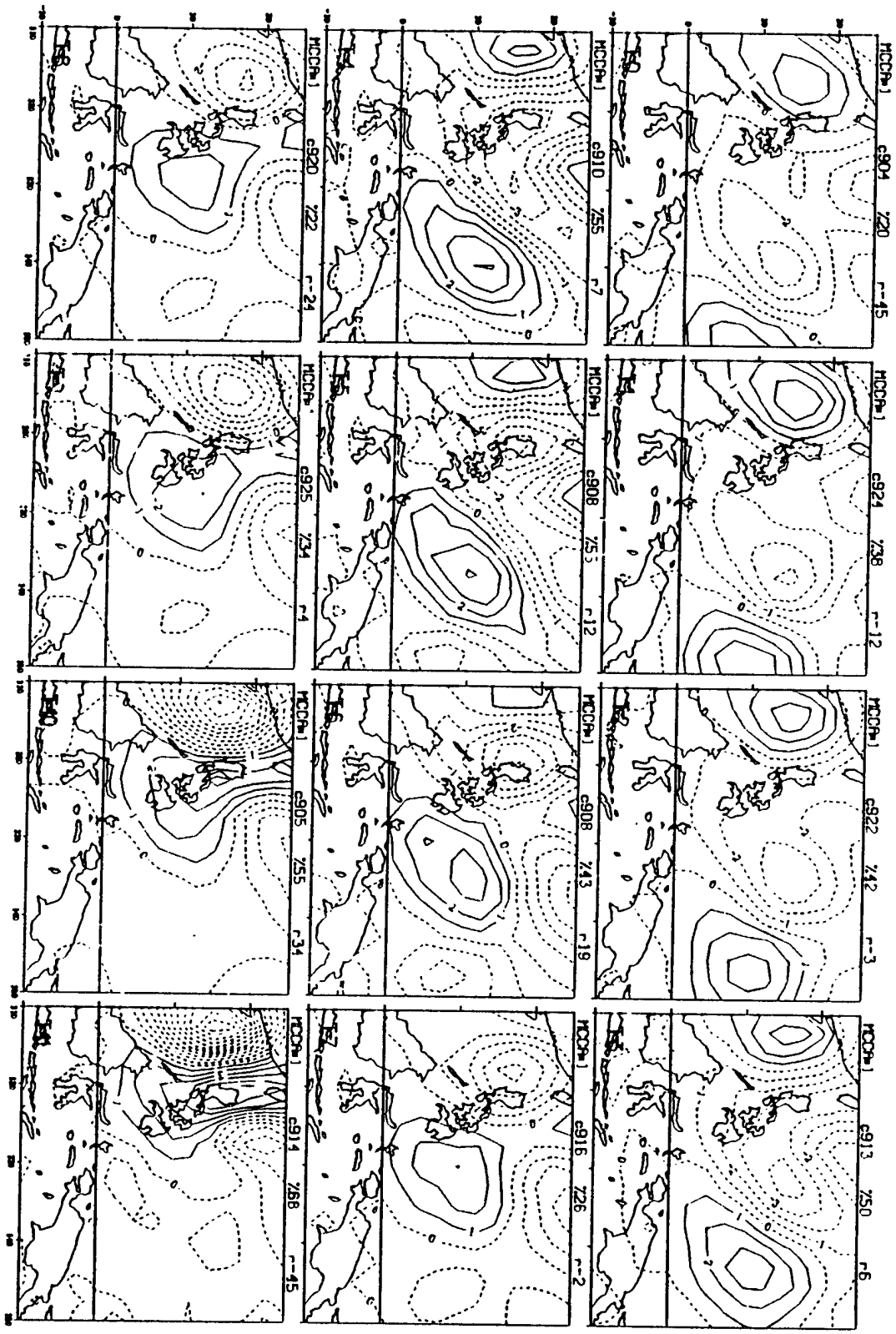

Figure A5: Same as the Figure A1 except for year 1978

Figure A6: Same as Figure A1 except for year 1979

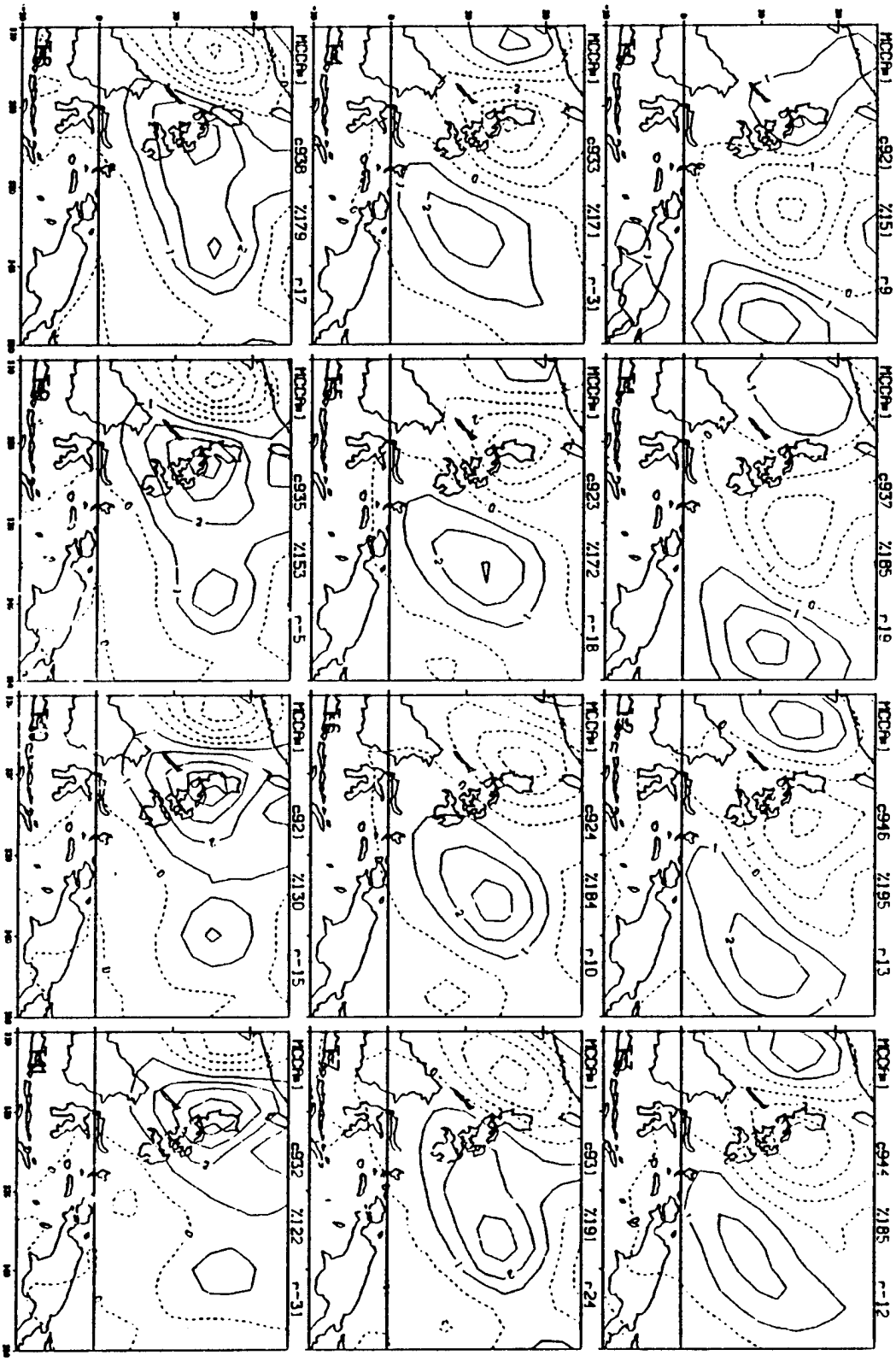

Figure A7: Same as Figure A1 except for year 1980

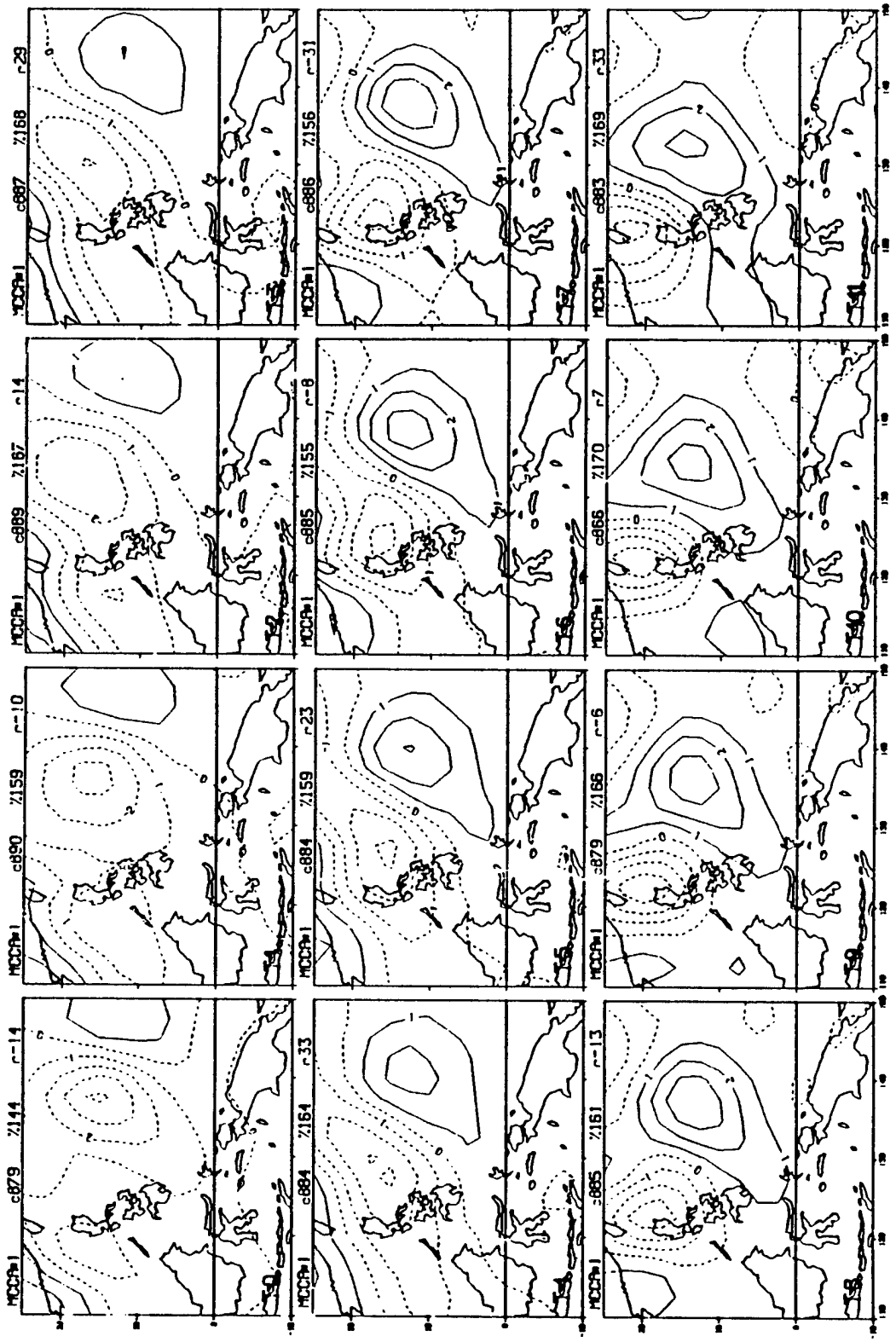

Figure A8: Same as Figure A1 except for year 1981

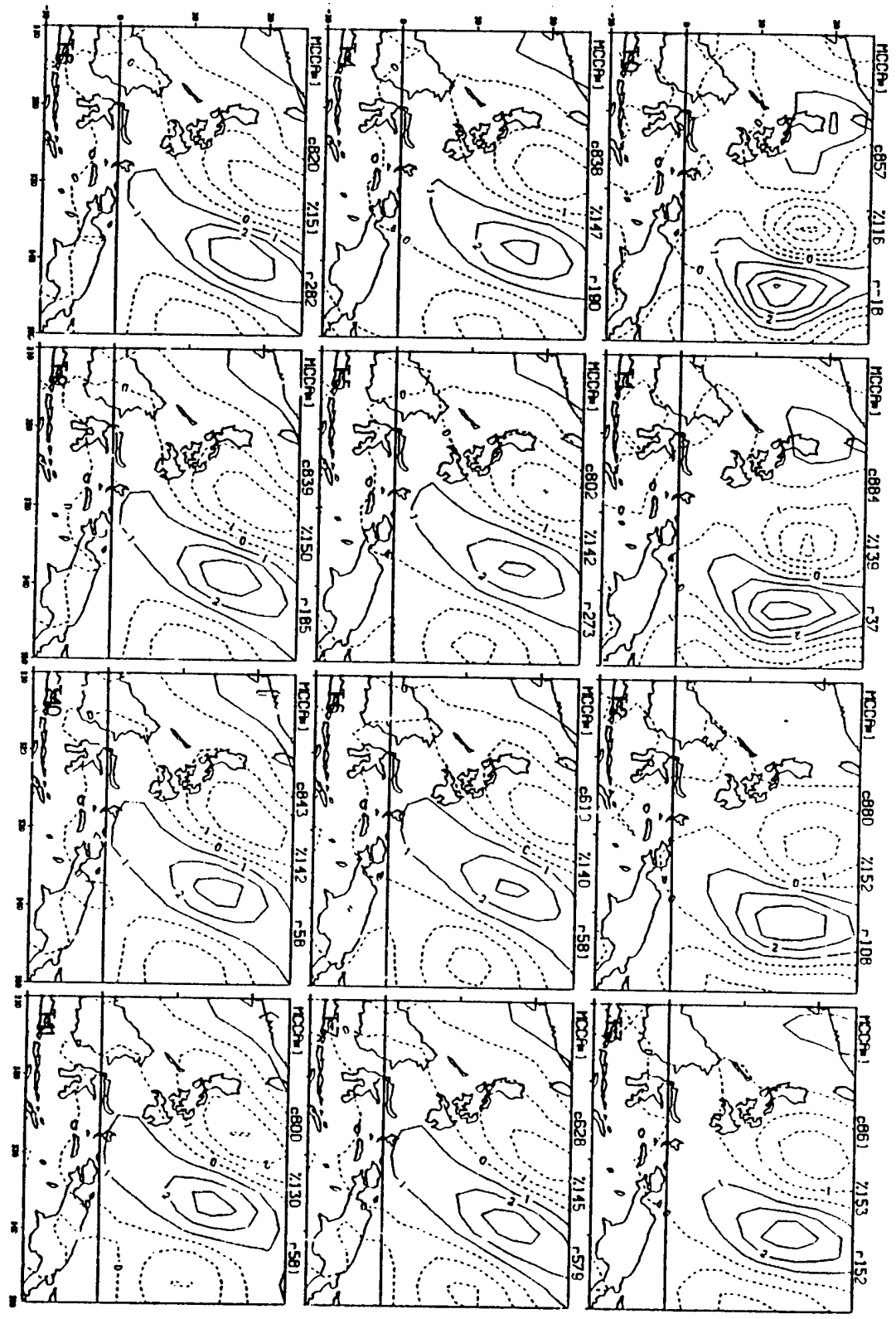

Figure A9: Same as Figure A1 except for year 1982

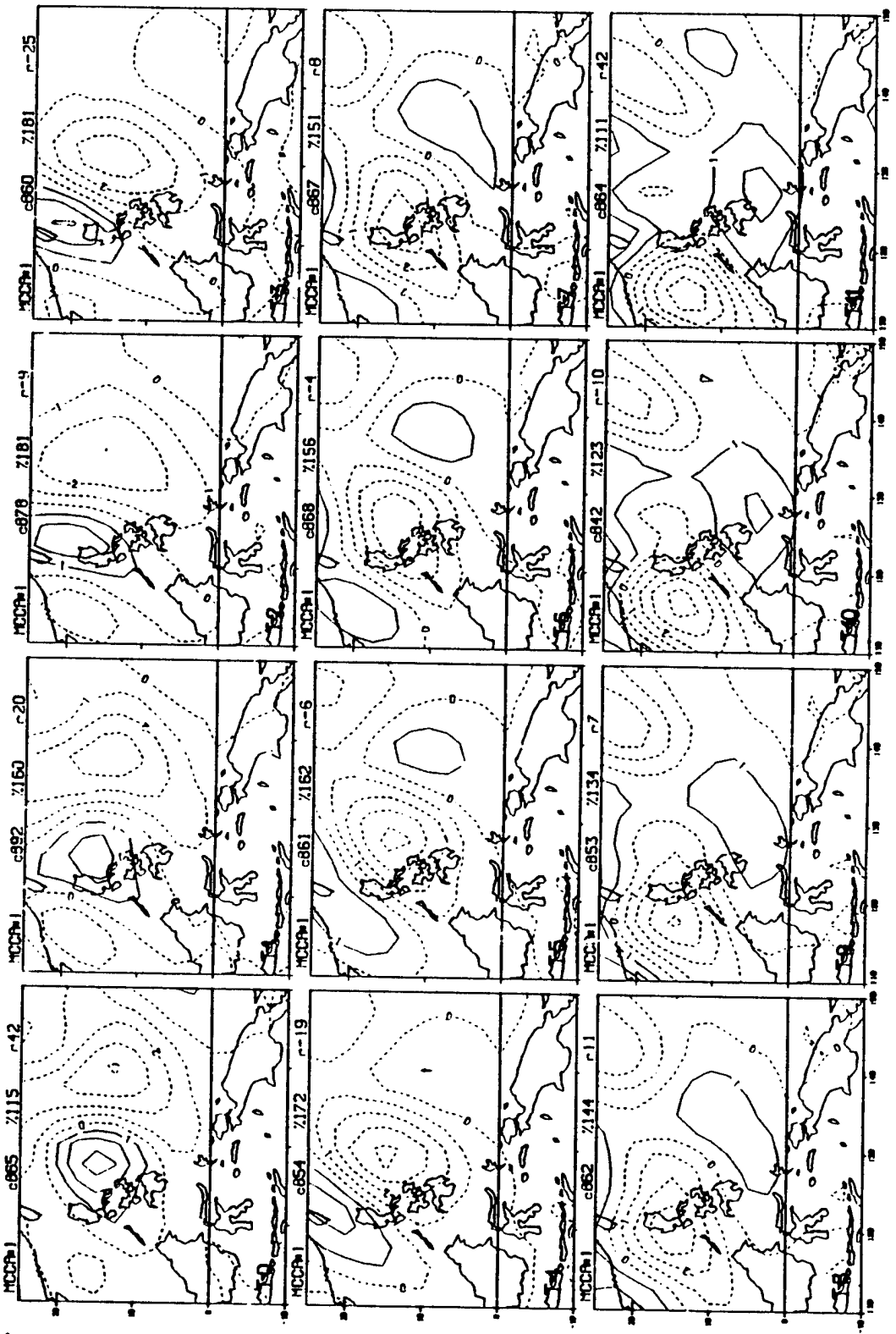

Figure A10: Same as Figure A1 except for year 1983

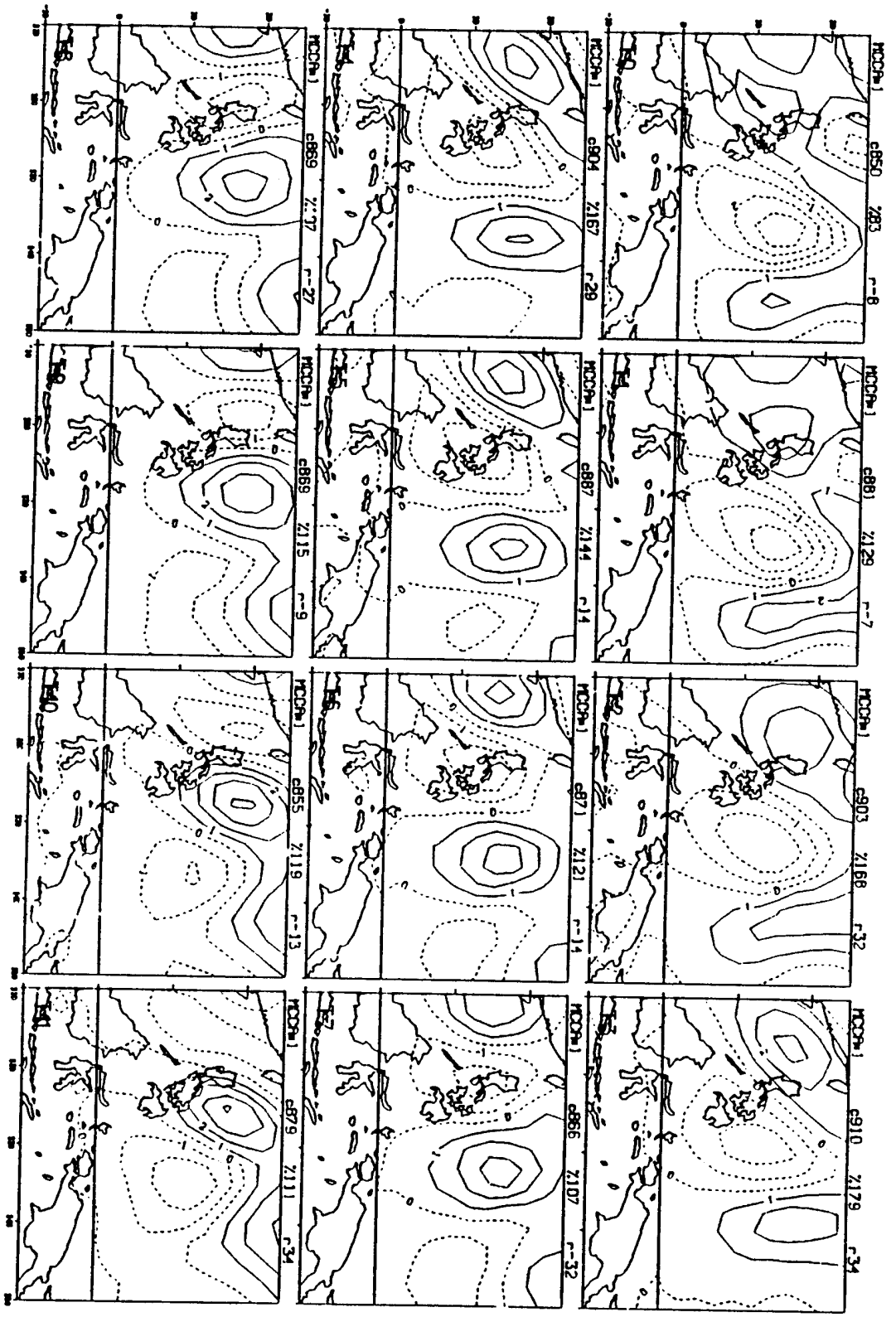

Figure A11: Same as Figure A1 except for year 1984

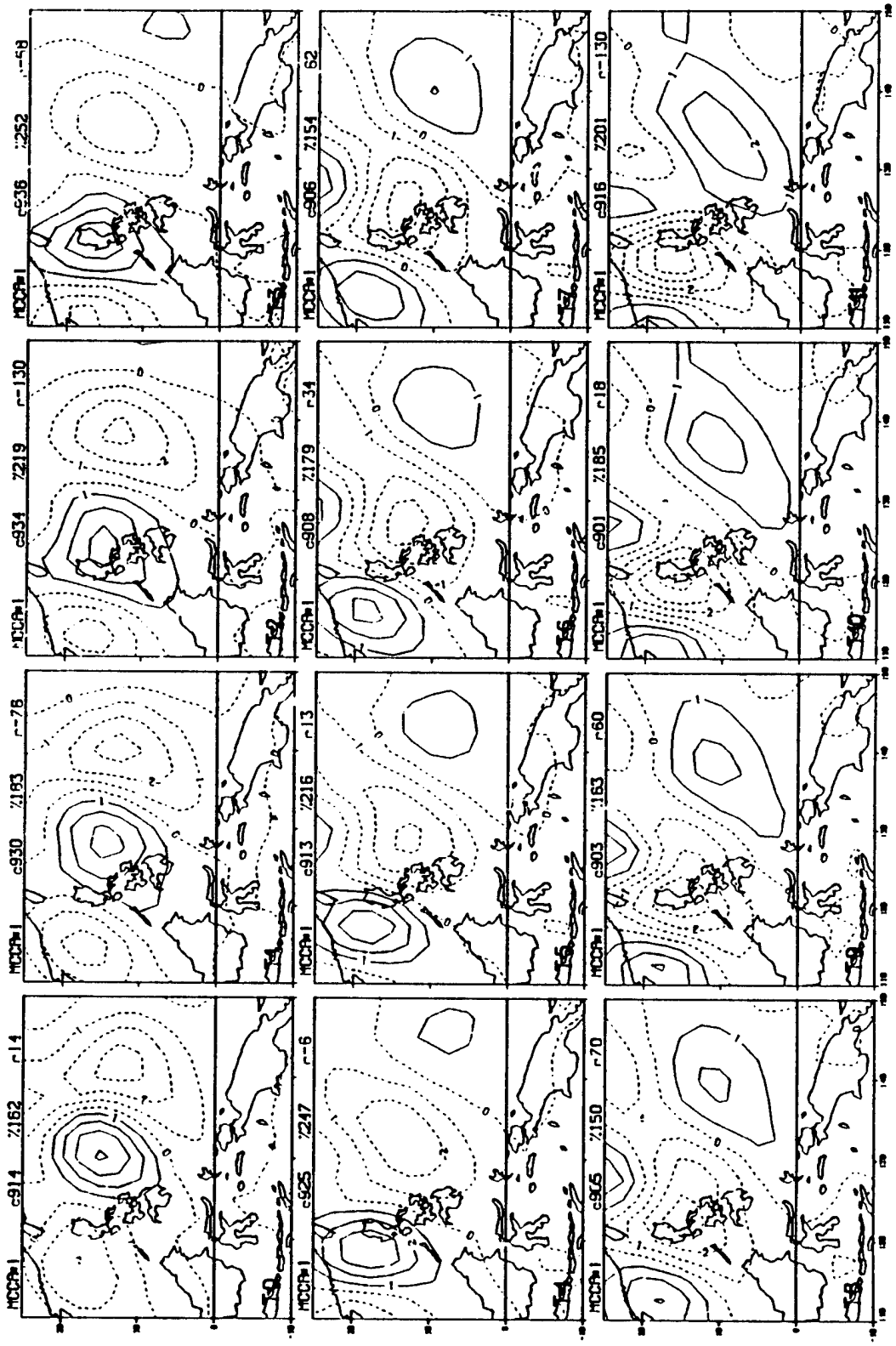

Figure A12: Same as Figure A1 except for year 1985

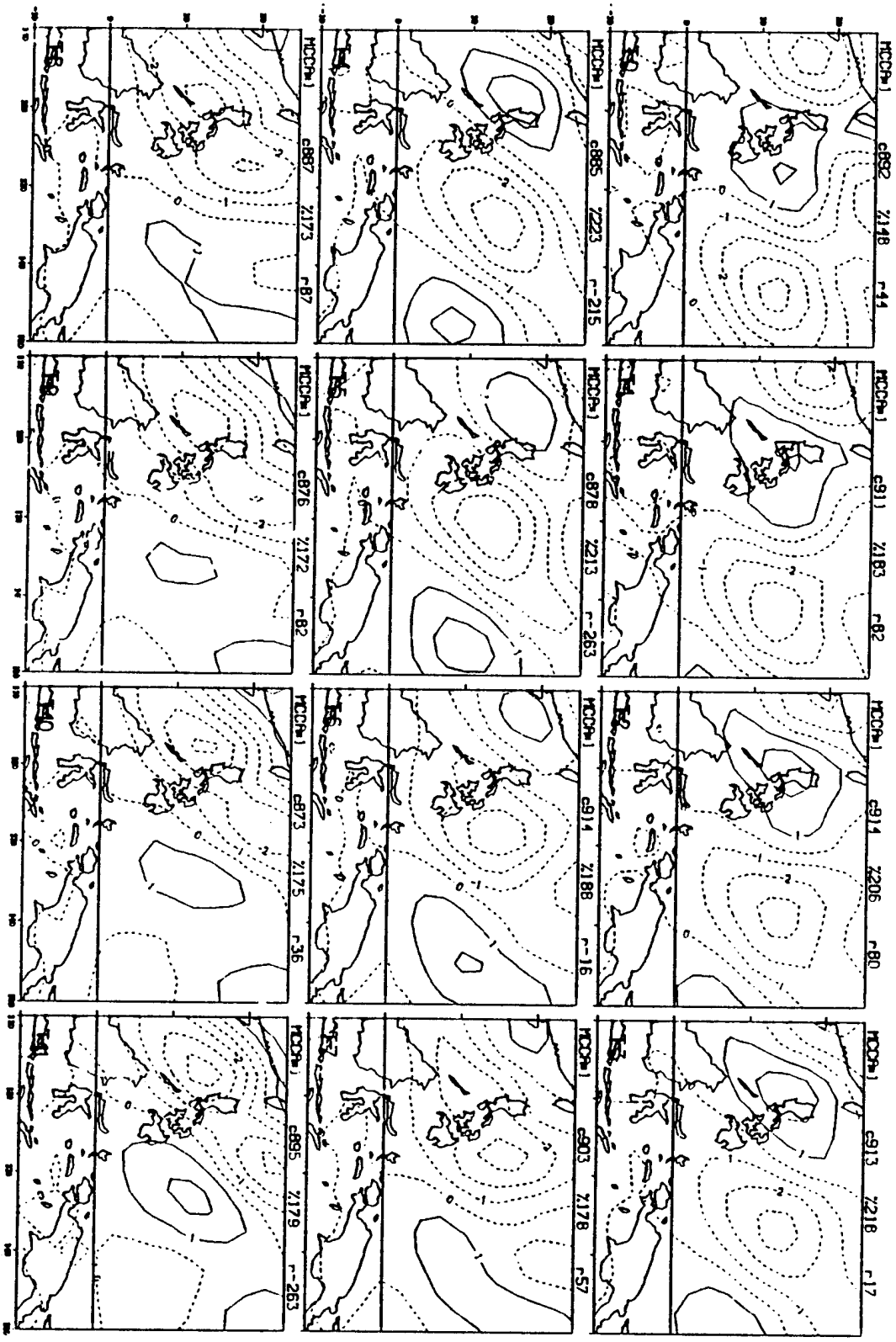

Figure A13: Same as Figure A1 except for year 1986

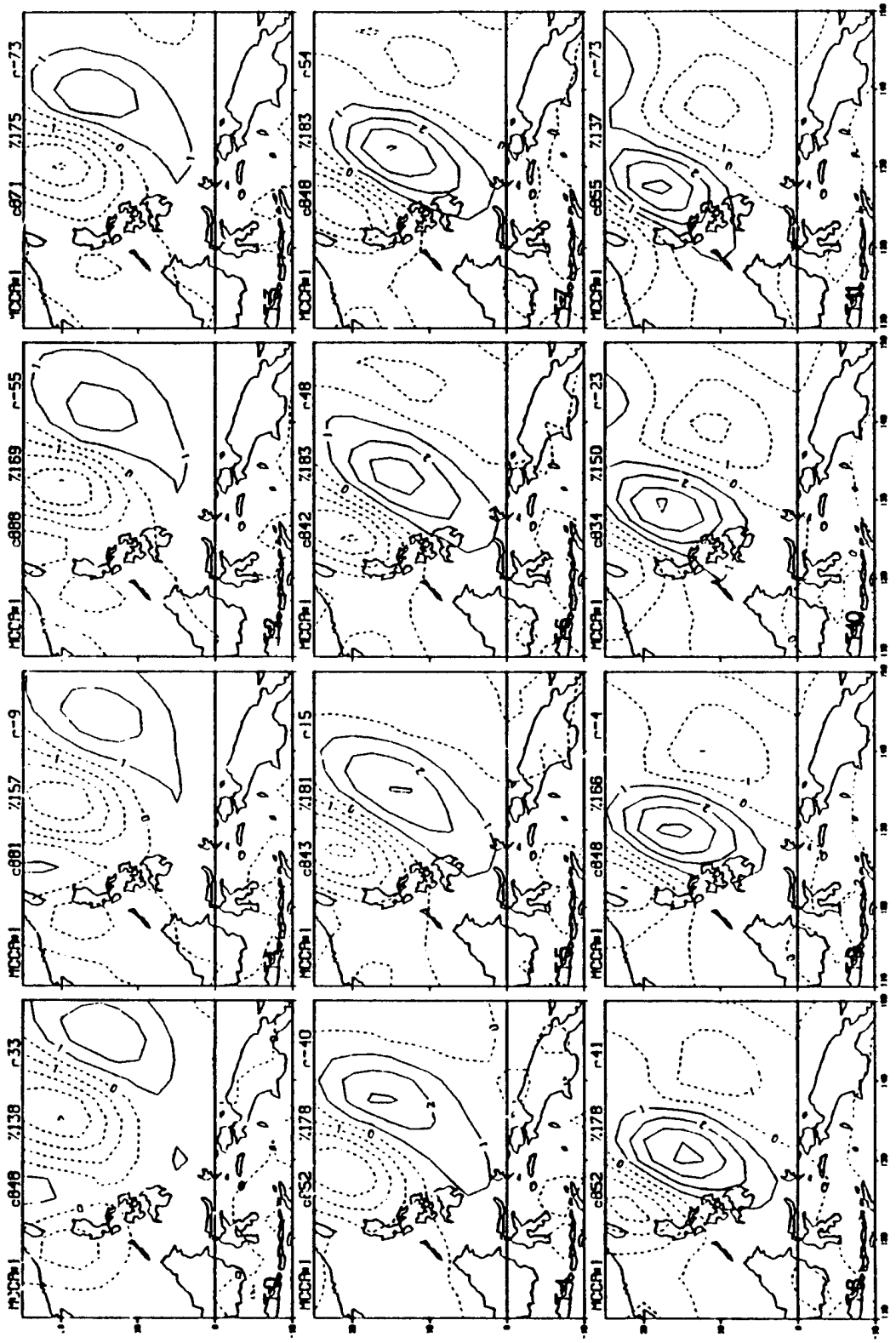

Figure A14: Same as Figure A1 except for year 1987

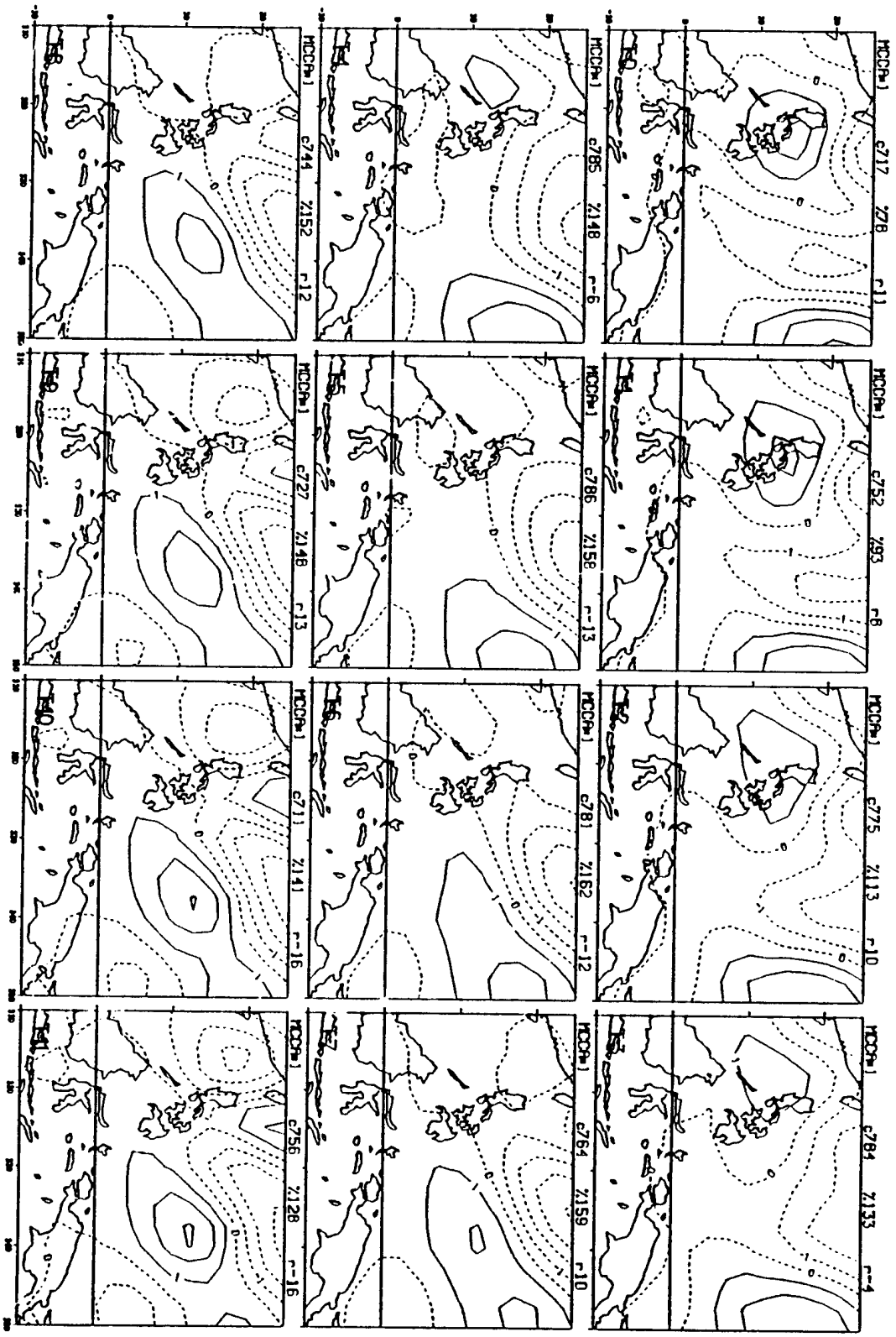

Figure A15: Same as Figure A1 except for year 1988.

LIST OF REFERENCES

Burpee,R.W.,1974: Characteristics of north African easterly waves during the summer of 1968 and 1969. *J.Atmos.Sci*,**31**,1556-1570.

Carlson,T.N.,1969: Some remarks on African disturbances and their progress over the tropical Atlantic. Mon.Wea.Rev.,97,716-726.

Chang,C.P. and C.R.Miller III,1977: Comparison of easterly waves in the tropical Pacific during two periods of contrasting sea-surface temperatures anomalies. *J.Atmos.Sci.*,**34**,615-628.

Chang,C.P., V.F.Morris and J.M.Wallace,1970: A statistical study of easterly waves in the western Pacific: July-December 1964: *J.Atmos.Sci.*,**27**,195-201.

Chang,C.P., J.M.Chen, P.Harr and L.Carr,1995: Northwestward propagating synoptic wave patterns over the tropical western Pacific and periodicity of tropical cyclone activity. Submitted to *Mon.Wea.Rev.*

Chang,C.P. and H.Lim,1988: Kelvin wave CISK: A plausible mechanism for the 30-50 day oscillation. **J.Atmos.Sci.**,1709-1720.

Chang,C.P.,1977: Viscous internal gravity waves and low frequency oscillations in the tropics. *J.Atmos.Sci.*,**34**,901-910.

Chang,C.P.,and L.Zambresly,1994: Observed and navy global model climatologies of synoptic disturbances over the tropical western Pacific during Northern Winter 1991-1992: A spectral analysis. *Mon.Wea.Rev.*, 122.page

Chen,J.M. and C.P.Chang,1994: Multiple-set canonical correlation analysis, Part II: A reliability case study. *Mon.Wea.Rev.*, 122.page

Chen,J.M.,C.P.Chang and P.A.Harr,1994: Multiple-set canonical correlation analysis, Part I: The method. *Mon.Wea.Rev.*, 122.page

Chen,T.C.,R.Y.Tzeng and M.C.Yen,1988: Development and life cycle of the Indian Monsoon: Effect of the 30-50 day oscillation. *Mon.Wea.Rev.*,**116**,2183-2199.

Dunn,G.E.,1940: Cyclogenesis in the tropical Atlantic. *Bull.Amer.MetSoc.*,**21**,215-229.

Dunkerton,T.J.,1993: Observation of 3-6 day meridional. wind oscillations over the tropical Pacific, 1973-1992: Vertical structure and interannual variability. *J.Atmos.Sci.*,**50**,3292-3307.

Glahn,H.R.,1968: Canonical. correlation and its relationship to discriminant analysis and multiple regression. *J.Atmos.Sci.*,**25**,23-31.

Harr,P.A.,1993: Large-scale circulation regimes and tropical cyclone characteristics over the western Pacific ocean. Ph.D thesis,Dept.of Meteorology,Naval Postgraduate School, Monterey, CA,275pp.

Holton,J.R.,1971: A diagnostic model for equatorial wave disturbances: The role of vertical shear of the mean zonal wind. *J.Atmos.Sci.*, **28**,55-64.

Horst,P.,1965: Factor analysis of data matrices. New York: Holt,Rinehart and Winston,730 pp.

Hotelling,H.,1933: Analysis of a complex of statistical variables into pricipal components. *J.of Edu.Psych.*, **24**,417-441,498-520.

_____,1935: The most predictible criterion. *J.of Edu.Psych.*,**26**,139-142.

_____,1936: Relations between two sets of variates. *Biometrika*,**28**,321-377.

Ketterning,J.R.,1971: Canonical analysis of several. sets of variables space. *Phil.Biometrika*,**58**,433-460.

Krishnamurti,T.N.,J.Molinari,H.Pan,and V.Wong,1977: Downstream amplification and formation of monsoon disturbances. Mon.Wea.Rev. 105,1281-1297.

Krishnamurti,T.N.,1985: Summer Monsoon experiment -A review. *Mon.Wea.Rev.*,**113**,1590-1626.

Krishnamurti,T.N.,and H.N.Bøhlme,1976: Oscillations of a Monsoon system: Part I: Observational aspects. *J.Atmos.Sci.*,**33**,1937-1954.

Krishnamurti,T.N.,and D.Subrahmanyan,1982: The 30-50 day mode at 850 mb during MONEX. J.Atmos.Sci., 39,2088-2095.

Krishnamurti,T.N.,and P.Ardanuy,1980: The 10-20 day westward propagating mode and "breaks in the Monsoon". *Tellus*,**33**,15-26.

Krishnamurti,T.N.,P.K.Jayakaumar,J.Sheng,NSurgi,and A.Dumar,1985: Divergent circulation on the 30-50 day time scal.e. *J.Atmos.Sci.*,**42**,364-375.

Lau,K.M.,and P.H.Chan,1986: Aspects of the 40-50 day oscillation during the northern summer as inferred from outgoing longwave radiation. *Mon.Wea.Rev.*,**114**,1354-1367.

Lau,K.H.,and N.G.Lau,1990: Observed structure and propagation characteristics of tropical. summertime synoptic scal.e disturbance. *Mon.Wea.Rev.*,**118**,1888-1913.

Lau,K.H.,and L.Peng,1987: Origin of low frequency (intraseasonal.) oscillations in the tropical. atmosphere. Part I: Basic theory. *J.Atmos.Sci.*,**44**,950-972.

Li,C.Y.,and Y.P.Zhou,1992: The quasi-biweekly (10-20day) oscillation in the tropical. atmosphere. *Sci.Atmos.Sinica*, 16(in chinese).

Liebemann,B.,and H.H.Hendon,1990: Synoptic scale disturbances near the equator. *J.Atmos.Sci.*,**47**,1463-1479.

Lorenc,A.C.,1984: The evolution of planetary scale 200 mb divergence during the FGGE year. Meteorological Office Tech.NoteII/ 210,1-23.

Lorenz,E.N.,1956: Empirical. orthogonal functions and statistical weather prediction. Sci.Report No.1 Statistical

Forecasting Project,MIT,Dept.of Meteorology, Cambridge, Mass., 49 pp.

Madden,R,and P.Julian,1971: Detection of a 40-50 day oscillation in the zonal wind. *J.Atmos.Sci.*,**28**,702-708.

_____,and_____,1972: Description of global scale circulation cells in the tropics with a 40-50 day period. *J.Atmos.Sci.*, **29**,1109-1123.

Nitta,T.,and Y.Takayabu,1985: Global analysis of the lower tropospheric disturbances in the tropics during the northern summer of the FGGE year. Part II: Regional characteristics of the disturbances. *Pure Appl. Geophys.***123**,272-292.

_____,Y.Nakagomi,Y.Susuki,N.Hasegawa,and A.Kadokura,1985: Global. analysis of the lower tropospheric disturbance in the tropics during the northern summer of the FGGE year. Part I: Global features. *J.Meteorol.Sci.Japan*,**63**,1-19.

Norquist,D.C.,E.E.Recker and R.J.Reed,1977: The energetics of African wave disturbances as observed phase III of GATE. *Mon.Wea.Rev.*,**105**,334-342.

Pearson,K.,1901: On lines and planes of closest fit to points in space. *Phil.Magazine*,**2**,559-572.

Piersig,W.,1936: Schwankungen von luftdruck and luftbewengung sowie ein ein beitrag zum wettergesschehen in passatgebiet des ostlichen nordatlantischen ozesns. *Arch.Dent.Seewarte*, 54(6).

Prohaska,J.T.,1976: A tecnique for anal.yzing the linear relationship between two meteorological. fields. *Mon.Wea.Rev.*, 104,1345-1353.

Reed,R.J.,and E.E.Recker,1971: Structure and properties of synoptic scale wave disturbance in the equatorial western Pacific. *J.Atmos.Sci.*,**28**,1117-1133.

_____,D.C.Norquist,and E.E.Recker,1977: The structure and Properties of african wave disturbances as observed during phase II of GATE. *Mon.Wea.Rev.*,**105**,317-333.

_____,E.Klinker and A.Hollingsworth,1988: The structure and characteristics of African wave disturbances as determined from the ECMWF operational analysis/forecast system. *Meteor.Atmos.Phys.*,**38**,22-33.

Regula,M.,1936: Druckschwandungen und tornados and der wesduste von Africa. Ann. *Hydrog.Mar.Metero.*,**64**,107-111.

Riehl,H.,1945: Waves in the easterlies and the polar front in the tropics Misc.Rep.No. 17 Dept.of Meteorology, University of Chicago, 79 pp.

Saha,K.,F.Sanders,and J.Shukla,1981: Westward propagating predecessors of Monsoon depressions. *Mon.Wea.Rev.*,**109**,330-343.

Steel,R.G.D.,1951: Minimum general.ized variance for a set of linear function. *Ann.Math.Statist*.**22**,456-60.

Takayabu,Y.N.,and T.Nitta,1993: 3-5 day period disturbances coupled with convection over the tropical Pacific ocean. *J.Meteor.Soc.Japan*,**71**,221-246.

Tao,S.Y.,and L.X.Chen,1987: A review of recent research of the east Asian summer monsoon in China. *Monsoon Meteorology*. Chang and Krishnamurti,eds.,Oxford Univ.Press.,60-92.

Wallace,J.M.,and C.P.Chang,1969: Spectral analysis of large scale wave disturbances in the tropical lower troposphere. *J.Atmos.Sci.*,**26**,1010-1025.

Wang,B.,1988: Dynamics of tropical low frequency waves: An analysis of the moist Kelvin waves. *J.Atmos.Sci.*,**45**,2051-2065.

Wu,P.L.,and C.Y.Li,1990: the 10-20 day oscillation in the atmosphere. Proceedings on Atmospheric Sciences, Scientific Press,Beijing,149-159 (in chinese).

Yanai,M.,T.Maruyama,T.Nitta and Y.Hayashi,1968: Power spectra of large scale disturbances over the tropical Pacific. *J.Meteorol.Soc.Japan*,**46**,308-323.

INITIAL DISTRIBUTION LIST

		No. Copies
1.	Defense Technical Information Center Cameron Station Alexandria, Virginia 22304-6145	2
2.	Library, Code 52 Naval Postgraduate School Monterey, California 93943-5101	2
3.	Chairman (Code OC/CO) Department of Oceanography Naval. Postgraduate School Monterey, California 93943-5002	1
4.	Chairman (Code MR/Hy) Department of Meteorology Naval. Postgraduate School Monterey, California 93943-5002	1
5.	Prof. Chih-Pei Chang (Code MR/Cp) Department of Meteorology Naval. Postgraduate School Monterey, California 93943-5002	2
6.	Pref. Jeng-Ming Chen (Code MR/Ch) Department of Meteorology Naval. Postgraduate School Monterey, California 93943-5002	2
7.	Dr. Patrick Harr (Code MR/Hp) Department of Meteorology Naval. Postgraduate School Monterey, California 93943-5002	1
8.	Ms. Bao Fong Jeng (Code MR/Jg) Department of Meteorology Naval. Postgraduate School Monterey, California 93943-5002	1
9.	Lcdr. Cheng,Chu-Chai No. 9-11, 5F, Ting Liao Rd., Pa Li Hsiang, Taipei Hsien, Taiwan. 249	2

10. P.O. Box 90175 1
Chinese Naval Academy library
Tsoying , Kaohsiung,
Taiwan.